ORAL DRUG DELIVERY – MOLECULAR DESIGN AND TRANSPORT MODELING

Naresh Pavurala

Dissertation submitted to the faculty of the Virginia Polytechnic Institute and State University in partial fulfillment of the requirements for the degree of

Doctor of Philosophy

In

Chemical Engineering

Luke E. Achenie, Chairman

Richey M. Davis

Eva Marand

Stephen Martin

November 14, 2013

Blacksburg, VA

Keywords:

Oral drug delivery, drug release model, ACAT model, pharmacokinetic model, simulation, optimization, molecular design, structure-property models, novel polymers, release kinetics, oral dosage form, tablet design

VIRGINIA POLYTECHNIC INSTITUTE AND STATE UNIVERSITY

ABSTRACT

Pharmacokinetic Modeling of Oral Drug Delivery

by Naresh Pavurala

Chairperson of the Supervisory Committee: Professor Luke Achenie

Department of Chemical Engineering

One of the major challenges faced by the pharmaceutical industry is to accelerate the product innovation process and reduce the time-to-market for new drug developments. This involves billions of dollars of investment due to the large amount of experimentation and validation processes involved. A computational modeling approach, which could explore the design space rapidly, reduce uncertainty and make better, faster and safer decisions, fits into the overall goal and complements the product development process. Our research focuses on the early preclinical stage of the drug development process involving lead selection, optimization and candidate identification steps. Our work helps in screening the most favorable candidates based on the biopharmaceutical and pharmacokinetic properties. This helps in precipitating early development failures in the early drug discovery and candidate selection processes and reduces the rate of late-stage failures, which is more expensive.

In our research, we successfully integrated two well-known models, namely the drug release model (dissolution model) with a drug transport model (compartmental absorption and transit (CAT) model) to predict the release, distribution, absorption and elimination of an oral drug through the gastrointestinal (GI) tract of the human body. In the CAT model, the GI tract is envisioned as a series of compartments, where each compartment is assumed to be a continuous stirred tank reactor (CSTR). We coupled the drug release model in the form of partial differential equations (PDE's) with the CAT model in the form of ordinary differential equations (ODE's). The developed model can also be used to design the drug tablet for target pharmacokinetic characteristics. The advantage of the suggested approach is that it includes the mechanism of drug release and also the properties of the polymer carrier into the model. The model is flexible and can

be adapted based on the requirements of the clients. Through this model, we were also able to avoid depending on commercially available software which are very expensive.

In the drug discovery and development process, the tablet formulation (oral drug delivery) is an important step. The tablet consists of active pharmaceutical ingredient (API), excipients and polymer. A controlled release of drug from this tablet usually involves swelling of the polymer, forming a gel layer and diffusion of drug through the gel layer into the body. The polymer is mainly responsible for controlling the release rate (of the drug from the tablet), which would lead to a desired therapeutic effect on the body.

In our research, we also developed a molecular design strategy for generating molecular structures of polymer candidates with desired properties. Structure-property relationships and group contributions are used to estimate the polymer properties based on the polymer molecular structure, along with a computer aided technique to generate molecular structures of polymers having desired properties. In greater detail, we utilized group contribution models to estimate several desired polymer properties such as grass transition temperature (T_g), density (ρ) and linear expansion coefficient (α). We subsequently solved an optimization model, which generated molecular structures of polymers with desired property values. Some examples of new polymer repeat units are $-\left[CONHCH_2-CH_2NHCO\right]_n-$, $-\left[CHOH-COO\right]_n-$. These repeat-units could potentially lead to novel polymers with interesting characteristics; a polymer chemist could further investigate these. We recognize the need to develop group contribution models for other polymer properties such as porosity of the polymer and diffusion coefficients of water and drug in the polymer, which are not currently available in literature.

The geometric characteristics and the make-up of the drug tablet have a large impact on the drug release profile in the GI tract. We are exploring the concept of tablet customization, namely designing the dosage form of the tablet based on a desired release profile. We proposed tablet configurations which could lead to desired release profiles such as constant or zero-order release, Gaussian release and pulsatile release. We expect our work to aid in the product innovation process.

To my Mother and Father:

Shri Venkateshwara Rao Pavurala

Shri Pushpavathi Pavurala

"Knowing is not enough, we must apply
willing is not enough, we must do…"

— *Johann Wolfgang von Goethe*

Acknowledgements

My Ph.D. program experience was the most challenging, yet enjoyable and rewarding, academic experience of my life, because I like to learn. It was an overwhelming experience as it opened my world throughout the years. I have met a lot of wonderful people. I have had the privilege of working with **Dr. Luke Achenie**, who was instrumental in helping me to complete my doctoral work. I sincerely thank him for his unending support and invaluable guidance throughout the period of my PhD.

I take the opportunity to express my deepest sense of gratitude to **Dr. Richie Davis, Dr. Eva Marand and Dr. Stephen Martin** for their constructive criticism, endless help, and guidance during my period of my PhD work.

I am also very thankful to my colleagues, for their suggestions and support during the course of my PhD. They include **Chris Christie, Zhenxing Wang (Jason), Nuttapol Lerkkasemsan and Syed Mazahir.**

I would like to thank **Riley Chan** for his ability to fix just about anything and **Cannaday Diane**, **Nora Bentley, Tina Kirk, Tammy Hiner Jo**, **Leslie Thornton- O'Brien**, **Shelley Johnson**, **Lois Hall**, **Dawn Maxey**, **Lisa Smith** ,**Ennis McCrery, Ruth Athanson, Graduate School and Cranwell International Center** for their assistance with countless matters.

I also thank the following for financial support: National Science Foundation, Department of Chemical Engineering, Virginia Tech.

My life at Virginia Tech is priceless and I am really fortunate to know wonderful people here. I would like to thank **Sonal Mazumder,** who has supported me through thick and thin - she had been a great friend, philosopher and guide. I would like to thank my committee (2010-2011) and members of **Indian Students Association** in Virginia Tech. I have gained immense experience and learnt various leadership and teamwork qualities while working with them.

Sincerest thanks to my father, **Venkateshwara Rao Pavurala,** and mother, **Pushpavathi Pavurala,** for being such wonderful parents providing constant support and encouragement.

Thanks to my brother, **Sahitya Pavurala** and my sister, **Swathi Pavurala** for everything. Thanks to my friends in India for all their support and love.

Finally, I would like to thank my professors from Indian Institute of Technology (IIT), Madras in India, who helped me to follow my dream and pursue my doctoral studies at Virginia Tech.

Naresh Pavurala

Blacksburg, Virginia-USA

November, 2013

Attribution

Professor Luke Achenie is my research advisor and committee chair. He provided guidance, help, and support throughout the work in this PhD dissertation. Also he significantly contributed to the written communication of the research.

TABLE OF CONTENTS

LIST OF FIGURES

Number *Page*

Chapter 1: Introduction

Chapter 2: Modeling of Drug Release from a Polymer Matrix

Chapter 3: An advanced pharmacokinetic model for oral drug delivery

Chapter 4: Designing polymer structures for oral drug delivery – a molecular design approach

Chapter 5: Customization of Oral Drug Dosage Form – Innovation in Tablet Design

LIST OF TABLES

Number *Page*

Chapter 2: Modeling of Drug Release from a Polymer Matrix

Chapter 3: An advanced pharmacokinetic model for oral drug delivery

Chapter 4: Designing polymer structures for oral drug delivery – a molecular design approach

ABBREVIATIONS

CAT	Compartmental Absorption and Transit
ACAT	Advanced Compartmental Absorption and Transit
AUC	Area under the curve
GI	Gastrointestinal
ADME	Absorption, Distribution, Metabolism and Excretion
NSC	Normalized Sensitivity Coefficient
CSTR	Continuous Stirred Tank Reactor
PFR	Plug Flow Reactor
CAMD	Computer Aided Molecular Design
MD	Molecular Dynamics
MILP	Mixed Integer Linear Programming
MINLP	Mixed Integer Nonlinear Programming
API	Active Pharmaceutical Ingredient
HPMC	Hydroxy Propyl Methyl Cellulose

CHAPTER 1

Introduction

1.1 Drug Delivery

Drug delivery can be described as application of chemical and biological principles to control the in vivo temporal and spatial location of drug molecules for clinical benefit. When a drug is administered, only a small fraction of the dose actually reaches the relevant receptors or sites of action, and most of the dose is wasted either by being taken up into the wrong tissue, removed from right tissue too quickly, or destroyed en route before arrival. The research in drug delivery is to tackle these issues in order to maximize drug activity and minimize side effects.

Till recently, injections (i.e. intravenous, intramuscular or subcutaneous route) remain the most common means for administering protein and peptide drugs like insulin. Patient compliance with drug administration regimens by any of these parenteral routes is generally poor and severely restricts the therapeutic value of the drug, particularly for disease such as diabetes (Soltero 2005). Among the alternate routes that have been tried with varying degrees of success are the oral, buccal (Sayani and Chien 1996), intranasal (Torres-Lugo and Peppas 2000), pulmonary (O'Hagan DT 1990), transdermal (Banga and Chien 1993), ocular (Lee and Yalkowsky 1999) and rectal (Pezzuto et al. 1993). Among these, oral route remains the most convenient way of delivering drugs. Oral administration presents a series of attractive advantages towards other drug delivery. These advantages are particularly relevant for the treatment of pediatric patients and include the avoidance of pain and discomfort associated with injections and the elimination of possible infections caused by inappropriate use or reuse of needles. Moreover, oral formulations are less expensive to produce, because they do not need to be manufactured under sterile conditions (Salama et al. 2006). In addition, a growing body of data suggests that for certain polypeptides such as insulin; the oral delivery route is more physiological (Hoffman A 1997). It is estimated that 90% of all medicines are oral formulations and oral drug delivery systems comprise more than half the drug delivery market. In 2008, the oral drug delivery market was a USD 35 billion industry and was expected to grow as much as 10% per year until at least 2012 (Gabor et al. 2010). Oral drug products are also profitable for the

pharmaceutical industry. However, biopharmaceutical issues such as physicochemical requirements of the drug and physiological conditions make oral delivery one of the most challenging routes. With recent developments in manufacturing technology, large quantities of oral formulations are produced with short production times. By following good manufacturing practices (GMP regulations), high quality oral delivery products are prepared in a reliable and reproducible manner.

Dissolution and absorption of drugs from the gastrointestinal (GI) tract is a very complex process involving multiple steps including drug disintegration and dissolution, degradation, gastric emptying intestinal transit, intestinal permeation and transport, intestinal and hepatic metabolism (Yu et al. 1996, Martinez and Rilyn 2002, Huang et al. 2009). It is influenced by many factors that not only vary among various compounds and formulations but also between different regions in the GI tract with respect to rate and extent of absorption. Absorption properties also vary from subject to subject and from time to time. The GI tract offers a large absorption surface and nearly one third of the blood from cardiac output flows through the gastrointestinal organs making it a very good site for drug absorption (Gabor et al. 2010). Most of the tablet formulations include a drug enclosed inside a swellable polymer. The delivery of drugs, peptides or proteins, occurs through a process of continuous swelling of the polymer carrier that is associated with simultaneous or subsequent dissolution of the polymer carrier. The drug is usually molecularly dispersed or dissolved in a polymer matrix at low or high concentrations. As water penetrates the polymer, swelling occurs and the drug is released to the external environment (Narasimhan and Peppas 1997).

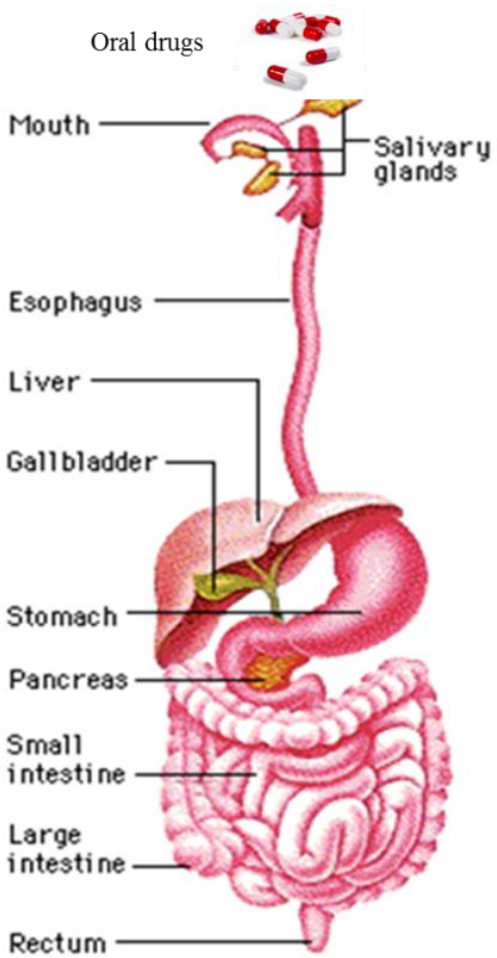

Figure 1: Schematic of gastrointestinal tract of human body (cinncinnati 2006)

Designing and formulating a protein and peptide drug for delivery though GI tract requires a multitude of strategies. The dosage form must initially stabilize the drug making it easy to take orally (Sayani and Chien 1996). It must then protect the drug from the extreme acidity and action of pepsin in the stomach. In the intestine, the drug should be protected from the surplus amount of enzymes that are present in the intestinal lumen. In addition, the formulation must facilitate both aqueous solubility at near-neutral pH and lipid layer penetration in order for the protein to cross the intestinal membrane and then basal membrane for entry into the bloodstream (Fig. 1). A primary objective of oral delivery systems is to protect protein and peptide drugs from acid and luminal proteases in the GIT. To overcome these barriers, several formulation strategies are being investigated. Some of them include enteric-coated dry emulsions, microspheres, and nanoparticles for oral delivery of peptides and proteins.

The drug discovery and development process involves several stages to bring a new drug (new chemical entity (NCE)) from laboratory to market. These include, target/disease identification, hit identification/discovery, hit optimization, lead selection and further optimization, candidate identification and clinical trials (Kuhlmann 1997). It involves identification and screening of tens of thousands of compounds to identify a few candidates (hits) with desired biological activity. These hits are further filtered based on their efficiency, and then tested in various pharmacological models. These candidates (leads) are further optimized based on their biopharmaceutical properties and filtered down to one or two best drug-like candidates for further development (Han and Wang 2005). Clinical trials are done on these drug like candidates of which only one compound makes to the market. Fig. 2 shows a schematic description of the drug discovery and development process along with a rough estimate of the number of candidates after each step.

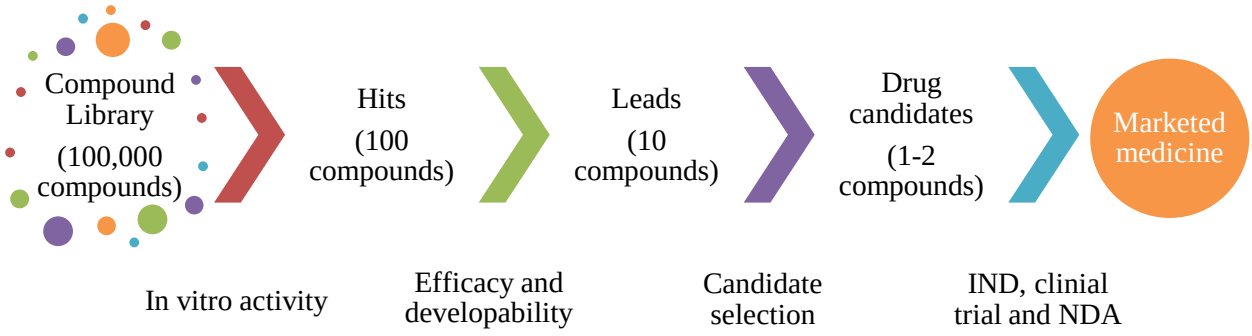

Figure 2: Schematic of the drug discovery and development process (Han and Wang 2005)

The entire drug discovery and development process costs around a billion dollars to bring a single new drug from laboratory to m/rket. This involves a lot of candidate failures to the early and late stages in the process. It was estimated that 39% of the failure was due to poor pharmacokinetic properties in humans; 29% was due lack of clinical efficiency; 21% was due to toxicity and adverse effects and 6% due to commercial limitations (Han and Wang 2005). The preclinical stage research includes about tens of million dollars of the total cost, whereas the clinical trials cost hundreds of millions of dollars. Therefore, a significant improvement in the

efficiency of the preclinical stage process will reduce potential failures in the later stages of the process and also save millions of dollars.

1.2 Problem Statement

In this dissertation we are trying to address the issue of reducing the number of experimental trials, time and effort needed for drug design and development. This work will help aid in the preclinical stage of the drug discovery and development process and help in reducing potential failures in the later stages. To address the stated issue we proceed as follows. We propose to accomplish a two way modeling approach i.e., given a drug tablet with initial dosage, the model can predict the pharmacokinetic behavior of the drug inside the body and its plasma concentration profile. Inversely, given the pharmacokinetic characteristics; the model can evaluate the design parameters and dosage of the drug tablet (Fig. 3).

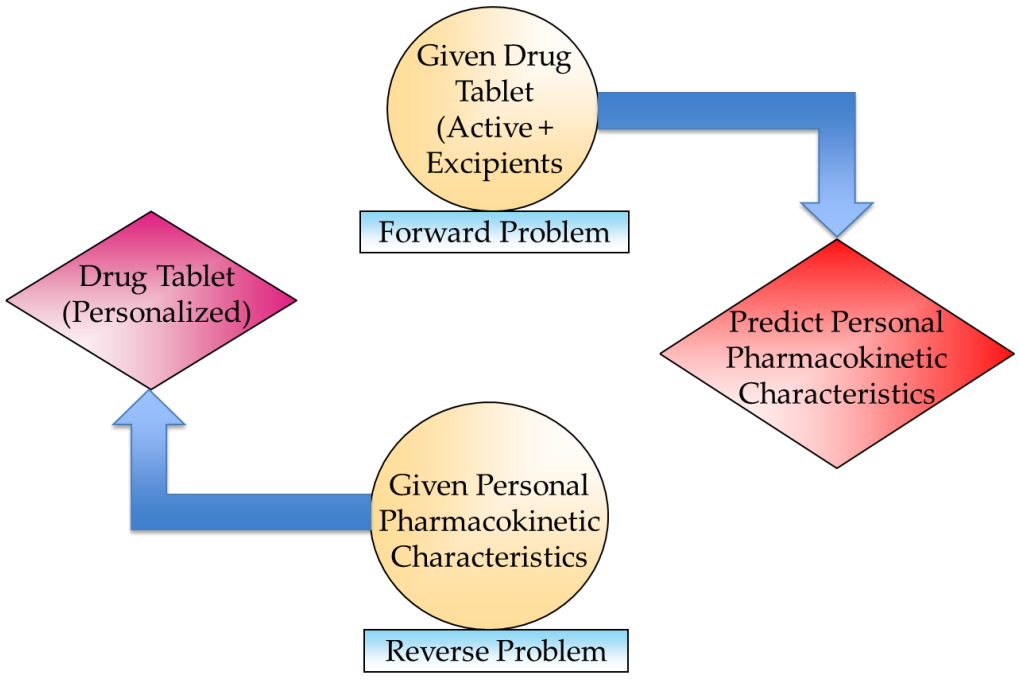

Figure 3: Proposed modeling strategy

We have defined the following aims to accomplish this task:

Aim 1

Develop a drug release model to predict the release of drug from an oral dosage form (drug enclosed in a polymer matrix) into the gastrointestinal (GI) tract of the human body

Aim 2

Develop a modeling platform to predict the plasma concentration profile and pharmacokinetic characteristics of an oral drug, given a drug release profile

Aim 3

Develop a modeling strategy to design the drug tablet using structure-property models and molecular design for a desired drug release profile

Aim 4

Design different dosage forms of the tablet to obtain specific desired drug release profiles – Tablet customization

In this thesis, the four specific aims are described in greater detail in chapters 2, 3, 4 and 5 respectively.

In chapter 2, we discuss a drug release model which predicts the release of drug from an oral drug tablet (drug enclosed in a polymer matrix) when it is taken into the gastrointestinal (GI) tract (Aim 1). This chapter discusses the various factors that influence the drug release and the effect of polymer matrix on the drug release. This work is expected to be very useful in the tablet design process.

After successfully developing a working drug release model, we develop a pharmacokinetic model which predicts the behavior of the drug as it passes through the GI tract in chapter 3 (Aim 2). The pharmacokinetic model is a combination of the drug release model developed in chapter 2 with a drug transport model. The developed model will be able to predict the plasma concentration profile and other pharmacokinetic characteristics such as peak plasma concentration, area under the curve and bioavailability. The plasma concentration profile represents the obtained therapeutic effect in the patient. This work is expected to be very useful in the drug discovery and development process.

Through Aim 1 and Aim 2, we were able to accomplish the forward problem as discussed in Fig. 3. Given a drug tablet, through the drug release model and the pharmacokinetic model developed in chapters 1 and 2, we will be able to predict the personal pharmacokinetic

characteristics of a patient. In the subsequent chapters, we tried to accomplish the reverse problem, i.e., developing the tablet formulation, given the personal pharmacokinetic characteristics.

In Chapter 4, we proposed a computer aided molecular design (CAMD) strategy which could aid in the drug tablet formulations. In this work, we specifically worked on the polymer component in the drug tablet. The polymer inside the tablet is majorly responsible for controlling the release rate of the drug from the tablet, hence controlling the drug release profile. A desired drug release profile is inspired by a desired plasma concentration profile. Through this approach, we were able to generate molecular structures of polymers which could be used as potential carrier materials for oral drugs. This work is expected to aid in the product development process.

In chapter 4, we discussed the concept of tablet customization, i.e., designing the dosage form of the drug tablet according to a desired drug release profile. In this work, we proposed tablet configurations which could lead to a desired release profiles such a constant release profile, a Gaussian release profile and a pulsatile release profile. The tablet design greatly influences the release characteristics. Tablet configurations could be customized based on the requirement of the patient, his physiological and genetic makeup, and the desired therapeutic effect. This work will greatly improve the patient compliance, reduce side effects, reduce dosage frequency and improve the overall efficiency of the drug tablet. This work is a significant forward step towards the development of personalized medicine.

1.3 References

Banga, A. K. and Y. W. Chien (1993). "Hydrogel-Based lontotherapeutic Delivery Devices for Transdermal Delivery of Peptide/Protein Drugs." Pharmaceutical Research **10**(5): 697-702.

cinncinnati, G. c. o. g. (2006). "Your digestive system and how it works ", from http://ssl.gcis.net/giconsults/gi-tract.htm.

Gabor, F., C. Fillafer, L. Neutsch, G. Ratzinger and M. Wirth (2010). Improving Oral Delivery

Drug Delivery. M. Schäfer-Korting, Springer Berlin Heidelberg. **197:** 345-398.

Han, C. and B. Wang (2005). Factors That Impact the Developability of Drug Candidates: An Overview. Drug Delivery, John Wiley & Sons, Inc.**:** 1-14.

Hoffman A, Z. E. (1997). "Pharmacokinetic considerations of new insulin formulations and routes of administration." Clin Pharmacokinet. **33**(4): 285-301.

Huang, W., S. Lee and L. Yu (2009). "Mechanistic Approaches to Predicting Oral Drug Absorption." The AAPS Journal **11**(2): 217-224.

Kuhlmann, J. (1997). "Drug research: from the idea to the product." Int J Clin Pharmacol Ther **35**(12): 541-552.

Lee, Y.-C. and S. H. Yalkowsky (1999). "Effect of formulation on the systemic absorption of insulin from enhancer-free ocular devices." International Journal of Pharmaceutics **185**(2): 199-204.

Martinez, M. a. and Rilyn (2002). "A Mechanistic Approach to Understanding the Factors Affecting Drug Absorption: A Review of Fundamentals." Journal of clinical pharmacology **42**(6): 620-643.

Narasimhan, B. and N. A. Peppas (1997). "Molecular analysis of drug delivery systems controlled by dissolution of the polymer carrier." Journal of Pharmaceutical Sciences **86**(3): 297-304.

O'Hagan DT, I. L. (1990). "Absorption of peptides and proteins from the respiratory tract and the potential for development of locally administered vaccine." Crit Rev Ther Drug Carrier Syst. **7**(1): 35-97.

Pezzuto, J. M., M. E. Johnson and H. Manasse Jr (1993). Biotechnology and pharmacy, Chapman & Hall.

Salama, N. N., N. D. Eddington and A. Fasano (2006). "Tight junction modulation and its relationship to drug delivery." Advanced Drug Delivery Reviews **58**(1): 15-28.

Sayani, A. P. and Y. W. Chien (1996). "Systemic Delivery of Peptides and Proteins Across Absorptive Mucosae." Critical Reviews in Therapeutic Drug Carrier Systems **13**(1&2): 85-184.

Soltero, R. (2005). Oral Protein and Peptide Drug Delivery. Drug Delivery, John Wiley & Sons, Inc.**:** 189-200.

Torres-Lugo, M. and N. A. Peppas (2000). "Transmucosal delivery systems for calcitonin: a review." Biomaterials **21**(12): 1191-1196.

Yu, L. X., E. Lipka, J. R. Crison and G. L. Amidon (1996). "Transport approaches to the biopharmaceutical design of oral drug delivery systems: prediction of intestinal absorption." Advanced Drug Delivery Reviews **19**(3): 359-376.

CHAPTER 2

Modeling of Drug Release from a Polymer Matrix System

Abstract

A drug release model is proposed to predict the behavior of an oral drug tablet when it is taken through the gastrointestinal (GI) tract. The model predicts the rate of change of tablet dimensions. The effect of polymer degradation rate on the tablet dissolution time and drug release kinetics was analyzed. The total tablet dissolution time decreased with increase in the polymer degradation rate constant (k_d). A power law model was fit to describe the relationship between tablet dissolution time and k_d . The model predicted initial burst release of the drug followed by a constant release. The time of burst release and the amount of drug undergoing burst release decreased with increase in k_d value.

Keywords: drug release model, drug diffusion, polymer matrix swelling, polymer dissolution, release kinetics

2.1 Problem Description

In this chapter, we propose a model to predict the release behavior of an oral drug from the solid drug tablet inside the GI tract of the human body. The model should be able to predict the amount of drug released into various regions of the GI tract. The model will provide insights on the various mass transport and chemical processes involved in drug delivery, as well as the effect of tablet design, geometry and drug loading on the release mechanism involved. The release behavior of a drug determines the pharmacokinetic behavior of the drug in the plasma. The proposed model will be a prelude to the development of the pharmacokinetic model discussed in chapter 3.

To address the problem as stated above, we employ a mechanistic modeling approach to construct the model. Mechanistic modeling takes into account the physical mechanisms that influence the process to develop the model. Therefore, it helps in better understanding of the processes which are difficult to explain experimentally. In this work, we developed a drug release

model based on the dissolution model proposed by Narasimhan and Peppas (Narasimhan and Peppas 1997, Brazel and Peppas 2000, Narasimhan 2001).

2.2 Background and Literature

There has been a significant change in the performance of drug delivery systems in the last 100 years. The delivery systems have evolved from simple pills to sustained/ controlled release and sophisticated programmable delivery systems (Grassi and Grassi 2005). Uncontrolled and immediate drug release kinetics is the characteristic of traditional delivery systems. This mainly led to abrupt increase in drug concentration on body tissues crossing the toxic threshold and then falling off below the minimum effective therapeutic level. The development of controlled drug delivery systems has greatly helped in solving this issue, and in maintaining the drug concentration in the blood and other tissues at a desired level for a longer time. In a controlled drug release system, a burst of drug is initially released to rapidly obtain the drug effective therapeutic concentration and then follows a controlled release behavior to maintain the drug concentration at the desired level. The development of controlled release systems has greatly improved patient compliance and drug effectiveness. They helped in reducing the dosage administration frequency and prevent side effects. Thus the design and development of controlled release systems has become a key issue in modern day research. Many engineers and pharmacists have come together to design and develop effective delivery systems. The use of mathematical modeling in this process is a very useful approach. It helps in predicting the drug release kinetics from a controlled release system and helps in further improving the design and development process.

The most common strategy to obtain a controlled drug release is by embedding a drug in a polymer matrix. The polymer used for this purpose can be a hydrophobic or a hydrophilic matrix depending on the nature of the drug. Some of the hydrophobic polymers include wax, polyethylene, polypropylene and ethylcellulose. Some of the hydrophilic polymers are hydroxypropylcellulose, hydroxypropylmethylcellulose, methylcellulose, sodium carboxymehylcellulose, alginates and scleroglucan (Finch 1995).

The drug release mechanism from a polymer matrix can be categorized based on three different processes, which are:

1) Drug diffusion from a non-biodegradable polymer (diffusion-controlled system)

2) Drug diffusion from a swellable polymer (swelling-controlled system)
3) Drug release due to polymer degradation and erosion (erosion-controlled system)

All the above-mentioned processes have a diffusion component. For a non-biodegradable polymer matrix, drug release is due to the concentration gradient caused by diffusion or polymer swelling. For a biodegradable polymer matrix, release is either controlled by polymer chain disentanglement which leads to matrix erosion or by diffusion when the erosion process is slow (Leong and Langer 1988, Fu and Kao 2010). There are several mathematical models proposed for drug release from tablets of different geometries as discussed above (Cabrera and Grau 2007, Siepmann and Siepmann 2008).

2.2.1 Diffusion-controlled systems

Diffusion-controlled systems are generally modeled using Fick's law of diffusion with appropriate boundary conditions. For example, the diffusion from a spherical micro particle is given by Eq. 1.

$$\frac{\partial C}{\partial t} = \frac{1}{r^2}\frac{\partial}{\partial r}\left[Dr^2 \frac{\partial C}{\partial r} \right] \tag{1}$$

where, the diffusion is assumed to be in the radial direction, D and C are the diffusion coefficient and the concentration of the drug in the polymer matrix. The boundary conditions are based on the mass transfer processes at the surface and the bulk surrounding the micro particle.

A reservoir system is a very good example of a diffusion-controlled system. In that system, the assumption is that the drug is confined in a spherical shell of inner radius (R_i) and outer radius (R_o) and the diffusion of drug takes place through the shell thickness of ($R_o - R_i$). The Fick's law defined in Eq. 1 is solved, with boundary conditions defined as in Eq. 2,

$$\begin{aligned} r &= R_i \qquad & C &= C_r \\ r &= R_o \qquad & C &= 0 \end{aligned} \tag{2}$$

where, the concentration of drug at the inner radius (R_i) is kept at a constant reservoir drug concentration (C_r) and the concentration at the outer radius (R_o) is assumed to be zero, since the surrounding bulk volume is large and there is no other mass transfer limitation (Arifin et al. 2006).

2.2.2 Matrix systems

In a typical matrix system, the drug is uniformly distributed within a non-biodegradable polymer matrix. The mechanism of drug release from a matrix system is dependent on the initial drug loading of the tablet and the solubility of drug in the polymer matrix. When the initial drug loading is lower than the drug solubility, the drug is assumed to be uniformly distributed in the polymer matrix. These kinds of systems are known as dissolved drug systems. In contrast, in a dispersed drug system the initial drug loading is higher than the drug solubility inside the polymer system. Here the system is divided into two regions namely, the non-diffusing region, where the undissolved drug is at the initial drug loading concentration and the diffusion region where the diffusion of the dissolved drug takes place. The drug diffusion through the diffusion region leads to shrinking of the non-diffusing region. Thus the boundary between the non-diffusing and the diffusing region continuously moves making it a moving-boundary problem (Arifin et al. 2006, Wu and Brazel 2008).

2.2.3 Swelling-controlled release systems

Swelling-controlled systems generally consist of a uniformly distributed drug within a biodegradable, swellable polymer. These swellable polymers are hydrophilic in nature so that when in contact with water, the latter is absorbed into the polymer, thereby swelling the polymer matrix. The swelling helps in loosening the polymer entanglement leading to disentanglement of the polymer. The polymer matrix swelling leads to the formation of a rubbery region, where there is better drug mobility due to lower polymer concentration. This helps in enhancing the release characteristics of the drug which is not only dependent on the diffusion rate of the drug but also on the polymer disentanglement and dissolution processes. A schematic showing the effect of polymer concentration on the polymer disentanglement rate is shown in Fig. 1.

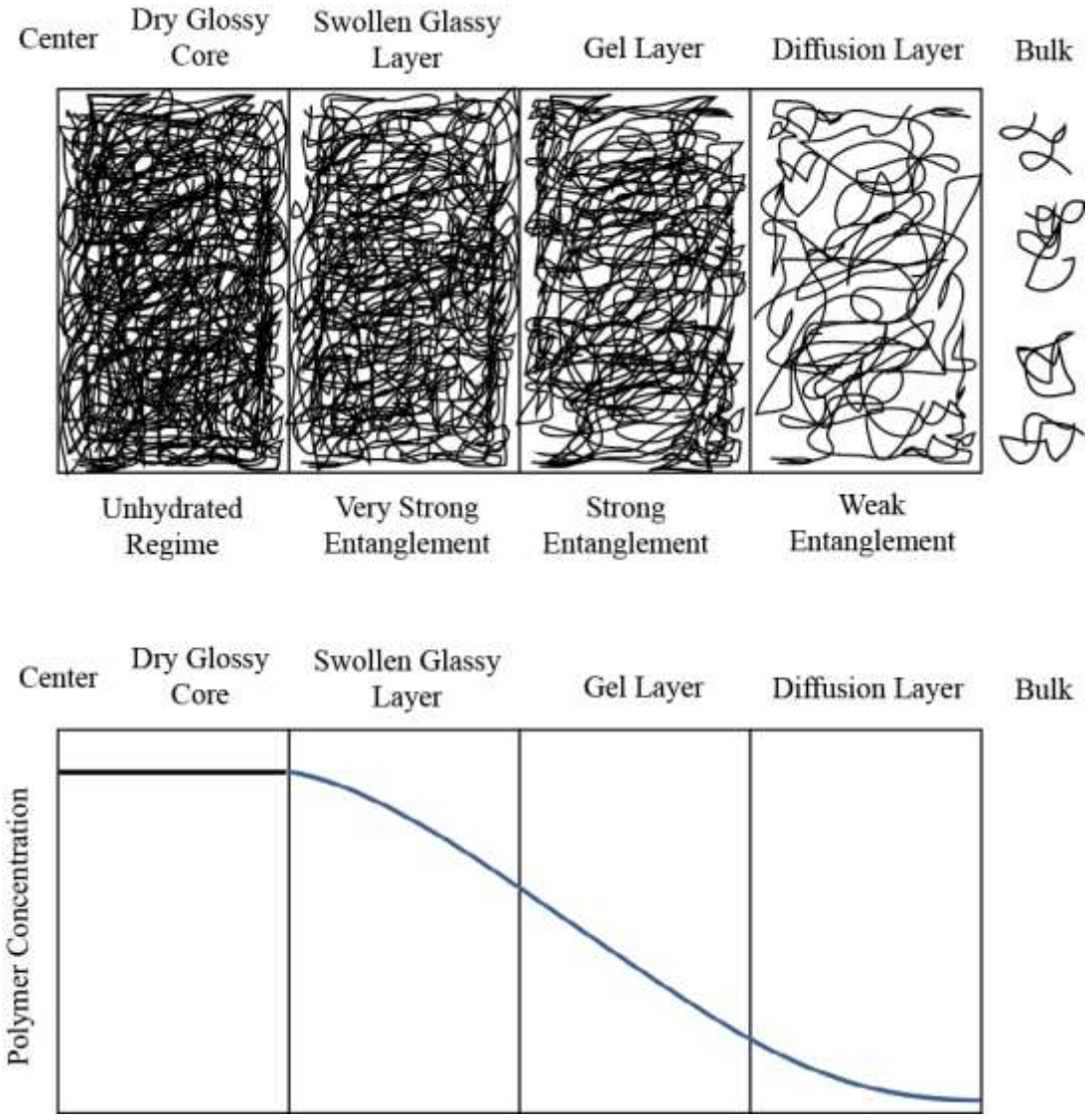

Figure 1: Schematic of polymer matrix disentanglement level as a function of polymer concentration in a swelling-controlled release system (redrawn from (Ju et al. 1995))

As the polymer absorbs water, there is a change in concentration of the polymer in the matrix. The polymer concentration is very high in the dry glassy core. The water diffusion in the swollen glassy layer creates a more mobile network, but restricted by very strong chain entanglement. In the gel layer, the concentrations of water and polymer become comparable with some reduction in the chain entanglement. Ultimately, the diffusion layer becomes very rich in water concentration, leading to weak chain entanglement and the polymer starts to disentangle and dissolve at the interface (Arifin et al. 2006).

2.2.4 Literature on modeling of tablet swelling and dissolution

The modeling of drug release from polymer matrices can greatly improve the design and understanding of delivery systems. Availability of a reliable mathematical model could complement/augment the resource-consuming trial and-error procedures usually followed in the manufacture of drug delivery systems. Several modeling approaches are presented in the literature; those that are relevant to this work are described below.

Modeling drug release behavior by swelling and dissolving in polymer matrices described in the literature considers either polymer slabs or spheres (Mallapragada and Peppas 1997, Narasimhan and Peppas 1997); very few models consider the cylindrical geometry of tablets (Siepmann et al. 1999, Siepmann et al. 1999, Siepmann et al. 2000, Siepmann and Peppas 2000, Siepmann et al. 2002). Tablet models tend to employ simplified one-dimensional transport assumptions (Ju et al. 1995, Kiil and Dam-Johansen 2003).

The model by Borquist et al. (Borgquist et al. 2006) considered drug release from a swelling and dissolving cylindrical polymeric tablet and can predict drug release from formulations containing soluble as well as poorly soluble drugs. The mass transfer rate includes the contributions from diffusion as well as swelling (diffusion induced convection). The transformation from solid to gel phase is assumed to be limited by the rate of penetrant transport into the solid phase, corresponding to a critical penetrant concentration. At the gel–solvent interface, it is assumed that equilibrium exists between the hydrodynamic forces and polymer entanglement. This implies that the surface polymer concentration reaches a constant value after the initial phase, and that this equilibrium exists for the rest of the dissolution process. Hence, the initial polymer dissolution rate is zero, until the entanglement strength has been reduced by the increased penetrant concentration. The model was used to study the influence of the drug diffusion coefficient, the drug solubility and the initial drug loading on the drug release profile. The model presented in this paper can simulate the drug and polymer release from swelling and dissolving polymer tablet. The model was verified against drug release and polymer dissolution data for the slightly soluble drug Methyl Paraben and the soluble drug Saligenin, showing good agreements in both cases. The drug diffusion coefficient was fitted to data, and the values obtained were considered to be accurate, thus confirming the reliability of the model.

The immersion of pure Hydroxypropylmethylcellulose (HPMC) tablets in water and their water uptake, swelling and the erosion during immersion were investigated in drug-free and drug-loaded systems (Chirico et al. 2007). A novel approach by image analysis to measure polymer and water masses during hydration was described. It was found that that the model consisting in the transient mass balance, accounting for water diffusion, diffusivity change due to hydration, swelling and erosion, was able to reproduce experimental data.

In Kill et al. (Kiil and Dam-Johansen 2003), a detailed mathematical model capable of estimating radial front movements, transient drug fluxes, and cumulative fractional drug release behaviors from a high-viscosity HPMC matrix was presented. Simulations produced with the model were compared to the measurements reported by Bettini et al. (Bettini et al. 1994, Bettini et al. 2001) and Colombo et al. (Colombo et al. 1999). However the model could not describe the continued swelling of the matrix, subsequent to the disappearance of the swelling front. Models of drug release from hydrogel based matrices of HPMC were presented by Lamberti et al. (Lamberti et al. 2011).

The effect of polymer relaxation constant on water uptake and drug release was shown in a mathematical model for the simulation of water uptake by and drug release from homogeneous poly-(vinyl alcohol) hydrogel (Wu and Brazel 2008). Another work showed that swelling of the hydrogel carrier begins from the edge to the center. At the beginning the drug release is by anomalous transport followed by Fickian diffusion when the swelling of the hydrogel approaches to a new equilibrium state (Zhang and Jia 2012).

A mathematical model was developed to describe the transport phenomena of a water-soluble small molecular drug (caffeine) from highly swellable and dissoluble polyethylene oxide (PEO) cylindrical tablets (Wu et al. 2005).The work considered several important aspects in drug release kinetics such as swelling of the hydrophilic matrix and water penetration, three-dimensional and concentration-dependent diffusion of drug and water, and polymer dissolution. In vitro study of swelling, dissolution behavior of PEOs with different molecular weights and drug release were carried out. When compared with experimental results, this theoretical model agreed with the water uptake, dimensional change and polymer dissolution profiles very well for pure PEO tablets with two different molecular weights. Drug release profiles using this model were predicted with a very good agreement with experimental data at different initial loadings. The

overall drug release process was highly dependent on the matrix swelling, drug and water diffusion, polymer dissolution and initial dimensions of the tablets. When their influences on drug release kinetics from PEO with two different molecular weights were investigated, it was found that swelling was the dominant factor in drug release kinetics for higher molecular weight of PEO ($Mw=8\times10^6$) while both swelling and dissolution were important to caffeine release for lower molecular weight PEO ($Mw=4\times10^6$). It was found that when initial drug loading increases, polymer dissolution became more and more important in the release process. Besides swelling and dissolution properties of polymer, the ratio of surface area to volume and the aspect ratio of initial tablets were found to be influential in the overall release profile.

A novel method was developed by Kimber et. al. (Kimber et al. 2012) to simulate polymer swelling and dissolution by combining a discrete element method (DEM) with inter-particle mass transfer. The method was applied to simulate the behavior of cylindrical tablets. The model considered the effects of several parameters such as the concentration-dependent diffusion constant of water in polymer, dissolution rate constant of polymer and the disentanglement threshold of polymer on the tablet behavior. A new drug component was included in the DEM method and the effects of drug distribution, maximum swelling ratio of polymer and drug-polymer diffusivity on the tablet behavior were studied (Kimber et al. 2013). The model was able to explicitly define the drug distribution in the tablet. The model showed that for a homogeneously dispersed drug, the release was slow over time, but for a heterogeneous distribution, there was an initial burst release followed by a slower release.

2.3 Dissolution Model

The Dissolution Model (Narasimhan and Peppas 1997, Brazel and Peppas 2000, Narasimhan 2001) explains the release of a water soluble, crystalline drug enclosed within a swellable, hydrophilic glassy polymer, placed in contact with water or a biological fluid. It is a moving boundary problem formulated using a system of partial differential equations (PDE's) and ordinary differential equations (ODE's) which describe the (i) diffusion of water into the system; (ii) diffusion of drug out of the system; (iii) polymer chain disentanglement through the boundary layer and (iv) the left and right moving boundaries. All the diffusion processes take place along the tablet thickness indicated by X (Fig. 2) making it a 1-D problem in space.

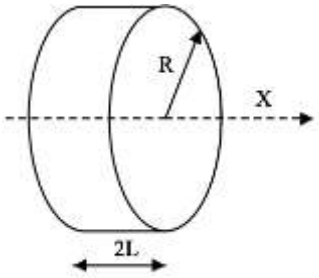

Figure 2: Schematic of the drug tablet of initial radius R and initial thickness 2L

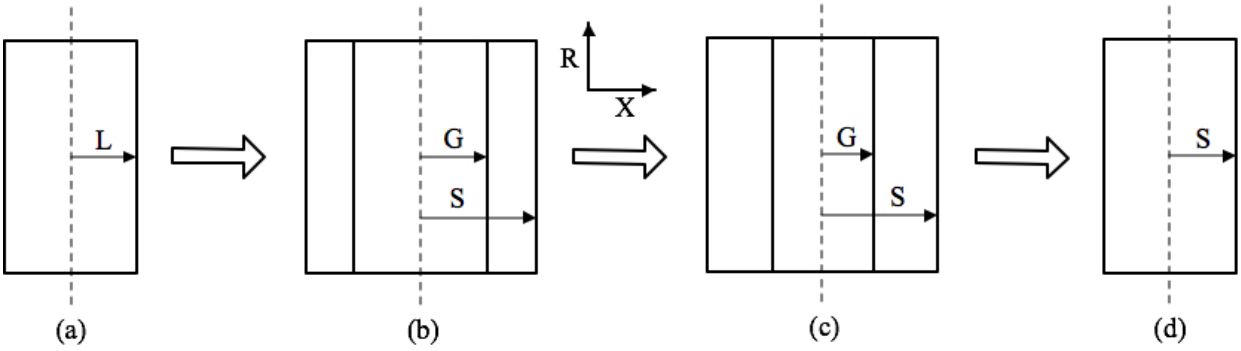

Figure 3: One-dimensional solvent diffusion and polymer dissolution process (Narasimhan and Peppas 1997)

In this model, when water comes in contact with the glassy polymer of initial thickness $2L$ (Fig. 3a), the polymer starts to swell and two distinct fronts are formed: the swelling interface at position G, and the polymer-water interface at position S (Fig. 3b). Initially, the front G moves inwards since the drug starts diffusing out of the gel layer and the front S moves outwards due to polymer swelling. When the concentration of water inside the polymer gel layer exceeds a critical value, v_1^*, polymer disentanglement begins and S starts to diminish. Hence, during the latter stage of the dissolution process, both G and S move towards the center of the tablet (Fig. 3c). The process continues, till the glassy core disappears and only the front S exists, which continues to diminish till the entire polymer is dissolved (Fig. 3d). A detailed description of the various equations used in the modeling of the dissolution model is given below.

Water transport into the polymer matrix is expressed using Fick's law as:

$$\frac{\partial v_1}{\partial t} = \frac{\partial}{\partial x}\left(D_1 \frac{\partial v_1}{\partial x} \right) \qquad G < x < S \tag{3}$$

where, v_1 is the volume fraction of water in the swollen polymer, D_1 is the diffusion coefficient of water in polymer and *x* is dimension along the tablet thickness. Eq. 3 is valid in the slab region between G and S (see Fig. 3b and Fig. 3c). The diffusion of drug out of the polymer is given by:

$$\frac{\partial v_d}{\partial t} = \frac{\partial}{\partial x}\left(D_d \frac{\partial v_d}{\partial x} \right) \qquad G < x < S \tag{4}$$

Here, v_d is the volume fraction of drug in the swollen polymer and D_d is the drug diffusion coefficient in the polymer. Eq. 3 and 4 describe the overall swelling/dissolution/release process and are solved with the following initial conditions

$$v_1(x,0) = 0 \qquad v_d(x,0) = v_{d0} \tag{5}$$

The first boundary condition for Eq. 3 and 4 is at the glass-rubbery interface G, given by:

$$v_1(G,t) = v_1^* \qquad v_d(G,t) = v_d^* \tag{6}$$

The critical volume fractions of water and drug at the interface, G, are v_1^* and v_d^*, respectively. Here v_1^* and v_d^* are functions of the thermodynamic conditions of glassy-rubbery transition, given by:

$$v_1^* = 1 - v_2^* - v_d^* \tag{7}$$

$$v_2^* = \frac{\frac{1}{\rho_2}}{\frac{1}{\rho_2} + \frac{(T_g - T)}{(\beta / \alpha_f)} \frac{1}{\rho_1} + \frac{1}{\rho_d}} \tag{8}$$

$$v_d^* = \frac{\frac{1}{\rho_d}}{\frac{1}{\rho_2} + \frac{(T_g - T)}{(\beta / \alpha_f)} \frac{1}{\rho_1} + \frac{1}{\rho_d}} \tag{9}$$

where, T_g is the glass transition temperature, T is the experimental temperature, α_f is the linear expansion coefficient of the polymer, β is the expansion coefficient contribution of water to

polymer, ρ_1 is the water density, ρ_2 is the polymer density and ρ_d is the drug density. The second boundary condition for Eq. 3 and 4 is at the rubbery-solvent interface, S, given by:

$$v_1(S,t) = v_{1,eq} \qquad v_d(S,t) = v_{d,eq} \tag{10}$$

where $v_{1,eq}$ and $v_{d,eq}$ are the equilibrium volume fractions of water and drug, estimated using the Flory-Rehner equation (Paul J. Flory 1943).

A mass balance at the interface G gives the moving boundary condition at the glassy-rubbery interface:

$$(v_1 + v_d)\big|_{(G,t)} \frac{dG}{dt} = -\left(D_1 \frac{\partial v_1}{\partial x} \right)\Bigg|_{(G,t)} - \left(D_d \frac{\partial v_d}{\partial x} \right)\Bigg|_{(G,t)} \tag{11}$$

The initial condition for Eq. 11 is given by, $G(0) = L$, where L is the initial half thickness of the tablet. The values of v_1 and v_d at interface G are given by Eq. 6. A mass balance at the interface S gives the moving boundary condition at the water-rubbery interface:

$$(v_1 + v_d)\big|_{(S,t)} \frac{dS}{dt} = -\left(D_1 v_1 \frac{\partial v_1}{\partial x} \right)\Bigg|_{(S,t)} - \left(D_d v_d \frac{\partial v_d}{\partial x} \right)\Bigg|_{(S,t)} - \left(D_p \frac{\partial v_2}{\partial x} \right)\Bigg|_{(S,t)} \tag{12}$$

The initial condition for Eq. 12 is given by, $S(0) = L$. The values of v_1 and v_d at interface S are given by Eq. 10.

As the polymer chains disentangle, they move out of the gel layer through a diffusion boundary layer (semi-dilute regime) of thickness δ_b. The polymer chain transport through this boundary layer is given by:

$$\frac{\partial v_2}{\partial t} = \frac{\partial}{\partial x}\left(D_p \frac{\partial v_2}{\partial x} \right) - \left(\frac{dS}{dt} \right) \frac{\partial v_d}{\partial x} \qquad S < x < S + \delta_b \tag{13}$$

The initial and boundary conditions to Eq. 13 are given by:

$$v_2(x,0) = 0 \tag{14}$$

$$v_2(S+\delta_b, t) = 0 \tag{15}$$

$$-D_p \left.\frac{\partial v_2}{\partial x}\right|_{(S^+,t)} = 0 \qquad 0 < t < t_{rept} \tag{16}$$

$$-D_p \left.\frac{\partial v_2}{\partial x}\right|_{(S^+,t)} = k_d \qquad t_{rept} \le t < t_c \tag{17}$$

$$v_2\big|_{(S^+,t)} = v_{2,eq} \qquad t_c \le t \tag{18}$$

where, t_{rept} is the reptation time defined as the minimum time taken by the polymer chains to disentangle, k_d is the polymer chain disentanglement rate and t_c is the critical time at which polymer concentration in the boundary layer reaches an equilibrium value, $v_{2,eq}$.

2.4 Solution Strategy

We developed a step by step algorithm to solve the dissolution model equations as described below:

Step 0: Initialization

Step 1: Let $S = (1+\varepsilon)G$, where ε is a small positive number. Solve the approximated versions of Eq. 11 and 12 simultaneously given by:

$$(v_1^* + v_d^*)\frac{dG}{dt} = -\frac{D_1}{(S-G)}\left[v_{1,eq} - v_1^*\right] - \frac{D_d}{(S-G)}\left[v_{d,eq} - v_d^*\right] \tag{19}$$

$$(v_{1,eq} + v_{d,eq})\frac{dS}{dt} = \frac{v_{1,eq}D_1}{(S-G)}\left[v_{1,eq} - v_1^*\right] + \frac{v_{d,eq}D_d}{(S-G)}\left[v_{d,eq} - v_d^*\right] - k_d \tag{20}$$

Obtain the new G and S values

Step 2: Solve Eq. 3, 4 and 13 using the new G and S values obtained from Step 1

Step 3: Solve Eq. 11 and 12 simultaneously (check for $G > 0$ during every iteration, because when $G = 0$, we have to solve only Eq. 12)

Step 4: If $S > 0$, go to Step 2

2.5 Results and discussions

We successfully solved the dissolution model using the modified strategy. The solution is divided into two parts. The first part of the solution includes solving for both G and S until the value of G (thickness of the solid drug tablet) becomes zero. The second part involves solving only for S (thickness of the swollen polymer) after G is zero. Here the contribution of water diffusion to the swelling of the polymer is negligible, only including the drug diffusion and the polymer disentanglement terms resulting in diminishing of S.

We first studied the effect of polymer disentanglement rate constant (k_d) on the rate at which the tablet dimensions G and S vary inside the body. The value of k_d has been varied by different factors and plotted curves showing the rate of change of G and S with time. Fig. 4, 5, 6 and 7 show the rate of change of G and S with increasing k_d values of 0.012, 0.024, 0.036 and 0.048 mm/min, respectively.

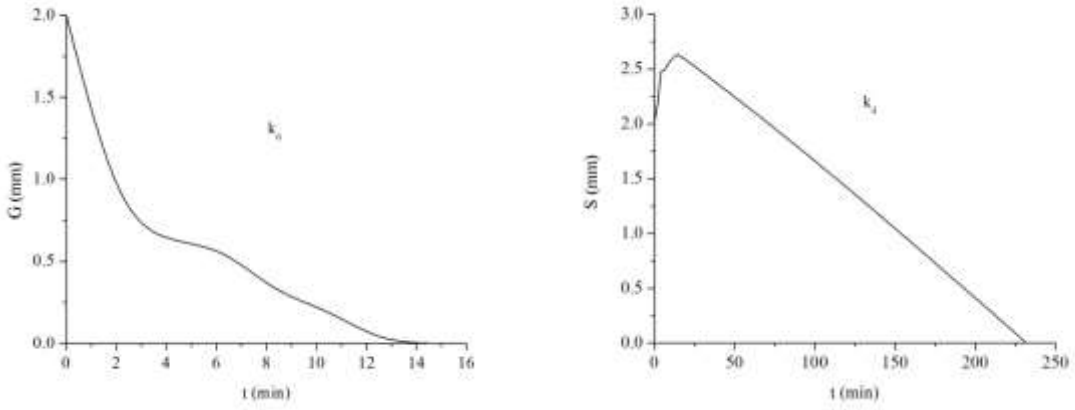

Figure 4: Rate of change in tablet interface dimensions G and S for k_d value of 0.012 mm/min

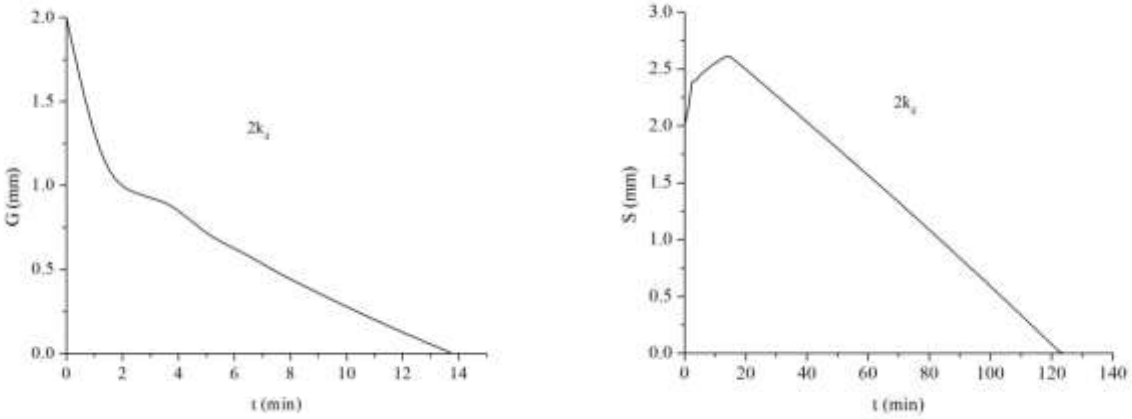

Figure 5: Rate of change in tablet interface dimensions G and S for k_d value of 0.024 mm/min

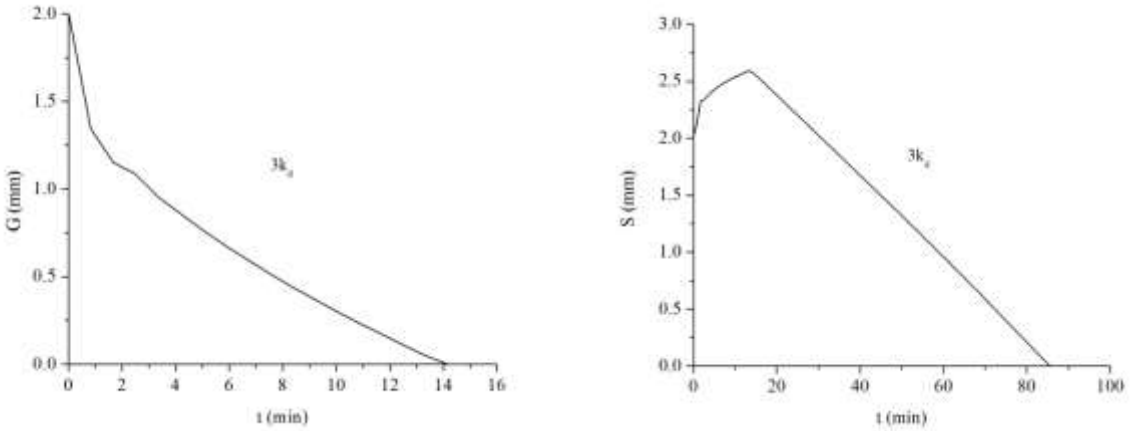

Figure 6: Rate of change in tablet interface dimensions G and S for k_d value of 0.036 mm/min

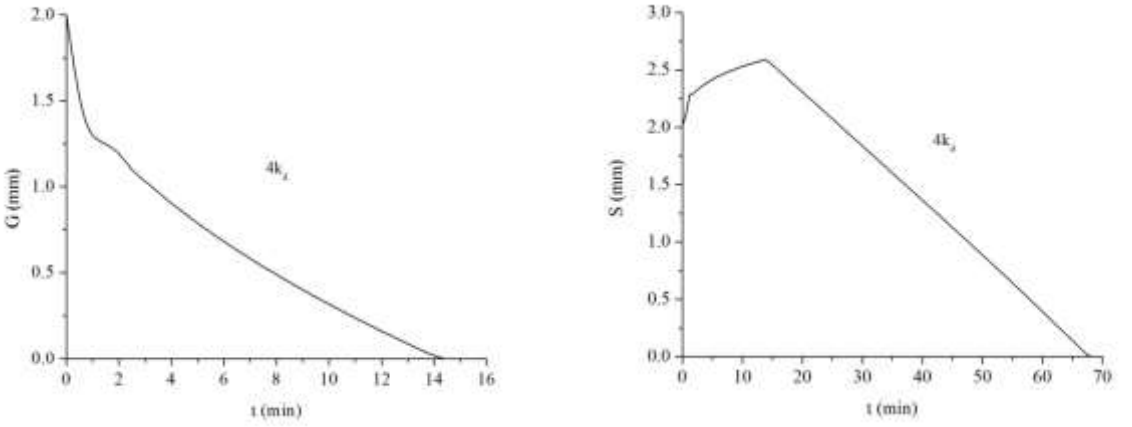

Figure 7: Rate of change in tablet interface dimensions G and S for k_d value of 0.048 mm/min

Here G is a measure of the solid tablet thickness and S is a measure of the total tablet thickness along with the swollen polymer. An expected trend is observed both in the case of G and S as discussed in section 2.3. The solid tablet thickness (G) decreases with time as the tablet traverses through the GI tract and comes into contact with the bodily fluid. This is due to the continuous diffusion of drug out of the solid tablet and the conversion of solid polymer in the tablet to rubbery (swollen) form. The total tablet thickness (S) initially increases with time because of the polymer swelling and then eventually falls after the concentration of polymer in the gel layer reaches the critical limit and the polymer starts degrading from the tablet.

We observed that, in each of the profiles containing a change in G, there is initial time period of fast decrease rate in the value of G followed by a relatively slower decrease rate. However, with increase in the k_d value, there is a noticeable drop in the time period for rapid decrease of G. This initial rapid fall in the value of G can be attributed to the initial burst release of the drug from the tablet. With increasing k_d value, there is a much faster burst release, leading to decrease in the time for burst release. The change in k_d value, did not have much impact on the total time taken for the solid part of the tablet to dissolve. This is because the dissolution of the solid drug tablet is independent of the polymer disentanglement rate. We observe that with increase in the k_d value, there is a significant drop in the total time for dissolution of the drug tablet including the swollen gel layer (looking at the trends for change of S), which is expected.

We have plotted the drug release profiles for different values of k_d, i.e., the cumulative (%) mass of drug released with time respect to the time of release (t) as shown in Fig. 8. The total amount of drug released in each of these profiles is 400 mg. Each of the release profiles showed an initial burst release followed by a constant release. This can be clearly observed in Fig. 8, where each of the curves has a constant slope after a certain initial burst release, indicating a constant rate of drug release.

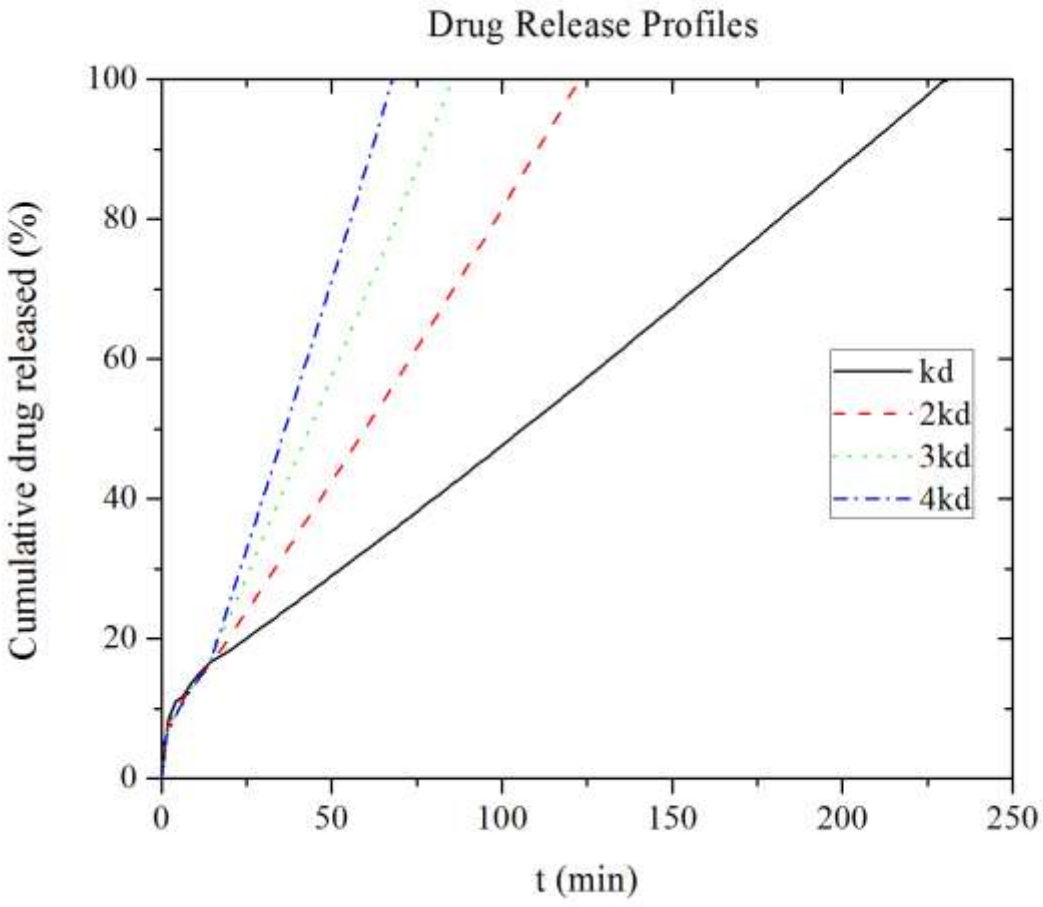

Figure 8: Effect of polymer degradation rate constants (k_d) on cumulative (%) drug released. The total amount of drug released for each of the k_d values is a constant of 400 mg

We have plotted the rate of drug release (dM/dt) for different values of k_d to more clearly observe the burst effect followed by the constant release (Fig. 9). We observed that, the burst effect is faster with increase in the k_d value i.e., the time taken for initial burst release is lower for higher k_d values. This could indicate that the burst effects can be controlled by varying the k_d value accordingly. The area under the curve values for each of the curves in Fig. 9 is a constant value of 400 mg, indicating that a constant amount of drug is released for different k_d values.

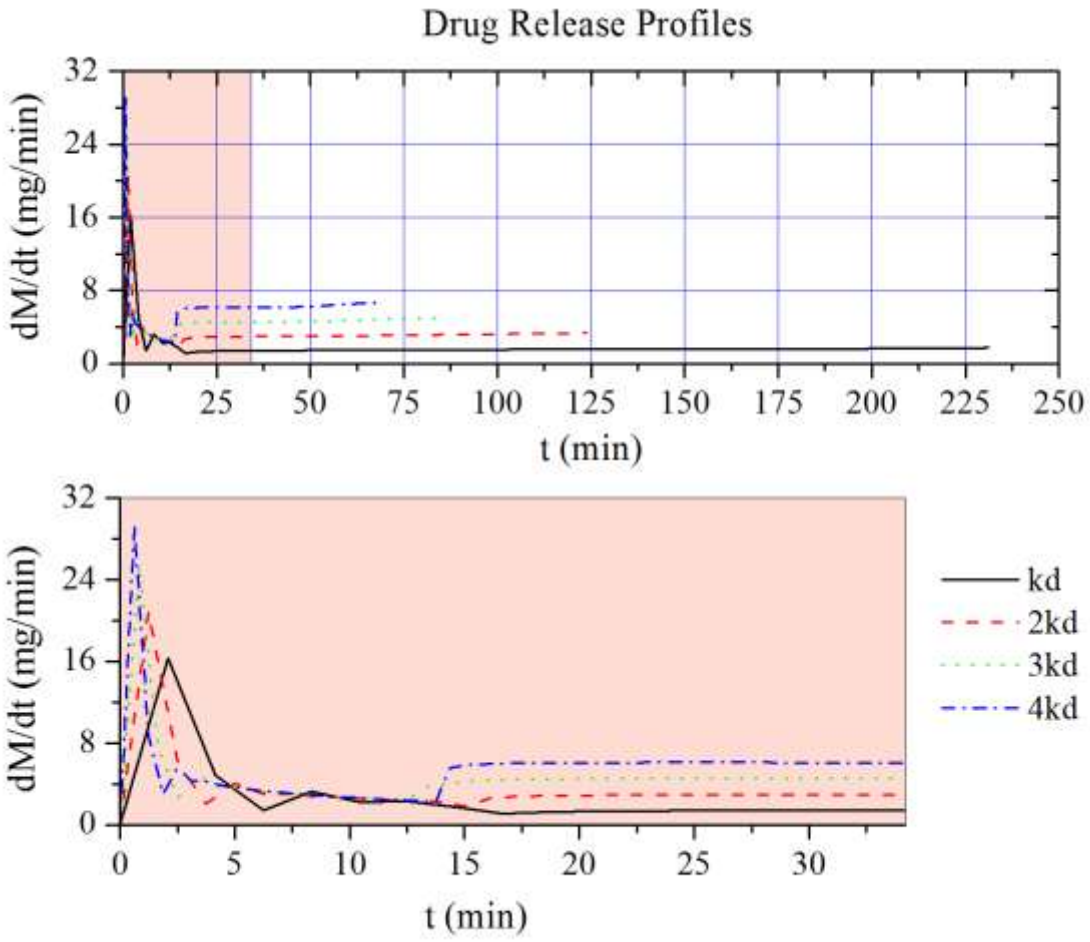

Figure 9: Effect of polymer degradation rate constants (k_d) on drug release rate (dM/dt)

We studied the effect of polymer degradation rate constant (k_d) on the total dissolution time of the tablet. Table 1 shows the various tablet dissolution times obtained when the value of k_d is changed by an increasing factor from 1 to 10. As expected, with increase in the k_d value, there was a drop in the total dissolution time. This is because, as the value of k_d increases, the polymer in the tablet dissolves at a much faster rate leading to a drop in the total dissolution time. We observed a dependence of the total degradation time on k_d followed a smooth trend (Fig. 10). Hence we tried to a fit a classical Freundlich equation to the data obtained in Table 1.

Table 1: Effect of polymer degradation rate on the tablet dissolution time

Polymer degradation rate constant (k_d) (mm/min)	Tablet dissolution time (min)
0.012	231.2500
0.024	123.7500
0.036	85.6240
0.048	68.1250
0.06	47.5000
0.072	40.0000
0.084	34.3330
0.096	30.2500
0.108	27.0830
0.12	24.5000

The classical Freundlich equation (power law) is of the form given in Eq. 21.

$$y = ax^b \tag{21}$$

where, y is the total tablet dissolution time in our case and x is the polymer degradation rate constant (k_d), a and b are the parameters that are estimated to fit the data. The data analysis and curve fitting was done in OriginPro 8 software. The results are given below.

Table 2: Statistics of the Freundlich curve fitting and parameter values

Number of Points		10
Degrees of Freedom		8
Residual Sum of Squares		88.75276
Adj. R-Square		0.99732
Fit Status		Succeeded (100)
Parameter	Value	Error
a	3.52103	0.25055
b	-0.94796	0.01764

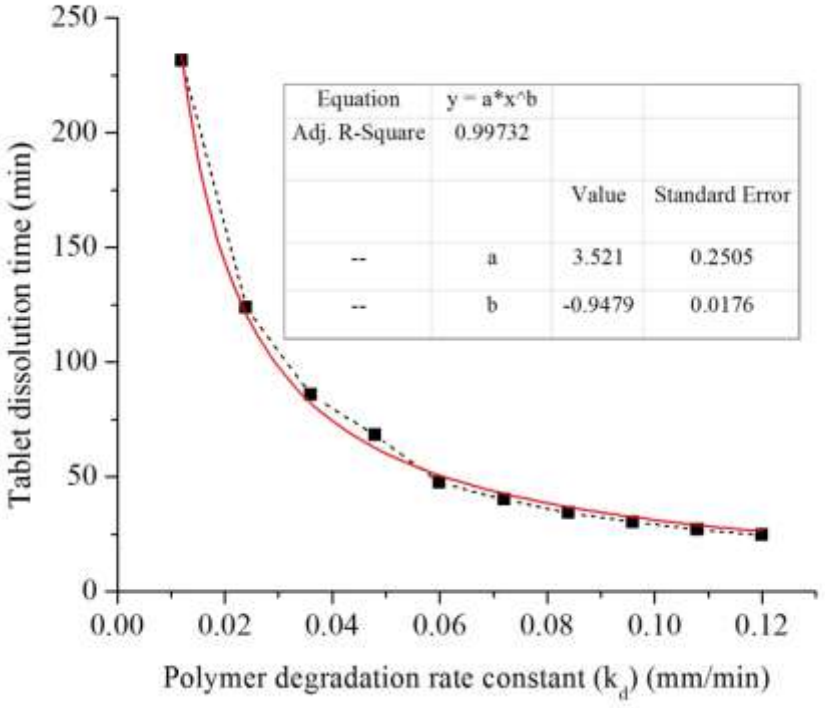

Figure 10: Effect of polymer degradation rate constant (k_d) on the tablet dissolution time

The classical Freundlich equation was an excellent fit to the data with an R^2 value of 0.99732 as shown in Table 2. This correlation between the tablet dissolution time and polymer degradation rate constant is very useful, since we will be able to estimate the dissolution times of a tablet without experimental data. We will be able to determine the type of polymer required to make the tablet in order to obtain a desired tablet dissolution time.

2.6 Conclusions

We successfully developed a drug release model by modifying a dissolution model proposed by Narasimhan and Peppas (Narasimhan and Peppas 1997). The developed model can be used to predict the release behavior of an oral drug from the solid drug tablet inside the GI tract of the body. A solution strategy is proposed to solve the moving boundary problem encountered in solving the drug release model. Using this model, we studied the effects of model parameters such as the polymer degradation rate constant (k_d), on the tablet dissolution rate. We specifically studied the effect on the thickness of the solid tablet (G) as well as the total tablet including the swollen gel layer (S). The value of G continuously decreased with time, while the value of S

initially increased and then decreased as expected. The profiles indicated a burst release during the initial stages of the release process.

We studied the effect of k_d on the total tablet dissolution time. There was a significant drop in the tablet dissolution time with increase in the k_d value. We fit a classical Freundlich equation to estimate the tablet dissolution time with change in k_d value. The obtained correlation could be very beneficial in estimating the tablet dissolution time without the need of any experimentation, as well as to estimate the k_d value for a desired tablet dissolution time. The model predicted the initial burst release of the drug followed by a constant release.

The solution which we have employed in this model to solve the moving boundary problem is an approximate solution. There is need of a more improved and continuous solution to the moving boundary problem which will help us to make more accurate predictions. One more major assumption is our model is that the drug release takes place only along the tablet thickness (axial direction). Hence it is a 1-D model. A model considering the release in all the directions is desired (a 2-D model). The model solution strategy employed in this paper is a discreet approach, where the time and space are divided in small fractions and the model is solved in each of these fractions. We need a much better solution which is more continuous and less discreet and give a more accurate representation of the drug release process.

The developed model will provide insights into the various mass transport, diffusion and degradation processes involved in the mechanism of drug release from a swelling polymer matrix. This model will greatly aid in simulating some of the in vitro dissolution tests and reduce the number of experiments, and hence reduce the time and effort involved.

2.7 Nomenclature

L	Initial half thickness of the drug tablet
v_1	Volume fraction of water in the swollen polymer
v_d	Volume fraction of drug in the swollen polymer
v_1^*	Critical volume fraction of water at the interface
v_d^*	Critical volume fraction of drug at the interface
$v_{1,eq}$	Equilibrium volume fraction of water
$v_{d,eq}$	Equilibrium volume fraction of drug
v_{d0}	Initial volume fraction of the drug
T_g	Glass transition temperature
T	Experimental temperature
α_f	Linear expansion coefficient of the polymer
β	Expansion coefficient contribution of water to polymer
ρ_2	Polymer density
ρ_d	Drug density
D_1	Diffusion coefficient of water in polymer
D_d	Diffusion coefficient of drug in polymer
k_d	Polymer chain disentanglement rate

2.8 References

Arifin, D. Y., L. Y. Lee and C.-H. Wang (2006). Mathematical modeling and simulation of drug release from microspheres: Implications to drug delivery systems.

Bettini, R., P. L. Catellani, P. Santi, G. Massimo, N. A. Peppas and P. Colombo (2001). "Translocation of drug particles in HPMC matrix gel layer: effect of drug solubility and influence on release rate." Journal of Controlled Release **70**(3): 383-391.

Bettini, R., P. Colombo, G. Massimo, P. L. Catellani and T. Vitali (1994). "Swelling and drug release in hydrogel matrices: polymer viscosity and matrix porosity effects." European Journal of Pharmaceutical Sciences **2**(3): 213-219.

Borgquist, P., A. Körner, L. Piculell, A. Larsson and A. Axelsson (2006). "A model for the drug release from a polymer matrix tablet—effects of swelling and dissolution." Journal of Controlled Release **113**(3): 216-225.

Brazel, C. S. and N. A. Peppas (2000). "Modeling of drug release from Swellable polymers." European Journal of Pharmaceutics and Biopharmaceutics **49**(1): 47-58.

Cabrera, M. I. and R. J. A. Grau (2007). "A generalized integral method for solving the design equations of dissolution/diffusion-controlled drug release from planar, cylindrical and spherical matrix devices." Journal of Membrane Science **293**(1–2): 1-14.

Chirico, S., A. Dalmoro, G. Lamberti, G. Russo and G. Titomanlio (2007). "Analysis and modeling of swelling and erosion behavior for pure HPMC tablet." Journal of Controlled Release **122**(2): 181-188.

Colombo, P., R. Bettini, P. L. Catellani, P. Santi and N. A. Peppas (1999). "Drug volume fraction profile in the gel phase and drug release kinetics in hydroxypropylmethyl cellulose matrices containing a soluble drug." European Journal of Pharmaceutical Sciences **9**(1): 33-40.

Finch, C. A. (1995). "Treatise on controlled drug delivery—fundamentals, optimisation—applications, edited by Agis Kydonieus. Marcel Dekker Inc., New York, 1992. pp. x+553, price US$155.00. ISBN 0-8247-8519-3." Polymer International **36**(4): 374-374.

Fu, Y. and W. J. Kao (2010). "Drug release kinetics and transport mechanisms of non-degradable and degradable polymeric delivery systems." Expert Opin Drug Deliv **7**(4): 429-444.

Grassi, M. and G. Grassi (2005). "Mathematical modelling and controlled drug delivery: matrix systems." Curr Drug Deliv **2**(1): 97-116.

Ju, R. T., P. R. Nixon and M. V. Patel (1995). "Drug release from hydrophilic matrices. 1. New scaling laws for predicting polymer and drug release based on the polymer disentanglement concentration and the diffusion layer." J Pharm Sci. **84**(12): 1455-1463.

Kiil, S. and K. Dam-Johansen (2003). "Controlled drug delivery from swellable hydroxypropylmethylcellulose matrices: model-based analysis of observed radial front movements." Journal of Controlled Release **90**(1): 1-21.

Kimber, J. A., S. G. Kazarian and F. Štěpánek (2012). "Modelling of pharmaceutical tablet swelling and dissolution using discrete element method." Chemical Engineering Science **69**(1): 394-403.

Kimber, J. A., S. G. Kazarian and F. Štěpánek (2013). "Formulation design space analysis for drug release from swelling polymer tablets." Powder Technology **236**(0): 179-187.

Lamberti, G., I. Galdi and A. A. Barba (2011). "Controlled release from hydrogel-based solid matrices. A model accounting for water up-take, swelling and erosion." International Journal of Pharmaceutics **407**(1–2): 78-86.

Leong, K. W. and R. Langer (1988). "Polymeric controlled drug delivery." Advanced Drug Delivery Reviews **1**(3): 199-233.

Mallapragada, S. K. and N. A. Peppas (1997). "Crystal dissolution-controlled release systems: I. Physical characteristics and modeling analysis." Journal of Controlled Release **45**(1): 87-94.

Narasimhan, B. (2001). "Mathematical models describing polymer dissolution: consequences for drug delivery." Advanced Drug Delivery Reviews **48**(2–3): 195-210.

Narasimhan, B. and N. A. Peppas (1997). "Molecular analysis of drug delivery systems controlled by dissolution of the polymer carrier." Journal of Pharmaceutical Sciences **86**(3): 297-304.

Paul J. Flory, J. R. (1943). "Statistical Mechanics of Cross-Linked Polymer Networks II. Swelling "

Journal of Chemical Physics **11**(11): 521-526.

Siepmann, J., H. Kranz, R. Bodmeier and N. A. Peppas (1999). "HPMC-Matrices for Controlled Drug Delivery: A New Model Combining Diffusion, Swelling, and Dissolution Mechanisms and Predicting the Release Kinetics." Pharmaceutical Research **16**(11): 1748-1756.

Siepmann, J., H. Kranz, N. A. Peppas and R. Bodmeier (2000). "Calculation of the required size and shape of hydroxypropyl methylcellulose matrices to achieve desired drug release profiles." International Journal of Pharmaceutics **201**(2): 151-164.

Siepmann, J. and N. A. Peppas (2000). "Hydrophilic Matrices for Controlled Drug Delivery: An Improved Mathematical Model to Predict the Resulting Drug Release Kinetics (the "sequential Layer" Model)." Pharmaceutical Research **17**(10): 1290-1298.

Siepmann, J., K. Podual, M. Sriwongjanya, N. A. Peppas and R. Bodmeier (1999). "A new model describing the swelling and drug release kinetics from hydroxypropyl methylcellulose tablets." Journal of Pharmaceutical Sciences **88**(1): 65-72.

Siepmann, J. and F. Siepmann (2008). "Mathematical modeling of drug delivery." International Journal of Pharmaceutics **364**(2): 328-343.

Siepmann, J., A. Streubel and N. A. Peppas (2002). "Understanding and Predicting Drug Delivery from Hydrophilic Matrix Tablets Using the "Sequential Layer" Model." Pharmaceutical Research **19**(3): 306-314.

Wu, L. and C. S. Brazel (2008). "Mathematical Model to Predict Drug Release, Including the Early-Time Burst Effect, from Swellable Homogeneous Hydrogels." Industrial & Engineering Chemistry Research **47**(5): 1518-1526.

Wu, N., L.-S. Wang, D. C.-W. Tan, S. M. Moochhala and Y.-Y. Yang (2005). "Mathematical modeling and in vitro study of controlled drug release via a highly swellable and dissoluble polymer matrix: polyethylene oxide with high molecular weights." Journal of Controlled Release **102**(3): 569-581.

Zhang, Y. and Y. Jia (2012). "Finite Flement Analysis of Controlled Drug Release Based on Biphasic Model of Hydrogel Carrier." Polymers & Polymer Composites **20**(1/2): 5-8.

CHAPTER 3

An advanced pharmacokinetic model for oral drug delivery

Abstract

A drug release mechanism is integrated with a Compartmental Absorption and Transit (CAT) model within a pharmacokinetic framework for predicting orally administered drug release and transport. The developed model is used to evaluate pharmacokinetic parameters such as peak plasma concentration ($C_{\max}$), area under the curve (AUC) and bioavailability. A comparative study has been performed on different cimetidine tablet formulations for which clinical drug profiles are available for model validation. The model predictions are in good agreement with the clinical results. Different scenarios based on the change in average patient body weight (W_p), fraction of drug in the tablet (f_d), tablet radius (R) and their corresponding effects on the model predictions are discussed. The changes in W_p and f_d have a strong effect on the model predictions. Within an optimization framework, the model is able to determine the optimal dimensions of a tablet of fixed dosage for a target plasma profile.

Keywords: oral drug delivery, ACAT model, dissolution model, pharmacokinetic simulation, optimization

3.1 Problem Description

In this chapter, we propose a modeling platform to predict the behavior of an oral drug inside the GI tract of the body. The model should be able to predict the plasma concentration curve for an oral drug and evaluate the pharmacokinetic characteristics such as C_{max}, AUC and bioavailability (Fig. 1). This model will have a great impact on the process of drug discovery and development. It will help in selecting the most favorable drug candidates with desired pharmacokinetic characteristics, thereby reducing the number of experimental trials required for drug design and development.

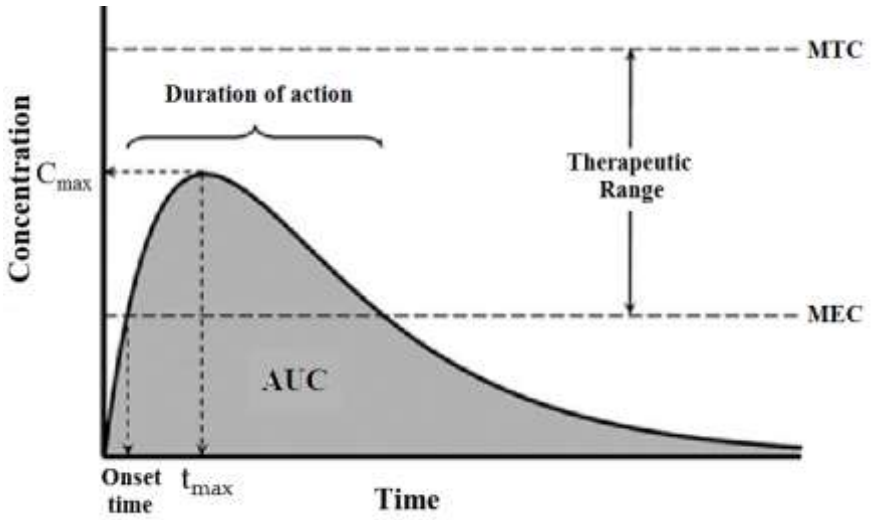

Figure 1: A typical plasma concentration profile and pharmacokinetic characteristics (Mehrotra et al. 2006)

To address the problem as stated above, we employ a semi-empirical modeling approach. In this work, we employ two models in series. The first step is a dissolution model, which describes the mechanism of drug release from the tablet into the system. The second step is an advanced compartmental and transit (ACAT) model which describes the dissolution, absorption, metabolism and transport of the drug in the GI tract into the blood stream.

We have performed a comparative case study using the developed model on three different cimetidine tablet formulations for which clinical drug profiles are available. We investigated three different scenarios, namely using plasma concentration profile, AUC and C_{max} as performance objective functions.

3.2 Background and Literature

The drug discovery process involves the use of considerable resources to analyze the pharmacokinetic properties of the potential drug candidates. Pharmacokinetic modeling aids in optimizing the use of such resources in the *in vivo* testing by predicting the pharmacokinetic behavior of the drug candidates. These models have the potential to filter out the most promising drug candidates for development and separate them from the ones with low probability of success (van de Waterbeemd and Gifford 2003). A very good way to develop a pharmacokinetic model is by incorporating the processes of absorption, distribution, metabolism and excretion (ADME) into

one global model. Mechanistic models strive to represent the physiological and pharmacological processes as accurately as possible using first principles approach. They incorporate our current understanding of the structure of the physiological system and the biological processes involved such as drug dissolution, degradation, gastric emptying, intestinal transit, intestinal permeation and transport, intestinal metabolism and hepatic metabolism (Marshall et al. 2006).

A typical CAT model (Yu et al. 1996, Yu and Amidon 1999) divides the GI tract into three segments namely, stomach, small intestine and colon, while the transit flow in the small intestine is separated into seven compartments. The model considers simultaneous small intestinal transit flow and drug absorption. In addition the model assumes instantaneous dissolution, linear transfer kinetics and equal transit times in all the compartments, very low absorption in stomach and colon. The dependence of the fraction of dose absorbed on the effective permeability of various drugs with different absorption characteristics was well captured by the model (Yu and Amidon 1999). This model serves as a basis for most of the compartment models being used in pharmacokinetics.

The advanced compartmental and transit (ACAT) model (Agoram et al. 2001, Bolger 2009) is based on the CAT model and accounts for the first-pass metabolism and colon absorption. It successfully predicted oral absorption for drugs like propranolol undergoing first-pass hepatic metabolism, midazolam which was undergoing first-pass in both intestine and liver, digoxin which was undergoing efflux transport and saquinavir undergoing both first-pass metabolism and efflux transport (Agoram et al. 2001). The Grass Model (Grass 1997) is a physiologically based multiple-compartmental model. It describes the gastric emptying, transit in the GI tract based mainly on solubility, permeability, and tissue surface area; it also calculates the drug absorption in each compartment. This model accurately predicted plasma concentration profiles and pharmacokinetic parameters (i.e. AUC, C_{max} and bioavailability) for drugs such as ketorolac and ganciclovir. The ADAM model is similar to the ACAT model (Dokoumetzidis et al. 2007, Jamei M 2007, Darwich et al. 2010). This model accounts for the GI physiology, dissolution process, gut wall permeation, drug degradation and all other factors accounted in the ACAT model. Additionally, it accounts for the heterogeneous distribution of the enterocytic blood flow and enzymes in the gut wall, food effects such as gastric emptying, splanchnic blood flow and luminal pH.

There are different kinds of mechanistic models such as dispersion models and compartmental models. There are dispersion models that define the GI tract as a single tube with

spatially varying properties (pH, surface area, etc.) along the tube (Ni et al. 1980) in contrast to compartmental models which represent the small intestine as a series of compartments with linear transfer kinetics, with uniform concentration in each compartment. Compartment models are easier to comprehend and model but tend to have many parameters that have to be fitted. Therefore sensitivity analysis may be used to identify a subset of the most sensitive parameters. On the other hand tube models represent a greater challenge in modeling; however they tend to have much less number of parameters.

The movement of drugs through the intestine was modeled by Willmann and co-workers (Willmann et al. 2007) through the introduction of an intestinal transit function (defined as the fractional drug dose in a specific GI segment at a given time) into the dispersion model. The model accounted for effects of solubility and permeability on the drug absorption and successfully simulated the fraction of dose absorbed for a wide variety of drugs in rats (Willmann et al. 2003), humans (Willmann et al. 2004) and monkeys (Willmann et al. 2007). It was observed that the dispersion model predicted well for passively absorbed drugs. However, assumptions such as negligible first-pass effect and passive intestinal permeability do not appear justified.

3.2.1 Advanced Compartmental and Transit (ACAT) Model

Yu and Amidon developed CAT model to simulate the rate and extent of drug absorption. The CAT model is based on the transit time distribution of seven small intestine compartments, described by a set of differential equations considering the simultaneous movement of drug in solution through the GI tract and absorption of dissolved drug from each compartment into the portal vein (Yu and Amidon 1999). However, this model did not account for many factors that describe the absorption process in a more realistic way. In order to account for all these factors an Advanced CAT (ACAT) model was developed. In this work we used a modified form of the ACAT model (Agoram et al. 2001) as a basis for developing the pharmacokinetic model. It includes linear transfer kinetics, six plausible states of the drug component (unreleased, undissolved, dissolved, degraded, metabolized and absorbed), nine compartments (stomach, seven segments of the small intestine, and colon), and three states of the excreted material (unreleased, undissolved and dissolved) (Fig. 2). Physiological factors such as gastric emptying, intestinal transit rate, first-pass metabolism, luminal transport and physicochemical factors (e.g. pKa, solubility, particle size,

particle density, permeability) and dosage factors including dosage form and dose are taken into account in predicting the oral drug absorption (Huang et al. 2009).

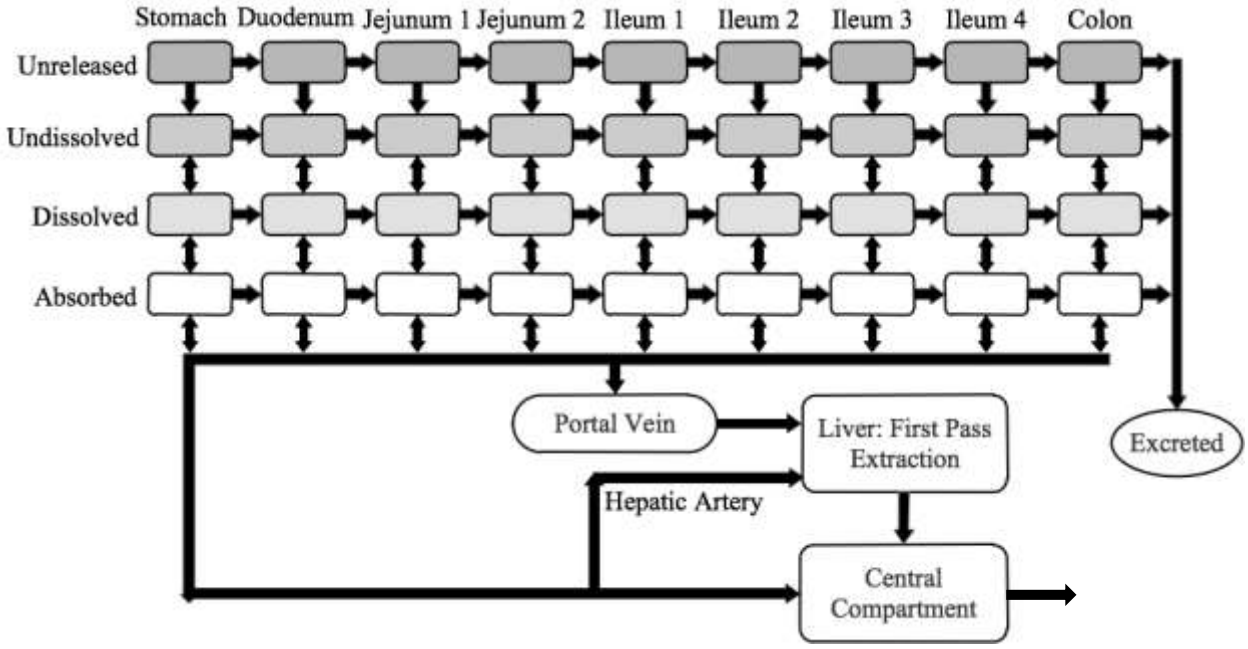

Figure 2: A schematic of the ACAT model (Agoram et al. 2001, Huang et al. 2009)

In the ACAT model, the drug passing through the small intestine has transit time specific to each compartment. The rate of drug transit is determined by a transfer rate constant, k_t, which is a reciprocal of the mean transit time between each compartment. The dissolution process is defined by a simple rate constant, k_d (Eq. (1)), which is calculated from the solubility of the drug (C_S) (as a function of pH), lumen concentration (C_L), its effective particle size (r_0), particle density (ρ), molecular diffusion coefficient (γ) and diffusion layer thickness (T). Hence it does not account for the process of dissolution as in (Narasimhan and Peppas 1997) where the disentanglement of the polymer is also taken into account along with the drug dissolution, clearly explaining the dissolution process. The time scale for the absorption process is set by a rate constant, k_a (Eq. (2)), which is expressed in terms of the effective permeability (P_{eff}) of the drug and absorption scale factor (α) for each compartment. A detailed description of the various equations used in the ACAT model for each compartment is included in Appendix A.

$$k_{(i)d} = 3\gamma \frac{C_{(i)S} - C_{(i)L}}{\rho r_0 T} \qquad (1) \qquad k_{(i)a} = \alpha_i P_{eff\,(i)} \qquad (2)$$

Here, '*i*' is the compartment number, which in our case varies from 1 to 9.

3.3 Proposed Methodology

In order to accomplish our objective we have identified a drug release model from the literature to describe the release of drug from a polymer matrix enclosed drug tablet (discussed in chapter 2). The model accounts for drug absorption and transit model to describe the absorption, transport, metabolism and excretion of drug in the gastrointestinal tract. Subsequently we combine the drug release model with the drug absorption and transit model to develop a pharmacokinetic model. The developed pharmacokinetic model is used to predict pharmacokinetic parameters such as peak plasma concentration, area under the curve and bioavailability. We have incorporated the model into an optimization framework to optimize key parameters such as tablet size.

3.4 Modeling Strategy

3.4.1 Modified Pharmacokinetic Model

In the ACAT model, the mechanism of drug release is not taken into account. For drug delivery systems trying to achieve a controlled release, the process of drug release from the system into the body is very important. It determines the amount of drug released into the body along the GI tract with time. Therefore, by incorporating a drug release model into the ACAT model, we are making the model closer to a realistic controlled release mechanism, which will in turn improve the overall prediction capabilities of the model. With the inclusion of the drug release model, we have also taken into account the properties of the polymer carrier used in the tablet. This will give us an opportunity to achieve one of our objectives of incorporating polymer molecular modeling into our model. This aspect is more thoroughly discussed in the subsequent chapters.

A schematic of our modeling methodology is given in Fig. 3. The model employs linear transfer kinetics with two plausible states of the drug component (dissolved and absorbed) as shown in Fig. 4. The first two layers in the ACAT model (Fig. 2) representing the unreleased and released states of the drug component are replaced by input from the dissolution model as shown in Fig. 4. The basic approach is that the amount of dissolved drug, which enters each of the compartments in the ACAT model, is evaluated using the dissolution model. The latter assumes that the drug tablet is cylindrical and that dissolution occurs along the tablet thickness in the axial

direction. Hence, the drug feed into each of the compartments is evaluated using the density of the drug, thickness of the tablet, fraction of drug in the tablet and the compartment volume obtained from Bolger et al. (Bolger 2009) (Eq. (3)). The drug feed determines the plasma concentration profile of the drug. Note that the drug dissolves gradually as it travels down the GI tract; therefore compartments along the tract are exposed to some of the freshly released drug. A description of the various equations used in the modified pharmacokinetic model is included in Appendices A and B. Specifically, Appendix A includes the equations used in the modified ACAT model and Appendix B includes the dissolution model equations which are used to evaluate the feed into the modified ACAT model.

The mass $M_{t_k,i}$ of drug into the i^{th} compartment at time t_k is given by

$$M_{t_k,i} = \frac{\pi R^2 (h_{t_{k-1},i} - h_{t_k,i}) \rho_d f_d}{V_{com,i}} \tag{3}$$

Here, $h_{t_k,i}$ is the half thickness of the drug tablet at time t_k in the i^{th} compartment $h_{t_{k-1},i}$ is the half thickness of drug tablet at previous time point t_{k-1} in the i^{th} compartment, R is the radius of the tablet, f_d is the fraction of drug, ρ_d is the density of the drug and $V_{com,i}$ is the compartment volume.

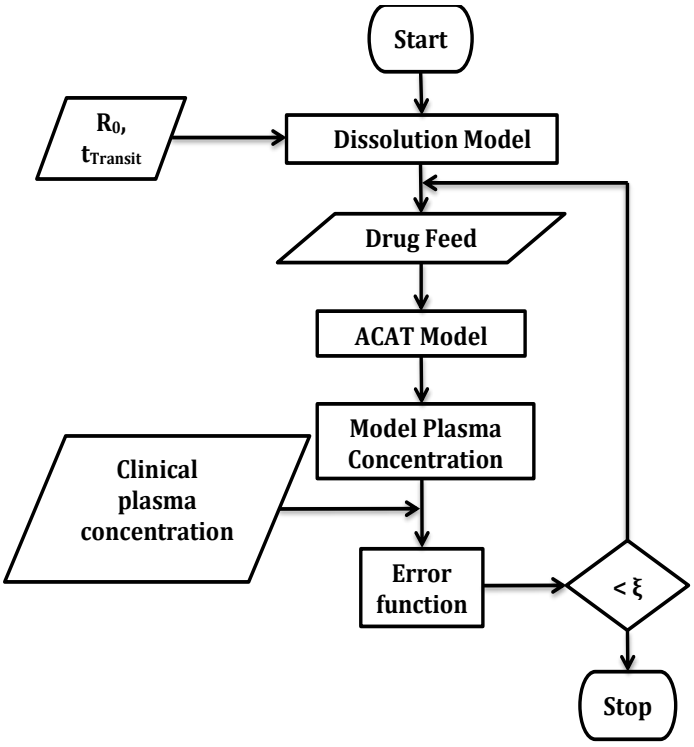

Figure 3: Schematic of the modeling methodology

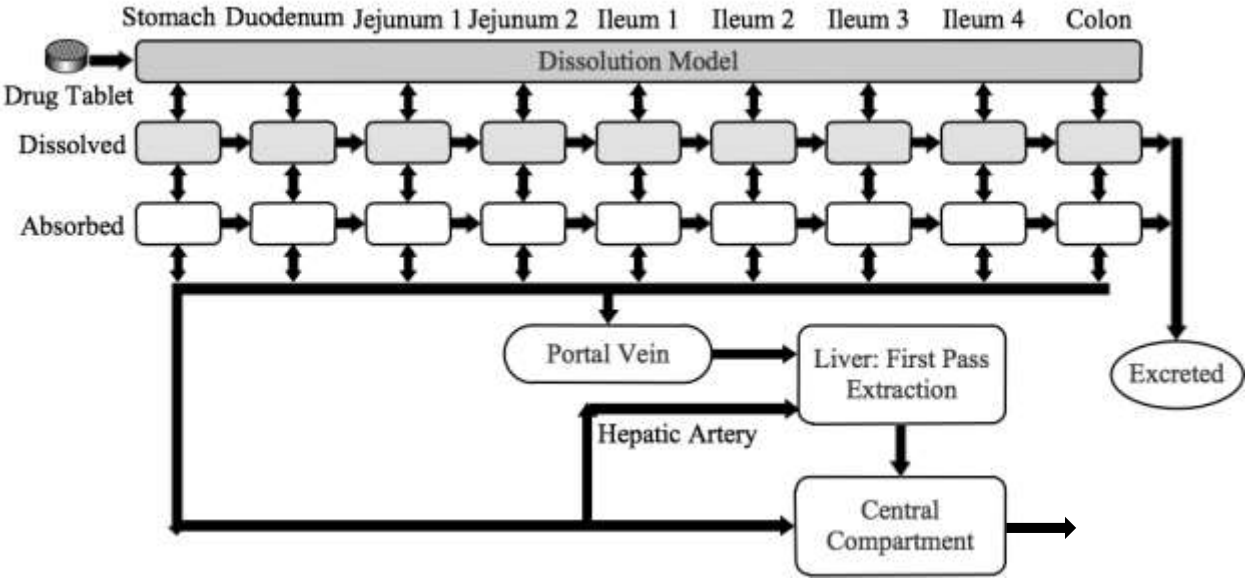

Figure 4: Schematic of the developed pharmacokinetic model

3.5 Case Study

In this paper, Cimetidine is used as a model drug to test the pharmacokinetic model. The drug is available in a variety of oral dosage forms for the treatment of duodenal and gastric ulcers (Somogyi and Gugler, 1983). Cimetidine is an antagonist of the Histamine H_2-receptor that inhibits the secretion of gastric glands. Bioavailability and pharmacokinetics of cimetidine was studied in 10 healthy volunteers after administration of doses (100,400, and 800 mg) in Grahnén et. al. (Grahnén et al. 1979). The solubility of cimetidine is approximately 6 mg/mL at 37˚C.

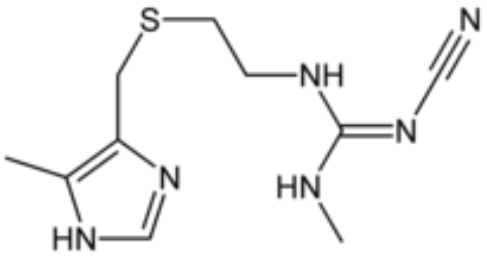

Figure 5: Molecular Structure of Cimetidine

Plasma concentration-time profiles of Cimetidine in 12 healthy patients (average body weight of 59.5Kg) following oral administration of a commercially available immediate release formulation (Tagamet) as well as three extended release formulations was presented in Jantratid et. al. (Jantratid et al. 2006). The cimetidine tablets used in the study were manufactured with an initial radius of 8mm. The author presented the relationship between in vitro absorption performances of immediate-release formulations containing cimetidine. We consider pharamcokinetic data of three different cimetidine 400mg formulations (Jantratid et al. 2006) containing: (i) 7.5% methacrylate copolymer cimetidine tablet; (ii) 15% methacrylate copolymer cimetidine tablet; (iii) 26% methacrylate copolymer cimetidine tablet.

3.6 Sensitivity Analysis

Parameter sensitivity analysis plays an important role in analyzing the relative sensitivity of system response with respect to the changing model parameters and identifying the most important ones. It gives us an insight into the model behavior. In this paper, we employ a local sensitivity analysis method (Chung et al. 2009). The model parameters are sequentially varied by fixing all the other

parameters to their nominal values and the system response is determined. Normalized sensitivity coefficient (NSC) values are evaluated from the values obtained using equation 4 (Chung et al. 2009). NSC values indicate the importance of a parameter on the system response.

$$NSC = \frac{(\phi - \phi_0)/\phi_0}{(P - P_0)/P_0} \tag{4}$$

Here ϕ_0 is the nominal value of the system response at P_0 the nominal value of the parameter; similarly ϕ is the system response at P. The system response (ϕ) in this paper is evaluated as the root mean squared error between the model and clinical data given by Eq. 5.

$$\phi = \frac{\sqrt{\sum_{i=1}^{N}\left[C_{(i)}^{model} - C_{(i)}^{\exp}\right]^2}}{N} \tag{5}$$

Here $C_{(i)}^{model}$ are plasma concentration values resulting from the model at selected time points (see Appendix A and Appendix B). $C_{(i)}^{\exp}$ are the corresponding clinical values and N is the total number of time points. We used a total of 16 time points in our model.

We performed sensitivity analysis for all the model parameters such as, human effective permeability (P_{eff}), drug density (ρ_d), hepatic clearance rate of drug from the liver (CL_h), volume of liver (V_{liver}), hepatic blood flow rate (Q_h), volume of central compartment ($V_{central}$), diffusion coefficient of water in polymer (D_1), diffusion coefficient of drug in polymer (D_d), polymer chain disentanglement rate (k_d) and drug absorption scale factors (α_i). The P_{eff} value accounts for all the factors responsible for the transport of drug across GI-epithelium such as passive transport as well as active transport due to transporters. The CL_h value accounts for the drug metabolism happening inside the liver. The NSC values evaluated for five of the most sensitive parameters are shown in Fig. 8. All the parameters are subjected to 2.5, 5, 7.5 and 10% perturbations on either side of zero as shown in Fig. 6.

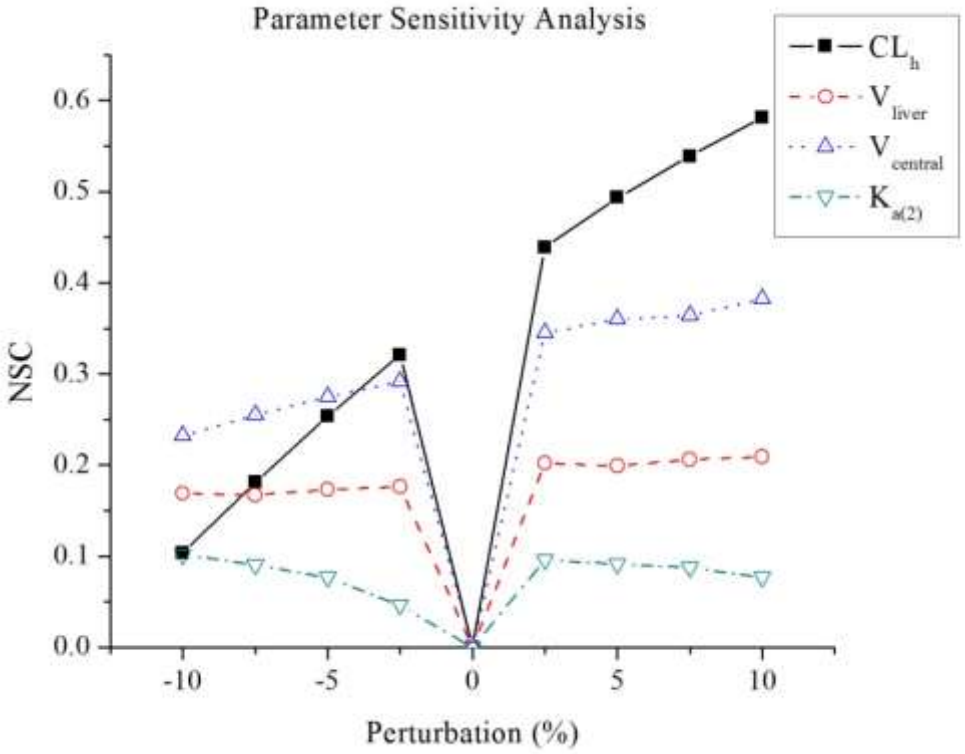

Figure 6: Comparison of NSC values for the parameters: hepatic clearance rate of drug from the liver (CL_h), volume of liver (V_{liver}), volume of central compartment ($V_{central}$) and absorption coefficient of 2nd compartment ($K_{a(2)}$)

We observe that in Fig. 6, when the value of P_{eff} is increased, there is a corresponding increase in the value of plasma concentration, which results in an increase in the system response value (Eq. 5); the reverse is true when P_{eff} is decreased. This is expected because the increase in drug permeability increases the drug absorption due to an increase in the absorption coefficient value (Eq. 2), which in turn increases the blood plasma concentration. The change in the absorption scale factor has a corresponding effect on the rate of drug absorption (Eq. 2), which will have an effect on the plasma concentration profile. The sensitivity of absorption scale factor is highest for the second and third compartments of the GI tract where most of the drug absorption takes place. In order to account for both P_{eff} and α_2 we performed the sensitivity analysis on the absorption coefficient of the second compartment ($K_{(2)a}$), where $K_{(2)a}$ is the product of P_{eff} and α_2 (Eq. 2). We observe that the curves for $V_{central}$ and V_{liver} follow a similar trend indicating a possible

correlation between the two. But both these parameters are independent of each other and we observe that in case of $V_{central}$ there is a slightly increasing trend in the curve, while the curve for V_{liver} is completely flat. The change in CL_h and $V_{central}$ has a direct effect on the plasma concentration as seen in Eq. A7 and Eq. A8. We observe that the NSC values are highest for CL_h indicating that it is the most sensitive among the parameters considered followed by $V_{central}$, followed by V_{liver} and finally $K_{(2)a}$ being the least sensitive among the parameters considered shown in Fig. 6.

3.7 Model Parameter Estimation

We employed the clinical pharmacokinetic data of cimetidine tablet (see Section 2.2) containing 7.5% methacrylate copolymer to estimate the various model parameters. The remaining two formulations of cimetidine are used for model validation to be discussed later. As discussed in Section 2.3, the sensitivity analysis identified the four most sensitive parameters as the effective permeability (P_{eff}), hepatic clearance rate of drug from the liver (CL_h), volume of central compartment ($V_{central}$) and absorption scale factor of 2nd compartment (α_2); these parameters were subsequently used in the parameter estimation step. Specifically, we minimized (Matlab function – fmincon) the system response (ϕ) using the parameters as the decision variables.

The parameter values used in the model are directly from the literature. Since we do not have access to the data that was used for parameter estimation, we cannot provide statistically valid confidence intervals. We instead provide approximate confidence intervals based on the standard deviation values provided from the literature. For a subset of the clinical data we perturbed some of the parameters in order to better fit the model predictions to the clinical data. This was subsequently followed by model validation using another subset of clinical data – data at two other compositions (15% and 26% methacrylate copolymer tablet). It is important to indicate that the estimated parameter values are specific to the population considered to obtain the clinical data. The approximate confidence intervals are given in Table 3.

The resulting model parameter values are given in Table 1. The absorption scale factors are given along with the transit rate constants and absorption rate constants evaluated using equation 1 and equation 2 in Table 2. The absorption rate constants are specific to each drug.

Table 1: Model Parameters used in the developed pharmacokinetic model

Parameter	Description	Value	Source
P_{eff} (cm/h)	Human effective permeability of the drug in the body	0.063	(Willmann et al. 2009)
ρ_d (gm/cm^3)	Density of the drug (cimetidine)	1.4	(Narasimhan and Peppas 1997)
V_{liver} (ml)	Volume of human liver	1539.6	(Agoram et al. 2001)
Q_h (ml/h/Kg)	Blood flow rate in the hepatic artery from central compartment into the liver	1260	(Agoram et al. 2001)
CL_h (ml/h)	Hepatic clearance rate of the drug from the liver	9036	(Gugler et al. 1982)
$V_{central}$ (ml)	Volume of central compartment	11900	(Gugle et al. 1982)
D_1 (cm^2/s)	Diffusion coefficient of water in polymer	2.5x10^{-7}	(Narasimhan and Peppas 1997)
D_d (cm^2/s)	Diffusion coefficient of drug in polymer	2.2x10^{-8}	(Narasimhan and Peppas 1997)
k_d (cm/s)	Disentanglement rate of polymer	3.3x10^{-7}	(Narasimhan and Peppas 1997)

Table 2: Compartment parameters used in the modified ACAT model, absorption rate constants and transit rate constants of each compartment

Compartment	Compartmental Absorption Scale Factor (α_i)	Compartment Radius (cm)	Absorption Rate Constant (h^{-1})	Compartment Transit Time (h)	Transit Rate Constant (h^{-1})
1	2	9.67	0.13	0.25	4.00
2	10	1.53	4.12	0.26	3.85
3	10	1.45	4.34	0.93	1.07
4	4	1.29	1.95	0.74	1.35
5	2	1.13	1.11	0.58	1.72
6	2	0.98	1.29	0.42	2.38
7	2	0.82	1.54	0.29	3.45
8	2	3.39	0.37	4.19	0.24
9	2	2.41	0.52	12.57	0.08

Table 3: Standard deviation and 95% confidence interval values for the estimated parameters

Parameter	Best-fit Value	Standard Deviation	95% Confidence Interval
P_{eff} (cm/h)	0.063	0.012	0.056 - 0.069
CL_h (ml/h)	9036	2778	7523 – 10549

$V_{central}$ (ml)	11900	6230	8506 – 15293
α_2	10	NA	NA

3.8 Results and Discussion

We validated the model after estimating the model parameters. Specifically, we compared the model data to the clinical data of the three different cimetidine formulations obtained from Jantratid (Jantratid et al. 2006). We evaluated the pharmacokinetic metrics (process variables or "parameters") including the AUC, $C_{\max}$ and bioavailability and statistically compared them with the model data.

We obtained clinical plasma concentration profiles for cimetidine 400mg tablet from Jantratid (Jantratid et al. 2006) for three different formulations: (i) 7.5% methacrylate copolymer cimetidine tablet (used in the parameter estimation); (ii) 15% methacrylate copolymer cimetidine tablet and (iii) 26% methacrylate copolymer cimetidine tablet. Each formulation had an initial dosage of 400mg containing excipients and 40% drug active. The clinical data indicates that the plasma profiles are a function of the drug-polymer ratio in the tablet; hence the model is constructed to reflect this ratio. The input mass for each of the three formulations is 1000mg, with drug-polymer ratios 5.33, 2.66 and 1.54 respectively. We set the total simulation time as 12 hours. The initial tablet radius was given as 8mm.

We estimated the error bars from the standard deviation values of $C_{\max}$ given by Jantratid (Jantratid et al. 2006), where the only standard deviation given is that of $C_{\max}$. From this standard deviation value we tried to estimate the standard deviation for each point on the plasma profile. Specifically, we assumed that the standard deviation was proportional to the concentration.

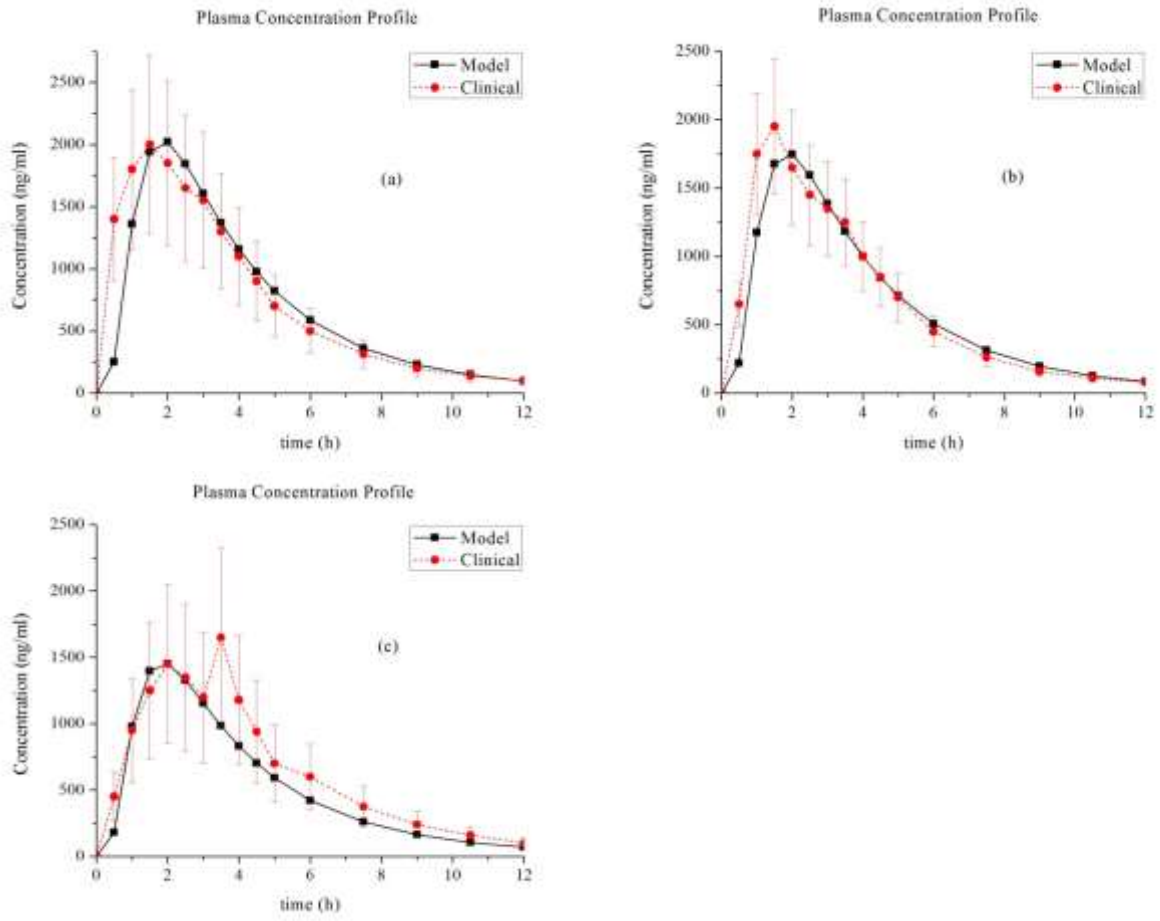

Figure 7: Comparison of model and clinical plasma concentration profiles for (a) 7.5% methacrylate copolymer cimetidine tablet; (b) 15% methacrylate copolymer cimetidine tablet; (c) 26% methacrylate copolymer cimetidine tablet, with estimated error bars for clinical plasma profiles. The experimental error bars are estimated from the standard deviation values provided in the literature

We compared the clinical profile for each of the formulations with the predicted plasma profile obtained from the model (Fig. 7). Fig. 7a shows the profiles for 7.5% methacrylate copolymer cimetidine tablet, which is used as the basis for parameter estimation; hence the model profile agrees well with the clinical profile with a low system response (ϕ) of 79.7 ng/ml evaluated using Eq. 5. A low system response indicates that the root mean squared error between the model predicted and clinical data is low. This implies that the model predicted data is quite close to the clinical data indicating a good prediction by the model. In Fig. 7b, the predicted plasma profile for

15% methacrylate copolymer cimetidine tablet agrees very well with the clinical profile with even lower system response value of 49.6 ng/ml. In Fig. 7c, the predicted plasma profile for 26 % methacrylate copolymer followed a similar trend as the 15% methacrylate copolymer cimetidine tablet with a low system response value of 55.3 ng/ml, strengthening the validity of the model with respect to the clinical profile. However, the second peak in the clinical profile being an anomaly could not be predicted by the model.

Table 4: Comparison of the pharmacokinetic parameters: C_{max} , t_{max} , AUC and bioavailability obtained from both the clinical experiments and the model. Clinical values are expressed as Value (Standard Deviation)

Sample	C_{max} **(ng/ml)**		t_{max} **(h)**		**AUC (ng h/ml)**		**bioavailability**	
	Clinical	Model	Clinical Range	Model	Clinical	Model	Clinical	Model
7.5% polymer	2000 (713)	2020	1.5 – 2	2	8975 (1784)	8791	61.5 (16.48)	62.11
15% polymer	1950 (494)	1745	1.5 – 2	2	7896 (1779)	7594	53.16 (12.68)	52.95
26% polymer	1450 (596)	1453	1.5 – 2	2	7722 (2444)	6326	52.09 (17.09)	45.32

We have summarized the various pharmacokinetic metrics (process variable or "parameter" values) obtained from the model and compared them with the clinical values in Table 1. We calculated all the clinical values in this table from the data given in Jantratid (Jantratid et al. 2006). We observe that the pharmacokinetic metric values for C_{max} , t_{max} , AUC and bioavailability values obtained from the clinical profile are very close to the predicted values for the 7.5 % methacrylate copolymer cimetidine tablet. This is expected since the parameter estimation was done using clinical data of 7.5 % methacrylate copolymer cimetidine tablet as the basis. We observe that the C_{max} values are 10 % lower than the clinical value for 15 % methacrylate copolymer cimetidine tablet and very close to the clinical value for 26% methacrylate copolymer cimetidine tablet (Table 4). We observe that the peak plasma concentration time (t_{max}) for all the three formulations is between the 1.5 – 2 hours range, which is generally the case for the clinical

values. We observe that the values of AUC predicted by the model are somewhat lower than that evaluated from the experiments for the 15 % and 26 % formulations. The AUC value for 15 % methacrylate copolymer cimetidine tablet is 3.8 % lower, while for 26 % methacrylate copolymer cimetidine tablet it is 18 % lower as shown in Table 4. The large difference in the AUC values for the 26% methacrylate copolymer cimetidine tablet is due to the unaccounted second peak in the clinical profile (Fig. 7c). However, all the $C_{\max}$ and AUC values evaluated from the model still fall within the clinical range of values given by Jantratid (Jantratid et al. 2006). We observe that the bioavailability values evaluated from the model are comparable to the clinical values except for the 26% methacrylate copolymer cimetidine tablet due to the large difference in AUC values.

3.9 Scenario Studies

We studied several scenarios by changing different inputs in the model and simulating their impact on the plasma concentration profile. The analysis was done using the clinical data for 7.5% methacrylate copolymer cimetidine tablet as the basis. Quantitative analysis was done by comparing the AUC values for different input values in each of the scenarios. We determined the optimal dimensions of drug tablet required for predicting a target plasma profile with maximum efficacy.

3.9.1 Average body weight of a patient (W_p)

Plasma concentration profiles are simulated after increasing the body weight by 30, 70 and 100% as shown in Fig. 6, along with the original predicted profile.

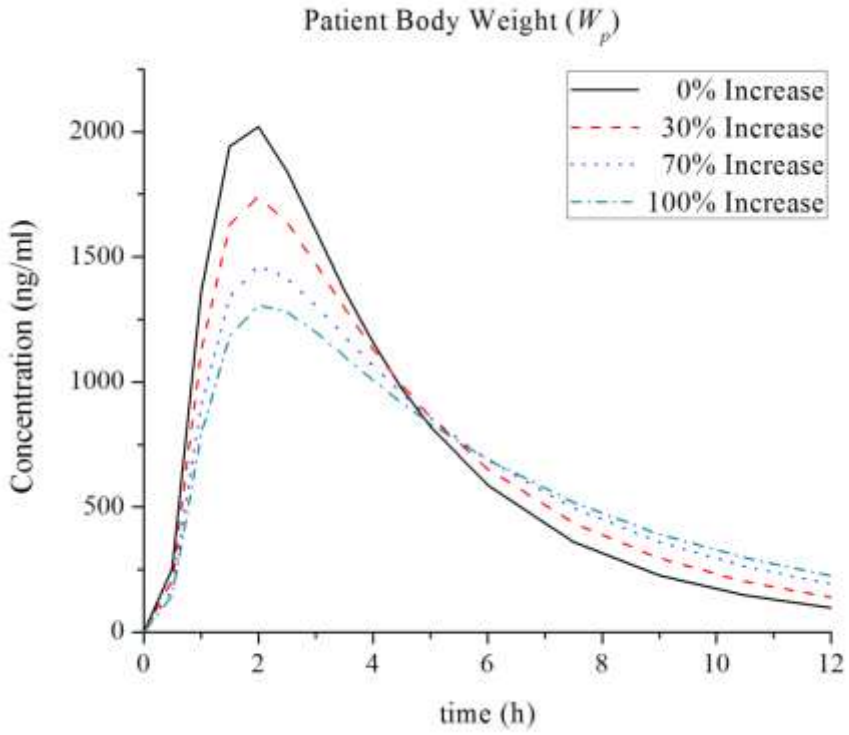

Figure 8: Comparison of model plasma profiles for different values of patient body weight

With an increase in the body weight, there is a significant negative shift in the plasma profile from the original. That is the plasma profile shifts below the original profile due to an increase in the parameter value as shown in Fig. 8. The negative shift is observed because, the increase in the body results in an increase in the values of hepatic blood flow rate (Q_h), volume of central compartment ($V_{central}$) and hepatic clearance rate of drug from the liver (CL_h), as all these values are evaluated using the body weight. This shows that the developed model can be used for different patients of different body weights. For patient body weight (W_p) increase of 0%, 30%, 70% and 100% (AUC values of 8791, 8580, 8229 and 7936 ng.h/ml respectively), the decrease in AUC values were 0%, 2.4%, 7.5% and 9.7% respectively. This low change in the AUC value indicates low effect of W_p on plasma concentration profile. We hypothesize that for a fixed drug dosage, two patients of varying body weights are expected to experience similar therapeutic effect of the drug.

3.9.2 Fraction of drug in polymer-drug system (f_d)

Plasma concentration profiles are simulated after decreasing the fraction of the drug by 0, 20, 40 and 60 % as shown in Fig. 9. The total mass of the drug tablet was 1000 mg as mentioned before containing 400 mg of drug.

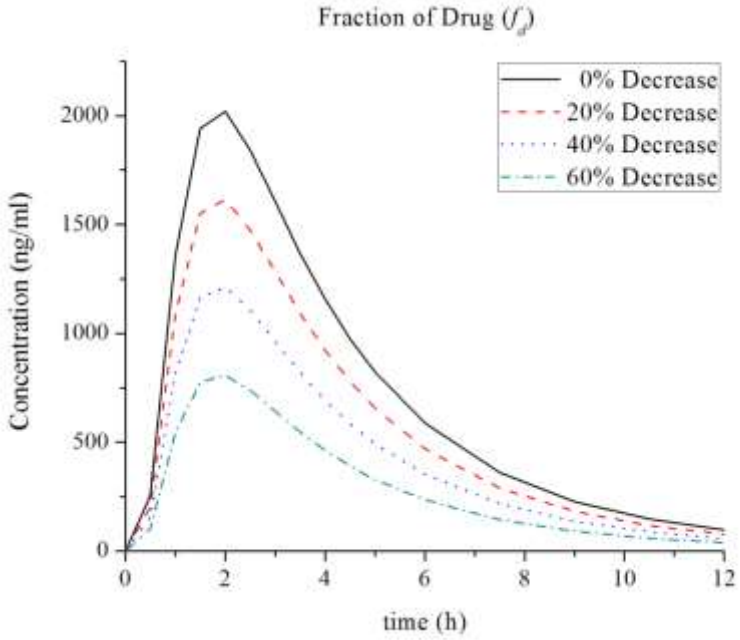

Figure 9: Comparison of model plasma profiles for different values of fraction of drug (f_d)

The decrease in the fraction of drug (f_d) is also an indication of the decrease in the drug loading of the tablet. The mass of drug released (*M*) into the modified ACAT is directly proportional to f_d as described by Eq. 3. Hence, the decrease in f_d will result in a corresponding decrease in the value of *M*, which decreases the overall plasma profile. The plasma profile shifts below the original profile due to decrease in the parameter value as shown in Fig. 9. The drug loading of a tablet is a measure of the effectiveness of the drug tablet. Pharmaceutical scientists thrive to produce drug formulations with maximum drug loading which could provide the most effective therapeutic effect with minimum amount of drug dosage. For fraction of drug (f_d) decrease of 0%, 20%, 40% and 60% (AUC values of 8791, 7030, 5276 and 3518 ng.h/ml respectively), the AUC values correspondingly decreased by 0%, 20%, 40% and 60% respectively. Thus f_d has a direct effect on the model predictions. We hypothesize that for a patient, the increase

in drug loading could lead to an overdose of the drug, and a decrease in drug loading could lead to a very low or no therapeutic effect at all. Thus the dosage should be carefully tailored to the drug loading of the tablet.

3.9.3 Tablet radius (*R*)

Plasma concentration profiles are plotted after increasing the tablet radius by 0, 20, 40 and 60% as shown in Fig. 10. The mass of the tablet is kept constant. Hence, with increase in tablet radius, there is a corresponding decrease in the tablet thickness.

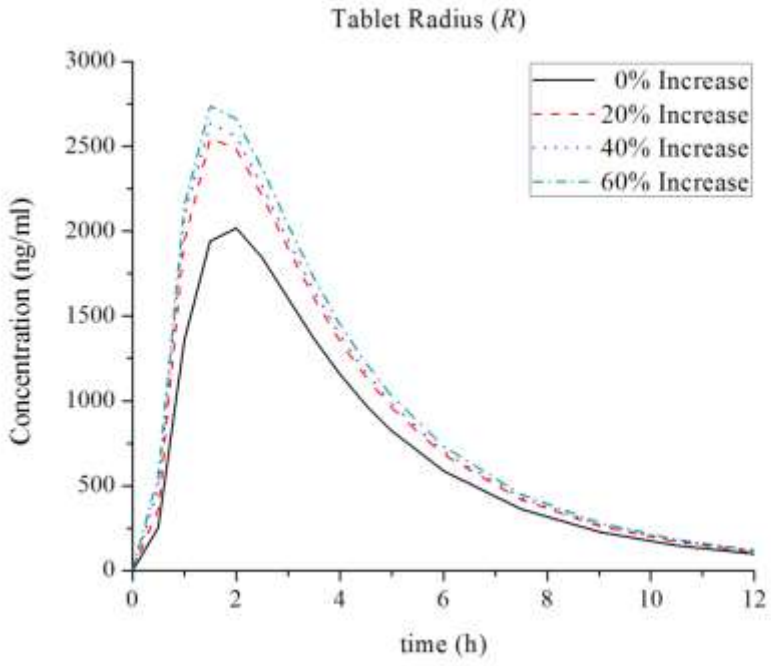

Figure 10: Comparison of model plasma profiles for different values of tablet radius

An increase in the tablet radius has low to moderate impact on the plasma concentration profile. There is a slight positive shift observed, with increase in the tablet radius (*R*). The mass of drug released (*M*) into the modified ACAT model is dependent on this tradeoff between the *R* and *h* values as described by Eq. 3. We observe that the overall effect on plasma profile is much less. Thus one can determine the optimal tablet radius, which corresponds to an optimal tablet thickness that has the maximum effect on the drug plasma profile. Most of the active drug is released in the axial direction for a typical cylindrical tablet considered in our model. In this case the change in the tablet radius will have a corresponding effect on the tablet surface area through which the axial

drug diffusion is taking place. This will have a significant impact on the drug release rate, which directly impacts the plasma concentration profile. For the tablet radius (*R*) increase of 0%, 20%, 40% and 60% (AUC values of 8791, 10707, 11105 and 11605 ng.h/ml respectively), the AUC values correspondingly increased by 0%, 22%, 26% and 32% respectively. This indicates that *R* has a significant effect on the model predictions up to a certain percentage of increase; the effect becomes low after that due to the tradeoff between *R* and *h* values as discussed above. Thus a tablet with higher radius is expected to have a greater therapeutic effect compared to the one with a lower radius, but risks crossing the toxicity threshold.

3.9.4 Optimization

In this scenario study, we consider tablet design before any experiments are performed. We are trying to address the question, "What tablet geometry maximizes the therapeutic affect?" To proceed, we make the assumption that the total volume of the tablet is constant and the overall tablet composition (drug, polymer and excipients) is fixed. We also make the assumption that the model parameters (such as permeability (P_{eff}), drug density (ρ_d), hepatic clearance rate of drug from the liver (CL_h), volume of liver (V_{liver}), hepatic blood flow rate (Q_h), volume of central compartment ($V_{central}$), diffusion coefficient of water in polymer (D_1), diffusion coefficient of drug in polymer (D_d), polymer chain disentanglement rate (k_d) and drug absorption scale factors (α_i).) do not change. We incorporated the developed pharmacokinetic model within an optimization framework as described in Eq. 6 to determine the optimal tablet dimensions for a given drug dosage. This will greatly help in determining drug tablet design, which will result in the maximum therapeutic effect. In this model, we fixed the tablet size (volume) and tablet composition.

$$\begin{aligned} &\underset{x}{Min}\, J = Performance\ \ Objective \\ &subject\ to \\ &\quad Pharmacokinetic\, Model \end{aligned} \tag{6}$$

Here, *J* is the objective function, which in our case is the AUC value; *x* is the optimization variable, which in this case is a tablet dimension. The pharmacokinetic model equations are defined by the ACAT model, while the dissolution model equations are given in Appendices A and B. For the 15% methacrylate copolymer cimetidine tablet considered for this study with an initial radius of 8

mm, the optimal tablet radius is obtained as R_{opt} = 15.6 mm. This optimal value is obtained when there are no constraints on the AUC value implying the maximum possible therapeutic effect. We performed the optimization using the interior-point function "fmincon" in Matlab. We used an Intel® Xeon(R) CPU E5405 2.00 GHz x 4 Processor; the simulation time was 37 minutes of CPU.

3.10 Conclusions

We have presented effective models for drug release, drug absorption and transit. The advantage of the suggested approach is that it can be used to test hypothesis about the mechanism involved in drug delivery into the blood circulatory system; these are issues we are exploring.

We concluded through parameter sensitivity analysis of the model that based on the NSC values, effective permeability (P_{eff}) is the most sensitive, followed by absorption scale factor of compartment 2 (α_2), hepatic clearance rate of drug from liver (CL_h), volume of central compartment ($V_{central}$) and volume of liver (V_{liver}) in that order.

Using a set of parameter estimated values, we performed a comparative study of plasma concentration profiles and pharmacokinetic metrics such as $C_{\max}$, AUC and bioavailability between model predictions and clinical data for three different cimetidine formulations, (i) 7.5% methacrylate copolymer cimetidine tablet; (ii) 15% methacrylate copolymer cimetidine tablet; (iii) 26% methacrylate copolymer cimetidine tablet. The predicted plasma concentration profiles match well with the clinical profiles for all the three cases. The estimated pharmacokinetic parameter values of $C_{\max}$, AUC and bioavailability fall well within the clinical range as given in Jantratid (Jantratid et al. 2006).

We presented scenario studies, which showed that the developed model is applicable to different patients with varying body weight (W_p). It is also applicable to different drug tablets with varying drug fraction (f_d) (or drug loading). We finally incorporated the model within an optimization framework to estimate the optimal geometry of the tablet which will give the maximum efficacy. The current model is limited to predicting the plasma concentration profiles similar to that shown in Fig. 7 where most of the drug absorption takes place within the initial few hours. We are extending the model to allow it to predict a plasma profile of a general shape.

This model is based on the ACAT model, which represents the GI tract as a series of well-mixed continuous stirred tank vessels similar to continuous stirred tank reactors (CSTRs); however, the GI tract is a continuous tube more closely represented by piece-wise tubular vessels similar. In the one-dimensional case the tubular model is similar to a set of plug flow reactors (PFRs). We are pursuing this angle as well with the understanding that higher model complexity and model accuracy would result.

3.11 Nomenclature

$k_{(i)t}$	Transit rate constant for the i^{th} compartment
$k_{(i)a}$	Absorption rate constant for the i^{th} compartment
P_{eff}	Effective permeability of drug in the body
α_i	Drug absorption scale factor
t_i	Transit time in each compartment of ACAT model
ρ_d	Drug density
f_d	Fraction of drug
L	Initial half thickness of the drug tablet
R_0	Radius of the drug tablet
$h_{t_k,i}$	Half thickness of the drug tablet at time t_k in the i^{th} compartment
$h_{t_{k-1},i}$	Half thickness of drug tablet at previous time point t_{k-1} in the i^{th} compartment
$V_{com,i}$	Compartment volume of the i^{th} compartment
ϕ_0	Nominal value of the system response
P_0	Nominal value of the parameter; similarly
ϕ	System response value
P	Model parameter value
$C_{\max}$	Peak plasma concentration
$t_{\max}$	Peak plasma concentration time
$C_{(i)}^{model}$	Plasma concentration value on the model predicted curve at selected time points
$C_{(i)}^{\exp}$	Plasma concentration values on the clinical curve at selected time points
N	Total number of time points considered to evaluate the system response
CL_h	Hepatic clearance rate of drug from the liver
V_{liver}	Volume of liver
Q_h	Hepatic blood flow rate
$V_{central}$	Volume of central compartment

D_1	Diffusion coefficient of water in polymer
D_d	Diffusion coefficient of drug in polymer
k_d	Polymer chain disentanglement rate
W_p	Average patient body weight
C_p	Plasma Concentration

3.12 References

Agoram, B., W. S. Woltosz and M. B. Bolger (2001). "Predicting the impact of physiological and biochemical processes on oral drug bioavailability." Advanced Drug Delivery Reviews **50, Supplement 1**(0): S41-S67.

Bolger, M. B. (2009). "Simulations of absorption, metabolism, and bioavailability." Methods and Principles in Medicinal Chemistry **40**(drug bioavailability): 453.

Bolger, M. B. (2009). "Simulations of the Nonlinear Dose Dependence for Substrates of Influx and Efflux Transporters in the Human Intestine." The AAPS Journal **11**(2): 353-363.

Chung, S.-W., F. L. Miles, R. A. Sikes, C. R. Cooper, M. C. Farach-Carson and B. A. Ogunnaike (2009). "Quantitative Modeling and Analysis of the Transforming Growth Factor ² Signaling Pathway." Biophysical journal **96**(5): 1733-1750.

Dokoumetzidis, A., L. Kalantzi and N. Fotaki (2007). "Predictive models for oral drug absorption: from in silico methods to integrated dynamical models." Expert Opinion on Drug Metabolism & Toxicology **3**(4): 491-505.

Grahnén, A., C. Bahr, B. Lindström and A. Rosén (1979). "Bioavailability and pharmacokinetics of cimetidine." European Journal of Clinical Pharmacology **16**(5): 335-340.

Grass, G. M. (1997). "Simulation models to predict oral drug absorption from in vitro data." Advanced Drug Delivery Reviews **23**(1–3): 199-219.

Gugler, R., B. Muller-Liebenau and A. Somogyi (1982). "Altered disposition and availability of cimetidine in liver cirrhotic patients." British Journal of Clinical Pharmacology **14**(3): 421-430.

Huang, W., S. Lee and L. Yu (2009). "Mechanistic Approaches to Predicting Oral Drug Absorption." The AAPS Journal **11**(2): 217-224.

Jamei M, Y. J., Turner D, Rowland-Yeo K, Tucker GT, Rostami-Hodjegan A (2007). A Novel Physiologically-Based Mechanistic Model for Predicting Oral Drug Absorption: The Advanced Dissolution, Absorption, and Metabolism (ADAM) Model. . PKUK. Edinburgh Caledonian Hotel, Edinburgh, UK.

Jantratid, E., S. Prakongpan, G. L. Amidon and J. B. Dressman (2006). "Feasibility of Biowaiver Extension to Biopharmaceutics Classification System Class III Drug Products: Cimetidine." Clinical Pharmacokinetics **45**(4): 385-399.

Marshall, S., F. Macintyre, I. James, M. Krams and N. E. Jonsson (2006). "Role of Mechanistically-Based Pharmacokinetic/Pharmacodynamic Models in Drug Development: A Case Study of a Therapeutic Protein." Clinical Pharmacokinetics **45**(2): 177-197.

Mehrotra, N., M. Gupta, A. Kovar and B. Meibohm (2006). "The role of pharmacokinetics and pharmacodynamics in phosphodiesterase-5 inhibitor therapy." Int J Impot Res **19**(3): 253-264.

Narasimhan, B. and N. A. Peppas (1997). "Molecular analysis of drug delivery systems controlled by dissolution of the polymer carrier." Journal of Pharmaceutical Sciences **86**(3): 297-304.

Ni, P. F., N. F. H. Ho, J. L. Fox, H. Leuenberger and W. I. Higuchi (1980). "Theoretical model studies of intestinal drug absorption V. Non-steady-state fluid flow and absorption." International Journal of Pharmaceutics **5**(1): 33-47.

S. Darwich, A., S. Neuhoff, M. Jamei and A. Rostami-Hodjegan (2010). "Interplay of Metabolism and Transport in Determining Oral Drug Absorption and Gut Wall Metabolism: A Simulation Assessment Using the Advanced Dissolution, Absorption, Metabolism (ADAM) Model." Current Drug Metabolism **11**(9): 716-729.

van de Waterbeemd, H. and E. Gifford (2003). "ADMET in silico modelling: towards prediction paradise?" Nat Rev Drug Discov **2**(3): 192-204.

Willmann, S., A. Edginton and J. Dressman (2007). "Development and Validation of a Physiology-based Model for the Prediction of Oral Absorption in Monkeys." Pharmaceutical Research **24**(7): 1275-1282.

Willmann, S., A. N. Edginton, M. Kleine-Besten, E. Jantratid, K. Thelen and J. B. Dressman (2009). "Whole-body physiologically based pharmacokinetic population modelling of oral drug administration: inter-individual variability of cimetidine absorption." Journal of Pharmacy and Pharmacology **61**(7): 891-899.

Willmann, S., W. Schmitt, J. Keldenich and J. B. Dressman (2003). "A Physiologic Model for Simulating Gastrointestinal Flow and Drug Absorption in Rats." Pharmaceutical Research **20**(11): 1766-1771.

Willmann, S., W. Schmitt, J. Keldenich, J. Lippert and J. B. Dressman (2004). "A Physiological Model for the Estimation of the Fraction Dose Absorbed in Humans." Journal of Medicinal Chemistry **47**(16): 4022-4031.

Yu, L. X. and G. L. Amidon (1999). "A compartmental absorption and transit model for estimating oral drug absorption." International Journal of Pharmaceutics **186**(2): 119-125.

Yu, L. X., E. Lipka, J. R. Crison and G. L. Amidon (1996). "Transport approaches to the biopharmaceutical design of oral drug delivery systems: prediction of intestinal absorption." Advanced Drug Delivery Reviews **19**(3): 359-376.

3.13 Appendix A

3.13.1 ACAT Model

According to the ACAT model, the rate of change of dissolved drug concentration in a GI compartment depends on:

1. Release of drug from the formulation into the compartment
2. Transit of drug into a compartment
3. Transit of rug out of a compartment
4. Absorption/exsorption of the drug

The model equations are given by:

Nomenclature	
Superscript	**Subscript**
Dissolved – 1	t – Transit
Absorbed – 2	a – Absorption

Stomach

The stomach is treated as another compartment (Compartment 1). Notes: (a) in Eqn. (A.1), carrier-mediated transport is ignored; (b) in Eqn. (A.2), gut metabolism is ignored; (c) level 2 is "enterocyte" (level 2).

$$\frac{dC_1^{(1)}}{dt} = C_{1\,feed} - k_{1t}^{(1)} C_0^{(1)} - k_{1a}^{(1)} (C_1^{(1)} - C_1^{(2)}) \qquad (A.1)$$

$$\frac{dC_1^{(2)}}{dt} = k_{1a}^{(1)} (C_1^{(1)} - C_1^{(2)}) - k_{1a}^{'(2)} (C_1^{(2)} - C_p) - k_{1t}^{(2)} C_1^{(2)} \qquad (A.2)$$

$$Initial\,Cond: C_1^{(1)}(0) = C_1^{(2)}(0) = 0$$

Small Intestine

The small intestine is divided into 7 compartments from (i = 2 to 8) and, i = 9 is the colon. The general equations for each of the compartments with different forms of the drug are given below *(assumes lateral and vertical transit coefficients have same values).*

Notes: (a) in Eqn. (A.3), carrier-mediated transport is ignored; (b) in Eqn. (A.4), gut metabolism is ignored; (c) level 2 is "enterocyte" (level 2).

$$\frac{dC_i^{(1)}}{dt} = C_{ifeed} + k_{(i-1)t}^{(1)} C_{(i-1)}^{(1)} - k_{it}^{(1)} C_i^{(1)} - k_{ia}^{(1)} (C_i^{(1)} - C_i^{(2)}) \qquad (A.3)$$

$$\frac{dC_i^{(2)}}{dt} = k_{ia}^{(1)} (C_i^{(1)} - C_i^{(2)}) + k_{(i-1)t}^{(2)} C_{(i-1)}^{(2)} - k_{ia}^{'(2)} (C_i^{(2)} - C_p) - k_{it}^{(2)} C_i^{(2)} \qquad (A.4)$$

$$Initial\ Cond: C_i^{(j)}(0) = 0 \qquad i = 2,...,9$$

$$Assume\ k_{ia}^{'(j)} = k_{ia}^{(j)}$$

Portal Vein (i.e. Plasma)

The rate of absorption of drug into the portal vein is given by:

$$R_{Abs} = \sum_{i=1}^{9} V_{com,i} k_{ia}^{'(2)} (C_i^{(2)} - C_p) \qquad (A.5)$$

This absorbed drug from the portal vein mixes with some of the recycled drug from the central compartment before it goes into the liver for first pass extraction. The mixing equation is given by:

$$C_{liver,in} = \frac{R_{abs}}{Q_H} + C_p \qquad (A.6)$$

Liver

The drug undergoes first pass elimination in the liver and the model equation is given by:

$$\frac{dC_{liver}}{dt} = \frac{\left[C_{liver,in} Q_H - C_{liver} CL_h - C_{liver} Q_H \right]}{V_{liver}} \qquad (A.7)$$

$$C_{liver}(0) = 0$$

Central Compartment

The final plasma drug concentration (C_p) is measured in the central compartment and the model equation is given by:

$$\frac{dC_p}{dt} = \frac{\left[C_{liver}Q_H - C_pQ_H\right]}{V_{central}} \qquad (A.8)$$

The various properties of compartments in the ACAT model such as the compartment volume, radius and length of each compartment, transit time in each compartment and the pH conditions in each compartment are given in Table A.1.

Table A.1: ACAT model compartment parameters for fasted human physiology (Bolger 2009)

Compartment	Volume (mL)	Radius (cm)	Length (cm)	Transit time (h)	pH
Stomach	47	9.67	28.3	0.25	1.3
Duodenum	42	1.53	14.1	0.26	6.0
Jejunum 1	154	1.45	58.4	0.93	6.2
Jejunum 2	122	1.29	58.4	0.74	6.4
Ileum 1	94	1.13	58.4	0.58	6.6
Ileum 2	71	0.98	58.4	0.42	6.9
Ileum 3	49	0.82	58.4	0.29	7.4
Caecum	47	3.39	13.2	4.19	6.4
Colon	50	2.41	27.6	12.57	6.8

CHAPTER 4

Identifying polymer structures for oral drug delivery – a molecular design approach

Abstract

A computer aided molecular design (CAMD) approach is proposed for generating molecular structures of polymer candidates which have the potential to be effective polymer carriers in drug delivery. A group contribution method has been used to predict properties such as glass transition temperature (T_g), expansion coefficient (α_f) and water absorption (W). A mixed integer nonlinear optimization technique was used to successfully generate some novel polymer structures not available in the literature. The generated polymers have been ranked according to a desirability curve. A solubility parameter analysis was done to further analyze and filter the generated polymers. The proposed new polymers need further investigation to be practically useful in oral drug delivery.

Keywords: oral drug delivery; molecular design; structure - property models; novel polymers; optimization

4.1 Problem Description

In this chapter, we propose a computer aided molecular design (CAMD) approach to generate molecular structures of polymer candidates with desired properties. This work is aimed towards drug product development process, where our focus lies in the development of novel polymers that can be used as potential carrier materials for drugs in drug delivery applications.

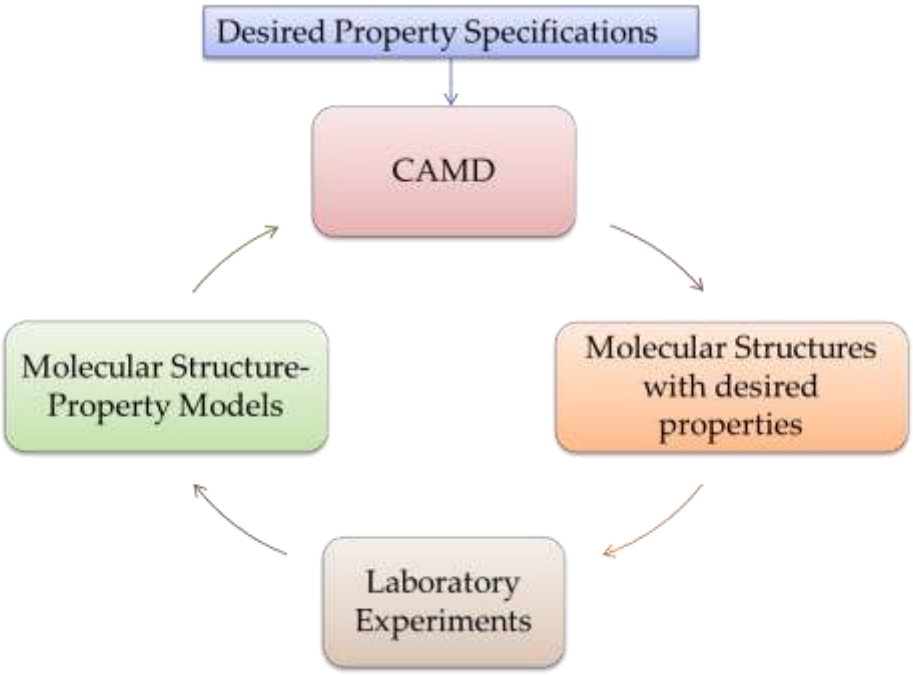

Figure 1: CAMD approach in product development process

To address the problem as stated above, we employ structure-property models, specifically group contributions to predict properties such as glass transition temperature (T_g), expansion coefficient (α_f) and water absorption (W). We then employ a mixed integer nonlinear optimization model to successfully generate molecular structures of novel polymers along with their properties. This approach can significantly reduce the number of laboratory experiments involved in the product development process by identifying a few viable candidates for development (Fig. 1).

4.2 Background and Literature

Polymers have a large impact on our everyday life because of their wide range of applications. Plastics, textiles and rubbers are the most common polymers with extensive use in the society. By convention all the polymers are designed through laboratory scale experiments using trial-and-error techniques. However it is inefficient to completely rely on experimental synthesis and testing of many alternatives, since the number of possibilities can be combinatorially large. Computational polymer molecular design can help in the screening of polymer structures, which can then be followed by laboratory scale experiments. This is economical and less time consuming.

The chemical industry is designing new polymers with desired functional properties for different applications. One such application is in the pharmaceutical industry, where a drug is to be encapsulated inside a polymer matrix to aid in oral drug delivery. For example the drug is to be protected from the various influences in the GI tract. There are several factors in the GI tract which may limit the absorption and solubility of the drug in the intestine; examples are the morphological barriers (mucus layer, micro villi, etc.), chemical barriers (acids, bicarbonates, etc.) and physiological barriers (a wide range of pH, enzymatic activities, specific transport mechanisms, etc.) (Gaucher et al. 2010). Therefore, the dissolution of a drug is quite often, the rate-limiting step, which ultimately controls the bioavailability of the drug. Polymers can be used as drug carriers because the chemical groups present in the structure can firmly bind with the drug and form an amorphous matrix. Polymers aid in targeted drug release in the small intestine where maximum absorption takes place.

4.2.1 Polymers in Oral Drug Delivery

Biodegradable polymers are defined as polymers which degrade in vitro and in vivo either into products that are normal metabolites of the body or into products that can be completely eliminated from the body with or without further metabolic transformation. The degradation products should be nontoxic, and that the rate of degradation and mechanical properties of the material should match the intended application. Nondegradable hydrophobic polymers initially used for drug delivery applications such as poly(dimethylsiloxane) (PS), polyurethanes (PU), and poly(ethylene-*co*-vinyl acetate) (EVA) (Mathiowitz 1999) were not suitable for in-vivo applications due to the need to remove them. Since biodegradable polymers do not have to be removed after delivery, they are preferred vehicles for drug delivery applications. The release of drugs is favored by bioerosion of polymer matrices. Thus, both natural and synthetic biodegradable polymers have been extensively investigated for drug delivery applications.

Natural polymers are mostly chosen due to their excellent biocompatibility, as structurally they closely mimic native cellular environments, have unique mechanical properties, and are biodegradable by an enzymatic or hydrolytic mechanism. However, they have certain inherent disadvantages associated with some of them such as risk of viral infection, antigenicity, unstable material supply, and batch-to-batch variation in properties (Barbucci 2002). Synthetic polymers, on the other hand, offer tremendous advantages over natural polymers from the material side. Due

to their synthetic flexibility it is possible to develop polymers having a wide spectrum of properties with excellent reproducibility. Furthermore, fine-controlling of the degradation rate of these polymers is highly feasible by varying their structure. The section below discusses the applications synthetic and natural biodegradable polymers in drug delivery.

4.2.2 Synthetic Biodegradable Polymers

In controlled drug delivery it is desirable to deliver a biologically active molecule for a desired time period and rate in order to maintain the drug level in the body within the therapeutic window. Synthetic biodegradable polymers have shown great promise in controlled drug delivery. The polymers are used as a matrix from where the drugs will released in a controlled manner. The rate of release of drugs from a matrix depends on several parameters such as nature of the polymer matrix, matrix geometry, properties of the drug, initial drug loading, and drug–matrix interaction (Bae YH 1998, Mathiowitz 1999, Hamdy Abdelkader 2008, Phaechamud 2008). The release of the drug from the polymer matrix can be by (i) a physical mechanism such as diffusion, (ii) solvent controlled or chemical mechanism such as by dispersion or (iii) conjugating drugs in the biodegradable polymer matrix. Several studies have been done to optimize parameters resulting in desired drug release profiles from polymeric matrices.

In case of synthetic biodegradable polymer, the drug release for the polymer matrices can be tuned by controlling the rate of degradation of the polymers by varying the nature and ratios of monomeric units. The biodegradable polymers can be used to form hydrogels. The most important biodegradable polymers for drug delivery applications are aliphatic polyesters such as PLA, PGA, and their copolymers (PLAGA) (Vert et al. 1998, Jain et al. 2011). Initally, monolithic formulations of these formulatios were studied where two-dimensional matrices of suitable geometry were prepared by casting an organic solution of polymer and drug followed by solvent evaporation or by compression/injection molding. Studies were performed to release cyclazocine from PLA implants. Among these, PLAGA became the most suitable polymer for drug delivery due to the ease of property manipulation possible with this polymer (Lewis 1990, Mathiowitz 1999). PEG (Bezemer et al. 2000) and poly (ester carbonates) (Nair and Laurencin 2006) are used as drug delivery systems. Hydrophobic polymers poly(ortho esters) are used treatment of postsurgical pain and ophthalmic diseases. Another aliphatic polyester that assumes importance

as a drug delivery matrix is poly(caprolactone) (PCL). Poly(caprolactone) (PCL) is a semicrystalline polyester, with a melting temperature around 55–60°C and a *T*g of – 60ºC. PCL is highly soluble in organic solvents, has low melting point and *T*g. It has an exceptional ability to form blends with a variety of polymers. It has a low degradation rate. Capronor, is the commercially available long-term contraceptive device based on PCL which releases levonorgestrel following zero order kinetics (Ueda 2003). It has low degradation rate and higher permeability of drugs compared to PLAGA. It has been extensively investigated drug delivery applications (Blanco et al. 2003, Magdalena M. Stevanović 2007, Cynthia D'Avila Carvalho Erbetta 2012). Poly(ortho esters) and polyanhydrides were developed as matrices for drug delivery to achieve zero-order release kinetics (Mathiowitz 1999, Attawia et al. 2001, Chiu Li et al. 2002, Heller et al. 2002).

Several other biodegradable polymer systems investigated as drug delivery matrices include polyphosphazenes (Lakshmi et al. 2003), polyphosphoesters (Zhao et al. 2003), poly(amino acids) , poly(alkyl cyanoacrylates) (Harmia et al. 1986, Nicolas and Couvreur 2009, Dossi et al. 2010), polyhydroxy alkanoates (Kassab et al. 1997, Shrivastav 2013) and poly(glutamic acid) (Li 1998, Yuan et al. 2010).

Langer et al. proposed polyanhydrides to be ideal candidates for drug delivery applications (Rosen et al. 1983, Jain et al. 2008). Poly[(carboxy phenoxy)propane-sebacic acid] (PCPP-SA) is a class of polyanhydride approved by FDA as a delivery matrix for the controlled delivery of the chemotherapeutic agent BCNU to treat brain cancer under the trade name Gliadel.

Poly amino acids like tyrosine-derived polycarbonates are hydrophobic amorphous polymers with *T*g less than 100 ºC and decomposition temperatures around 300 ºC (Ertel and Kohn 1994). Tyrosine carbonates (desaminotyrosyl-tyrosine alkyl esters, DTH) has been investigated for delivering dopamine drug as the polymer has similar structure to the drug and slow degradation rate. Biodegradable polyphosphazenes are now being extensively investigated as matrices for drug delivery applications, particularly protein delivery (Andrianov and Payne 1998, Lakshmi et al. 2003, Brüggemann 2013). Polyphosphoesters are currently being investigated as nerve conduits and as matrices for drug and gene delivery applications (Zhao et al. 2003). Poly(lactide-*co*-ethyl phosphate) matrices were used for delivery of chemotherapeutic drugs such as paclitaxol. They

showed zero order release and now under clinical trials under the trade name PACLIMER (Zhao et al. 2003).

4.2.3 Natural Biodegradable Polymers

Polysaccharides such as cellulose derivatives are important matrices for drug delivery applications (Swarbrick 1991, Robert 2006). Starch has several applications as drug delivery systems. A slow-release drug delivery system based on amylose-rich starch under the trade name Contramid is available in the market. Starch microspheres have been used as a bioadhesive drug delivery system for the nasal delivery of proteins (Illum, Fisher et al. 2001). Alginate hydrogels have shown potential as drug delivery systems (Mumper 1994, Tønnesen 2002, Izawa 2013). Alginate beads are employed for the controlled delivery of many cationic drugs and various growth factors. The drug loading and rate of release from these systems is greatly influenced by the ionic interaction between the drug and the alginate matrix. Polyelectrolyte complexes of alginate with other cationic polymers such as chitosan have been extensively investigated for cell encapsulation or as drug delivery matrices. Cross-linked chitosan hydrogel are attractive materials for controlling drug delivery by varying the cross-linking density. Other drug delivery systems include proteins, gelatin complexes etc.

Polyhydroxyalkanoates (PHA) are biocompatible, processable, and degradable and hence used as matrices for drug delivery applications (Kassab et al. 1997, Ueda 2003, Shrivastav 2013). Poly(γ-glutamic acid) (γ-PGA) was used to deliver a novel drug delivery system to deliver anticancer drug Taxol (Li 1998). The hydrogels of poly(glutamic acid) prepared by γ-irradiation are under investigation as drug delivery matrices (Choi 1995).

Synthetic and natural biodegradable polymers have huge impact as controlled drug delivery systems. However, investigation of more novel and functionalized polymers are required. The future development of biodegradable polymeric biomaterials will consider appropriate physical, mechanical, biological and degradation properties.

The rest of the manuscript is organized as follows. In section 4.3, we discuss some of the well-known property prediction methods available in our arsenal. Section 4.4 describes the computational method used to solve the CAMD problem. In section 4.5, the various aspects considered in developing the CAMD problem are discussed, such as the properties of the polymer

and the problem formulation. Section 4.6 includes the results and discussion followed by conclusions in section 4.7.

4.3 Polymer Property Prediction

A polymer is a macromolecule consisting of identical repeat units (monomers), which are linked by covalent bonds. A polymer containing identical repeat units is called a homo-polymer. The design of a polymer repeat unit requires the ability to estimate the physico-chemical properties of the repeat unit and by extension the polymer itself. There are several property prediction models, some of which are geared toward thermodynamic properties, whereas some are geared towards transport properties. We have employed a computer aided molecular design (CAMD) framework for the design of the repeat unit in a homo-polymer. Specifically desired property targets are to be achieved. In the literature there has been a significant amount of effort on the design of homo-polymer repeat units using CAMD (Venkatasubramanian 1994, Maranas 1996, Camarda and Maranas 1999). The authors used property models to estimate the properties of generated repeat units, which were then screened, based on the desired property constraints.

The accuracy of CAMD methodologies are dependent on the accuracy of the property prediction models. There are two types of property prediction methods, reference methods and approximate methods. Reference methods are generally used to verify or validate a theory. While approximate methods are developed by fitting them to an experimental data and try to match the proposed theory in a limited range (Gani and Constantinou 1996). Hence, the approximate methods are computationally inexpensive but less reliable while the reference methods are computationally intense but more reliable. Some of the reference methods known as mechanical methods are discussed below. Approximate methods are subcategorized into empirical and semi-empirical methods.

4.3.1 Molecular Modeling

Molecular mechanics, molecular dynamics and quantum mechanics are some of the well-known mechanical models. Some of the molecular properties such as electrostatic potentials or polarizability are accurately obtained using Quantum mechanics techniques (Gasteiger and Engel 2003). The calculations involved in Quantum mechanics are complex and slow because the

electrons are treated explicitly. On the other hand molecular mechanics treats electrons implicitly, which makes the calculations much faster than quantum mechanics. Most of the static properties are estimated using molecular dynamic (MD) techniques. Dynamic properties such as viscosity can be estimated using non-equilibrium MD. All the above methods can be used to simultaneously determine the molecular properties and their structure. However, the computational effort involved means that they cannot be used explicitly within a CAMD framework, unless an off-line mode of use is considered.

4.3.2 Empirical and Semi-Empirical Models

Empirical models are models developed based solely on the experimental observations. Some of the well-known empirical models are chemometrics (Timmerman 2008), quantitative structure activity relationship (QSAR) (Esposito 2004), and pattern matching and factor analysis (Wolber 2008). These models are more suitable to study known processes rather than new ones (Gani and Constantinou 1996). Hence, these models are not very applicable in CAMD based polymer design. Semi-empirical models are developed partly on theoretical concepts and partly on observations and are widely used by scientists for property estimation (Van Krevelen 1990).

Some of the most commonly known semi-empirical models are corresponding states models (Sola et al. 2008), topology or geometry based models (Moore and Peters 2005), models based on additivity of groups, atoms or bonds and hybrid methods, which is integration of two or more of the above models (Venkatasubramanian 1994). The group additivity and topology or geometry models are used quite often employed in CAMD algorithms (Derringer and Markham 1985, Venkatasubramanian 1995, Camarda and Maranas 1999). The following sub sections will give a brief theoretical description of the methods used in this work.

4.3.3 Group / Atom / Bond Additivity

Atom, group or bond additivity methods are used for estimating a property of a molecule based on the assumption that the interactions between atom or groups or bonds in a molecule or polymer are effective only within a short range. The property of a molecule using the additive atom or group or bond contribution method is given by Eq. (1).

$$F(Y) = \sum_{i}^{N} m \times p_i \tag{1}$$

Y is the property estimated, p_i corresponds to contribution of atom or group or bond, i, and m corresponds to the number of occurrences of atom or group or bond in a chemical structure. The group additive approach is widely used among these three additive methods. In a group contribution method, the contribution of an individual group is independent of the molecule in which the group occurs. Some of the major contributions in the area of group additivity based property estimation methods is by (Van Krevelen 1990, Gani and Constantinou 1996, Marrero and Gani 2001).

In the method by Marreo and Gani, the molecular structure of a compound is represented as a collection of three types of groups: first-order, second-order and third-order. The first-order groups are used to describe the whole molecular structures while the second- and third-order groups are used to provide more structural information of the molecular fragments (Marrero and Gani 2001). The method for estimating a property, *Y*, is given by Eq. 2.

$$f(Y) = \sum_{i} N_i C_i + w \sum_{j} M_j D_j + z \sum_{k} O_k E_k \tag{2}$$

where, C_i is the contribution of first-order group of type-i that occurs N_i times, D_j and E_k are the contributions of second-order groups of type- j and third-order groups of type- k, that occur M_j and O_k times, respectively. $f(Y)$ is a simple function of the property Y.

Van Krevlen (Van Krevelen 1990) proposed a simple group contribution method for estimating the properties from the homo-polymer repeat unit structures. These property models are quite accurate and have been used widely in different CAMD based applications (Derringer and Markham 1985, Venkatasubramanian 1995).

Property estimation methods based on topological information related to molecular structures commonly use connectivity indices (Kier and Hall 1986, Bicerano 2002). Application of this approach is well known for the estimation of physicochemical properties such as boiling point, partition coefficients, molar refraction, solubilities and many more (Randić 2001). Bicerano (Bicerano 2002) developed property models for estimating polymer properties from the polymer

repeat-unit structures using connectivity indices. A large range of properties can be estimated using this methodology.

4.4 Computational Techniques in Computer Aided Molecular Design

A computational technique is generally used in a CAMD algorithm to find a desired set of feasible chemical structures by generating and evaluating various alternatives. A set of structural and property constraints are used to identify the set of chemically feasible molecular structures that satisfy the design specifications. The generation of a wide range of feasible molecular structures and reliable property estimation of the generated molecular structures are the limiting steps in any CAMD based technique (Churi and Achenie 1996, Duvedi and Achenie 1996, Harper 1999, Karunanithi 2005, Karunanithi 2006).

In a Mathematical optimization technique the CAMD problem is formulated into an optimization problem. Here, the property constraints are formulated as mathematical constraints and the objective function is based on the performance criteria weighting the property values into a single score. Minimizing the objective function solves the optimization problem. A Mixed Integer Non Linear Programming (MINLP) method is commonly employed to solve the optimization problems encountered in CAMD. Application of an MINLP solution technique has disadvantage of (potentially) high computational cost and (potential) difficulties in finding the global optimum (Ostrovsky et al. 2002, Karunanithi 2005, Karunanithi 2006).

4.5 CAMD Model Development – Polymers as Drug Carriers

This section provides a detailed description of the various factors considered in developing the CAMD model. The first factor that is considered is identifying and studying the effect of various polymer properties on the rate of release of the drug from the polymer matrix. A detailed description of the problem formulation and the techniques used to solve the problem are discussed.

4.5.1 Properties of Polymers as Drug Carriers

There are several polymer properties that influence the rate of drug release from a polymer matrix enclosed drug system. Some of the most important properties are described below.

Glass Transition Temperature (T_g): Glass transition temperature is the temperature at which a polymer changes from a glassy state (hard and brittle) to a rubbery state (soft and flexible). It is defined for some crystalline as well as amorphous polymers. The T_g of a polymer is also a measure of the free volume within the polymer. The higher the free volume of the polymer, the lower the T_g and lower free volume implies a higher T_g (Jadhav 2009). For the polymer to be used as a drug carrier, it should be very stable (in glassy state) outside the body and transform into the rubbery state while inside the body to give a better release of the drug. The T_g is expected to be greater than the body temperature (37 ºC).

Molecular weight: Increase in molecular weight leads to decrease in chain end concentration. Higher molecular weight implies a bulkier polymer having a lower free volume, implying a higher T_g.

Expansion Coefficient (α_f): Higher expansion coefficient of polymer implies greater flexibility when it is in its rubbery state inside the GI tract. And greater the expansion, higher the rate of drug release from the polymer matrix.

Water absorption (W): Increase in moisture content leads to increase in free volume due to formation of hydrogen bonds with polymeric chains increasing the distance between polymeric chains (Jadhav 2009). The increased free volume between polymeric chains result in decreased Tg. Simultaneously, low hydrogen bonding between drug and polymer provides more hydrogen bonding sites for water molecules resulting in decreased physical stability.

pH: pH of the polymer plays a major role especially when the polymer is pH sensitive. Depending on the pH of the environment, the polymer will either swell or collapse. For polymers containing acidic groups such as –COOH, -SO3H, it will swell at basic pH (higher pH), which makes it quite stable under acidic conditions inside the stomach. For polymers containing basic groups such as –NH2, it will swell in acidic pH and hence making it unstable in the stomach.

Solubility: If the polymer is highly soluble in water, implying that it has hydrophilic groups in its molecular structure and hence will lead to a higher and faster release of drug. But a high solubility leads to instability in the aqueous medium or inside the GI system. If the polymer contains hydrophobic groups, it is more stable water but poorly soluble and gives a low release of drug. Hence, there is always a tradeoff between the release rate of drug and stability of the polymer based on the solubility.

Pore Size: Higher the pore size or porosity of the polymer, greater the amount of moisture it could absorb leading to a higher drug release rate.

Chemical Groups: Polymers having bulky groups in its structure are less flexible. Bulky groups lead to decrease in the free volume of the polymer, which results in a higher T_g . Higher T_g leads to lower drug release as discussed above. Having long side groups in the structure makes the polymer chains move apart from each other leading to an increase in the free volume. A higher free volume implies a higher drug release. Presence of polar groups in the molecule will lead to increase in the intermolecular forces, attraction within chains and cohesion. This will bring the molecules much closer leading to a lower free volume.

4.5.2 Problem Formulation

A step by step description of the CAMD problem formulation are described as given in Table 1

Table 1: Step by step procedure for formulating a CAMD problem

Step 1	Choose a basis set of groups which could be in the desired polymer repeat-unit
Step 2	Define structural constraints (min. and max. number of groups in the repeat-unit)
Step 3	Define desired property constraints using structure-property models and group contributions
Step 4	Solve Mixed-Integer Nonlinear Optimization Model to obtain repeat units satisfying the constraints from Step 2 and Step 3

According to step 1, the basis set of groups is determined by choosing the most probable groups which could be present in the polymer repeat unit. This is a result of determining all the groups which are present in the molecular structures of polymers currently being used as oral drug

carriers. Table A1 in the appendix gives a list of polymers which we have used to determine the groups and also the groups extracted from each of the polymers, resulting in the basis group set given in Table 2.

Table 2: Basis group set and the respective contributions for different properties

S. No	Group	Valence (v_i)	Molecular weight (M_i) (gm/mol)	Molar glass transition function (Y_{gi}) (gm.K/mol)	Molar volume (V_{gi}) (cm^3/mol)	Molar water content (H_i) (gm(water) /mol)
1	CH_3	1	15	8121.78	35.5	0
2	CH_2	2	14	2361.26	16.1	$3.3E^{-5}$
3	CH	3	13	987.78	-1	0
4	C	4	12	0	-19.2	0
5	$CH=CH$	2	26	5976.32	27	0
6	SiO	2	44	-18917.29	3.8	0.02
7	COO	2	44	21739.93	18	0.075
8	OH	1	17	17433.54	10	0.75
9	$CHCl$	2	48.5	19388.75	25	0.015
10	$CONH$	2	43	30748.83	9.5	0.75
11	CH_2O	2	30	5834.32	19.9	0.02
12	CH_2COO	2	58	15447.25	34.1	0.075
13	N	3	14	-31461.27	5	0
14	CCN	3	38	15883.2	4.8	0.065
15	$CHCN$	2	39	17695.43	23	0.065
16	$CONHCH_2$	2	57	23529.58	25.6	0.75
17	$CHCOO$	3	57	11629.78	17	0.075
18	CH_2NH	2	29	33150.95	20.6	0.64
19	CHO	3	29	2250.41	22.3	0.02

20	CH_2CO	2	42	13169.56	26.9	0.11

According to step 2, the structural constraints include the minimum ($n_{\min}$) and maximum ($n_{\max}$) number of groups, which could be present in the repeat unit given by Eq. (3). They include the valence constraint, which is the total valence of the polymer repeat unit defined using Eq. (4). The structural constraints make sure that the molecules obtained are physically realizable.

$$n_{\min} \le \sum_i n_i \le n_{\max} \tag{3}$$

$$\sum_i (2 - v_i) n_i = 2(k-1) \tag{4}$$

where, n_i and v_i are the number and valence, respectively, of the groups of type i; k in the equation takes the value of 1, 0 or -1 depending on the type of structures formed, namely acyclic, monocyclic and bicyclic. In our work, we concentrated on acyclic structures.

According to step 3, property constraints define the desired limits for property values and are given by Eq. (5). These properties are estimated using correlations and structure-property models such as group contributions.

$$P_l \le P(n_i) \le P_u \tag{5}$$

where, P_l and P_u are the lower and upper bounds of the properties specified for a polymer repeat unit structure and $P(n_i)$ is the predicted property value. In this work, three different properties are considered, namely, glass transition temperature (T_g), expansion coefficient (α_f) and water absorption (W) are estimated using Eq. (6).

$$T_g = \frac{\sum Y_{gi}}{\sum M_i} \qquad \alpha_f = \frac{0.115}{T_g} \qquad W = \frac{18 \sum H_i}{\sum M_i} \tag{6}$$

where, H_i, M_i and Y_{gi} represent the group contributions for molar water content, gram molecular weight and molar glass transition function respectively.

Finally in step 4, we solve the formulated problem using a computer aided technique such as mixed-integer nonlinear optimization to generate the molecular structures of repeat units satisfying the constraints defined in step 2 and step 3. The CAMD optimization problem can be expressed as given in Eq. (7).

$$\min f(x) \tag{7}$$

s.t.

$$0 \le Ax \le b \tag{8}$$

$$g(x) \le 0 \tag{9}$$

$$x \equiv \text{integer}$$

where, the linear constraints comprise of the structural constraints given by Eq. (8), and the nonlinear constraints comprise of the valence and property constraints given by Eq. (9). The performance objective function ($f(x)$) can be in different forms. In this work we used a desirability function for glass transition temperature (T_g) as the objective function and is given by Eq. (10).

$$f(x) = 1 - d_i(x) \tag{10}$$

where,

$$d_i = \begin{cases} \left[\dfrac{Y_i - Y_i^l}{c_i - Y_i^l} \right]^s & Y_i^l \le Y_i \le c_i \quad (11) \\ \left[\dfrac{Y_i - Y_i^u}{c_i - Y_i^u} \right]^t & c_i \le Y_i \le Y_i^u \quad (12) \end{cases}$$

where, Y_i is the predicted property value, Y_i^u and Y_i^l are the upper and lower bounds of the property, c_i is the most desirable value of the property, which corresponds to a desirability of 1. The values of s and t determine the rate at which the property is changing above and below c_i.

4.5.3 Mixed Integer Nonlinear Optimization – Outer Approximation Algorithm

The mixed integer nonlinear optimization problem discussed in step 4 is solved using a generalized outer approximation (GOA) algorithm. The algorithm involves successive solutions of nonlinear programs (NLP's) and mixed integer linear programs (MILP's). Here, each iteration generates an

upper and lower bound on the MINLP solution. A general form of the optimization problem is given by Eq. (13) (Floudas 1995).

$$\begin{aligned} \min_{x,y} \quad & f(x,y) \\ s.t. \quad & g(x,y) \le 0 \\ x \in R \quad & y \in Z \end{aligned} \tag{13}$$

In the first step, a resulting primal problem $P(y^1)$ is solved for an initial value of y^1 and the obtained solution is denoted by x^1. The primal problem is given by Eq. (14) is an NLP. The current upper bound is set as $UBD = P(y^1)$.

$$\begin{aligned} \min_{x,y} \quad & f(x,y^1) \\ s.t. \quad & g(x,y^1) \le 0 \\ x \in R & \end{aligned} \tag{14}$$

In the second step, the relaxed master problem given by Eq. (15), is solved. The relaxed master problem is an MILP. The solution to the relaxed master is given by y^{k+1} and μ^k at a general iteration step k.

$$\begin{aligned} \min_{x,y,\mu} \quad & \mu \\ s.t. \quad & \mu \ge f(x^k,y^k) + \nabla f(x^k,y^k)^T \begin{pmatrix} x - x^k \\ y - y^k \end{pmatrix} \\ & 0 \ge g(x^k,y^k) + \nabla g(x^k,y^k)^T \begin{pmatrix} x - x^k \\ y - y^k \end{pmatrix} \\ x \in R \quad & y \in Z \end{aligned} \tag{15}$$

where, x^k is the feasible solution to the primal problem $P(y^k)$. The lower is evaluated from the current step given by $LBD = \mu^k$. The primal problem for the next iteration is given by $P(y^{k+1})$. The steps 1 and 2 are repeated until Eq. (16) is satisfied i.e., until the upper and lower bounds are very close to each other.

$$UBD - LBD \le \varepsilon \tag{16}$$

The NLP's and the MILP's are solved using Matlab programming. The solution to the primal problem solved is the starting point for the MINLP. Since this is a local optimum, the optimal solution to the MINLP is obtained quite quickly.

4.6 Results and Discussion

Following the step by step procedure as discussed in the previous section, the resulting problem formulation is given in Table 3. The problem defined was to generate molecular structures of novel polymers which could be used as potential drug carriers.

Table 3: CAMD problem formulation

Basis Set	$CH_3, CH_2, CH, C, CH=CH, SiO, COO, OH, CHCl, CONH, CH_2O, CH_2COO, N, CCN, CHCN, CONHCH_2, CHCOO, CH_2NH, CHO, CH_2CO$	
Structural constraints	Minimum (n_{min})	Maximum (n_{max})
Groups/repeat unit	2	6
Valence constraint	$\sum(2-v_j)n_j = 0$	
Property constraints	Minimum	Maximum
Glass transition temperature (T_g)	37 ºC	177 ºC
Expansion coefficient (α_f)	0.1x10^{-4} K^{-1}	10x10^{-4} K^{-1}
Water absorption (W)	0.08 g (water)/g (polymer)	0.35 g (water)/g (polymer)

The resulting CAMD problem as shown in Table 3, is solved using a mixed-integer nonlinear optimization and the molecular structures generated are given in Table 4. The values of predicted properties such as T_g, α_f and W are provided along with the repeat unit structures in Table 4. The predicted structures have properties within the desired range. All these structures can be further evaluated with the help of a polymer chemist to be potential new polymers which can be used as efficient drug carriers for different types of drugs.

Table 4: Molecular structures of polymer repeat units and predicted properties

S. No.	Groups	Repeat unit structure	T_g (°C)	α_f (K^{-1}) x 10^4	W (g (water)/g (polymer))
1	16, 16	$-\left[CONHCH_2-CH_2NHCO\right]_n-$	139.8	2.786	0.2368
2	11, 16	$-\left[OCH_2-CONHCH_2\right]_n-$	64.5	3.407	0.1593
3	8, 19	$-\left[CHOH-O\right]_n-$	154.9	2.687	0.3013
4	8, 17	$-\left[CHOH-COO\right]_n-$	119.7	2.928	0.2007
5	2, 16	$-\left[CH_2-CONHCH_2\right]_n-$	91.6	3.154	0.1901
6	2, 11, 16	$-\left[CH_2-CH_2O-CONHCH_2\right]_n-$	41.1	3.661	0.1372
7	11, 16, 16	$-\left[CONHCH_2-CH_2O-CH_2NHCO\right]_n-$	94.3	3.131	0.1900
8	16, 16, 16	$-\left[\left(CH_2NHCO\right)_3\right]_n-$	139.8	2.786	0.2368
9	2, 10, 12	$-\left[CONH-CH_2-CH_2COO\right]_n-$	149.2	2.724	0.1291
10	8, 12, 17	$-\left[CHOH-COO-CH_2COO\right]_n-$	64.2	3.411	0.1227
11	16, 16, 20, 20	$-\left[\left(CONHCH_2\right)_2-\left(CH_2CO\right)_2\right]_n-$	97.7	3.102	0.1460
12	8, 16, 19, 20	$-\left[CONHCH_2-CHOH-O-CH_2CO\right]_n-$	115.8	2.957	0.2023
13	1, 4, 8, 12	$-\left[CCH_3OH-CH_2COO\right]_n-$	129.0	2.861	0.1456
14	3, 7, 8, 12	$-\left[CHOH-COO-CH_2COO\right]_n-$	148.3	2.729	0.1227
15	2, 8, 12, 19	$-\left[-CHOH-O-CH_2-CH_2COO\right]_n-$	44.7	3.619	0.1289
16	12, 12, 16, 16	$-\left[\left(CONHCH_2\right)_2-\left(CH_2COO\right)_2\right]_n-$	65.9	3.393	0.1291
17	3, 8, 11, 12	$-\left[-CHOH-CH_2O-CH_2COO\right]_n-$	63.5	3.418	0.1289

18	8, 10, 12, 17	$-\left[-CHOH-COO-CONH-CH_2COO\right]_n-$	157.0	2.674	0.1697
19	2, 8, 12, 14	$-\left[-CCNOH-CH_2-CH_2COO\right]_n-$	129.6	2.857	0.1261
20	11, 11, 16, 16, 20	$-\left[\left(CONHCH_2\right)_2-\left(CH_2O\right)_2-CH_2CO\right]_n-$	59.8	3.455	0.1375
21	8, 13, 18, 20, 20	$-\left[NOH-CH_2NH-\left(CH_2CO\right)_2\right]_n-$	42.7	3.643	0.2012
22	10, 10, 11, 12, 12	$-\left[\left(CONH\right)_2-CH_2O-\left(CH_2COO\right)_2\right]_n-$	150.4	2.716	0.1296
23	16, 16, 16, 16, 20	$-\left[\left(CONHCH_2\right)_4-CH_2CO\right]_n-$	124.4	2.894	0.2073
24	16, 16, 20, 20, 20	$-\left[\left(CONHCH_2\right)_2-\left(CH_2CO\right)_3\right]_n-$	87.7	3.188	0.1372
25	12, 15, 16, 16, 20	$-\left[\begin{matrix}CH_2COO-CHCN-\\\left(CONHCH_2\right)_2-CH_2CO\end{matrix}\right]_n-$	96.1	3.116	0.1245
26	4, 8, 8, 12, 20	$-\left[C\left(OH\right)_2-CH_2COO-CH_2CO\right]_n-$	161.8	2.645	0.2077
27	8, 12, 12, 14, 16	$-\left[-CCNOH-\left(CH_2COO\right)_2-CONHCH_2\right]_n-$	111.8	2.988	0.1354
28	4, 5, 8, 8, 12	$-\left[C\left(OH\right)_2-CH=CH-CH_2COO\right]_n-$	160.0	2.656	0.2181
29	8, 8, 12, 19, 19	$-\left[\left(CHOH-O\right)_2-CH_2COO\right]_n-$	92.4	3.147	0.1938
30	8, 8, 12, 14, 19	$-\left[CHOH-O-CCNOH-CH_2COO\right]_n-$	157.5	2.671	0.1879
31	1, 10, 12, 13, 18	$-\left[CH_3N-CONH-CH_2COO-CH_2NH\right]_n-$	79.2	3.265	0.1658

32	15, 15, 16, 16, 16, 16	$-\left[(CONHCH_2)_4-(CHCN)_2\right]_n-$	150.2	2.717	0.1841
33	16, 16, 18, 20, 20, 20	$-\left[(CONHCH_2)_2-CH_2NH-(CH_2CO)_3\right]_n-$	172.0	2.584	0.1653
34	10, 16, 16, 20, 20, 20	$-\left[(CONHCH_2)_2-CONH-(CH_2CO)_3\right]_n-$	141.5	2.774	0.1641
35	16, 16, 16, 16, 20, 20	$-\left[(CONHCH_2)_4-(CH_2CO)_2\right]_n-$	113.1	2.979	0.1858
36	16, 16, 16, 20, 20, 20	$-\left[(CONHCH_2)_3-(CH_2CO)_3\right]_n-$	97.7	3.102	0.1564
37	12, 12, 16, 16, 16, 16	$-\left[(CONHCH_2)_4-(CH_2COO)_2\right]_n-$	90.4	3.164	0.1648
38	16, 16, 16, 16, 16, 20	$-\left[(CONHCH_2)_5-CH_2CO\right]_n-$	127.0	2.875	0.2125
39	15, 16, 16, 16, 16, 20, 20	$-\left[CHCN-(CONHCH_2)_3-(CH_2CO)_2\right]_n-$	116.8	2.950	0.1552

The generated molecular structures are provided in the increasing order of the number of groups in the repeat unit. This method does not take into account the order in which the groups are attached to each other. As a result, with increasing number of groups in the repeat unit, there exist several combinations of the groups to form the repeat unit structure. For example, if we consider, repeat unit number 6, consisting of three different groups (group numbers 2, 11 and 16), there exist 3 different possible ways in which the repeat unit structure can be formed (not considering the

possibilities for isomers). The higher the number of groups in the repeat unit, the larger the number of possible structures. This method does not distinguish between the various possibilities, as the predicted property values are the same for all of them.

4.6.1 Ranking of Candidate Polymers

The candidate polymer structures generated can be further filtered based on their estimated properties. The candidates can be ranked based on the desirability function as given by Eq. (11) and Eq. (12). This method was developed by Harrington (Harrington 1965) and further modified by Derringer and Suich (Derringer and Suich 1980). For each predicted property Y_i, a desirability function (d_i) is evaluated. The value of d_i is always between 0 and 1. A d_i value of 1 implies that a polymer with this property value is the most useful for the application, while a value of 0 makes the polymer completely useless. Hence, the higher the value of d_i, the more useful the polymer for the application. If we have multiple polymer properties with desired values, the corresponding desirability can be evaluated using Eq. (17), where the composite desirability (D) is evaluated as the geometric mean of the individual desirability's.

$$D = (d_1 d_2 d_3 .... d_k)^{1/k} \tag{17}$$

where, k is the number of properties considered. The value of D represents the optimality of the polymer considered and has is value between 0 and 1 like the individual desirability's (Derringer and Markham 1985).

We plotted desirability curves based on some of the properties considered such as T_g and W. In case of T_g, as shown in Fig. 1, the most desirable value is 107 ºC, which is midway between 37 ºC and 177 ºC. The polymer must possess high glass transition so that the formulation can be transferred and stored for months. Also the polymer must not itself have a tendency to crystallize (Hancock and Parks 2000, Konno and Taylor 2006). It is preferable that all crystallinity of the drug substance be suppressed by the polymer carrier since small pockets of crystallinity can act as seeds, resulting in additional crystal growth and ultimately reduced shelf-life of the drug formulation (Florence et al. 2011). Normally during summers, the temperature in certain regions reaches close to 50 ºC. So the T_g value must be 40-50 ºC higher than the storage temperature. Therefore a

temperature around 100 ºC is a reasonable value for desirable T_g. The higher the value of T_g, the more difficult it is for the polymer to transform into rubbery state once it is inside the body. So a T_g value below 107 ºC is much more favorable compared to a value above 107 ºC. Hence in Fig. 3, the desirability function is adjusted in such a way that, the curve falls more slowly below 107 ºC and much faster above 107 ºC. This is done by adjusting the values of the variables s and t in Eq. (11) and Eq. (12). For Fig. 2, the value of s is 0.3 and the value of t is 3. Table 5 gives a list of the top six, most favorable structures based on desirability ranking using T_g.

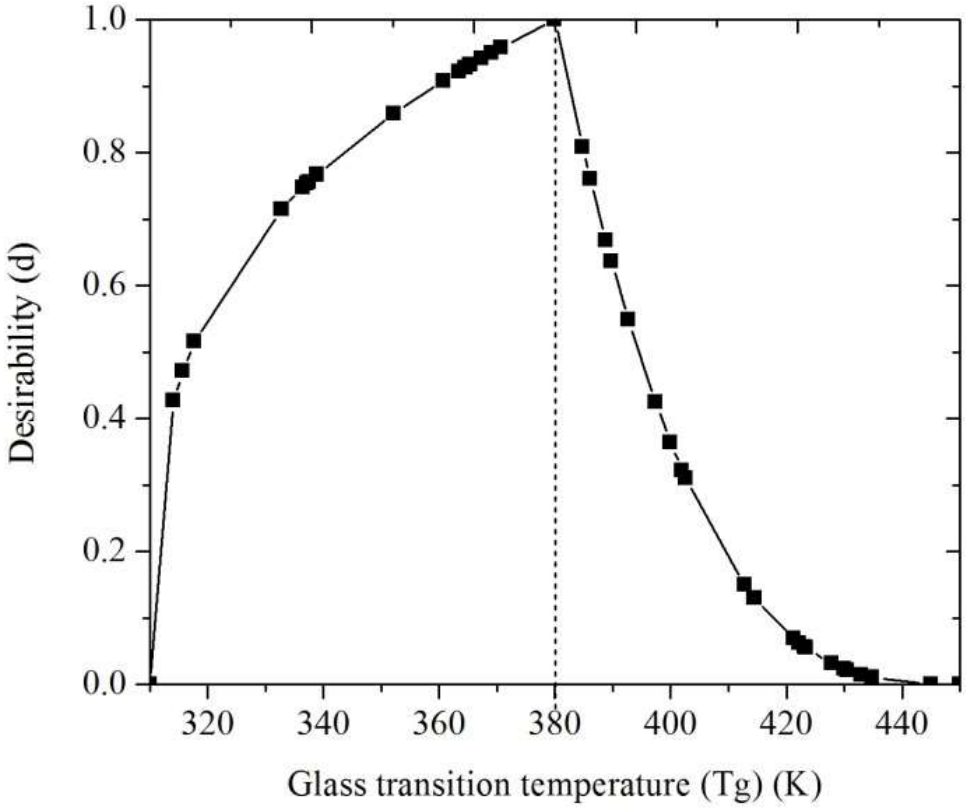

Figure 2: Desirability curve using glass transition temperature (T_g)

Table 5: Desirability and rank of repeat unit structures using glass transition temperature (T_g)

S. No.	Repeat unit structure	T_g (K)	Desirability using T_g	Rank
36	$-\left[(CONHCH_2)_3-(CH_2CO)_3\right]_n-$	97.7	0.9581	1
11	$-\left[(CONHCH_2)_2-(CH_2CO)_2\right]_n-$	97.7	0.9581	2
25	$-\begin{bmatrix} CH_2COO-CHCN- \\ (CONHCH_2)_2-CH_2CO \end{bmatrix}_n-$	96.1	0.9505	3
7	$-\left[CONHCH_2-CH_2O-CH_2NHCO\right]_n-$	94.3	0.9417	4
29	$-\left[(CHOH-O)_2-CH_2COO\right]_n-$	92.4	0.9322	5
5	$-\left[CH_2-CONHCH_2\right]_n-$	91.6	0.9281	6

In case of W , the higher the water absorption capacity of the polymer, the better the release of drug from the polymer matrix. Hence higher the value of W , more desirable is the polymer. Hence, the upper bound of W (W = 0.35) is the most desirable value (Fig. 3). Hence we only use Eq. (12) with a value of s as 1.5, to determine the most favorable polymers with most water absorption. A list of top six polymer structures are given in Table 6.

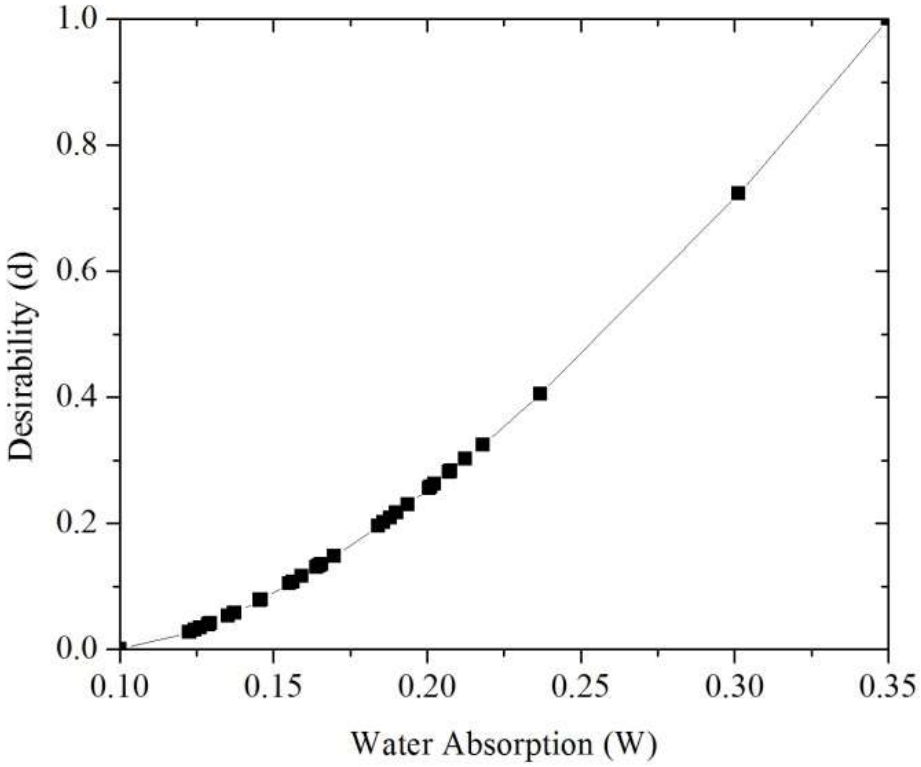

Figure 3: Desirability curve using water absorption (W)

Table 6: Desirability and rank of repeat unit structures using water absorption (W)

S. No.	Repeat unit structure	W (g (water)/ g (polymer))	Desirability using W	Rank
3	$-\left[CHOH-O\right]_n-$	0.3013	0.7225	1
8	$-\left[\left(CH_2NHCO\right)_3\right]_n-$	0.2368	0.4048	2
1	$-\left[CONHCH_2-CH_2NHCO\right]_n-$	0.2368	0.4048	3
28	$-\left[C\left(OH\right)_2-CH=CH-CH_2COO\right]_n-$	0.2181	0.3247	4
38	$-\left[\left(CONHCH_2\right)_5-CH_2CO\right]_n-$	0.2125	0.3019	5
26	$-\left[C\left(OH\right)_2-CH_2COO-CH_2CO\right]_n-$	0.2077	0.2827	6

4.6.2 Solubility Parameter Analysis

The solubility of a polymer is largely dependent on its chemical structure. The miscibility of two materials is more favored when they are structurally similar. The comparison of solubility parameters between two materials determines their extent of miscibility. The solubility parameter (δ) is a numerical value, which determines the relative miscibility between two materials and is defined as the square root of cohesive energy density (cohesive energy per unit volume). The cohesive energy of a solid is the energy required to break the atoms of the solid into isolated atomic species. The solubility parameter value can be estimated using a group contribution method proposed by Hansen (Hansen 1969), and is given by Eq. (18).

$$\delta = \sqrt{\delta_d^2 + \delta_p^2 + \delta_h^2} \tag{18}$$

where,

$$\delta_d = \frac{\sum F_{di}}{\sum V_i} \qquad \delta_p = \frac{\sqrt{\sum F_{pi}^2}}{\sum V_i} \qquad \delta_h = \sqrt{\frac{\sum F_{hi}}{\sum V_i}}$$

where, F_{di}, F_{pi} and F_{hi} are the additive atomic and group contributions to cohesive energy from dispersion forces, polarity and hydrogen bonds of a structural group i, and V_i is the group contribution for molar volume, respectively. Table 7 gives a list of some of the well-known pharmaceutical drugs and their corresponding solubility parameters (Gupta 2011). It also gives a list of the solubility parameters of the generated polymer structures evaluated using the Hansen method. This table contains only the list of polymers which have a comparable solubility parameter value to that of the drugs. Here the polymers are represented using their serial numbers, which are used in Table 4, and both the drugs and polymers are arranged in the increasing order of their δ value. For example, Ibuprofen has a solubility parameter closest to the polymer with S. No. 5, indicating that it is most miscible with that polymer.

Table 7: Comparison of solubility parameters of pharmaceutical drugs and generated polymers

Drug	Solubility Parameter (δ) ($MPa^{0.5}$)	Polymer S. No.	Solubility Parameter (δ) ($MPa^{0.5}$)
Ibuprofen	19.2	5	22.7
Napthalene	20.1	33	24.1
Pimozide	21.1	35	24.3
Haloperidol	22.1	36	24.3
Naproxen	22.7	38	24.3
Phenylbutazone	22.7	23	24.4
Diazepam	22.9	24	24.5
Caffeine	23.2	11	24.8
Prazepam	23.2	8	24.8
Niflumic acid	23.6	39	25.2
Trimethoprim	23.7	1	25.4
Rofecoxib	24.8	34	25.7
Diclofenac	25.1	20	25.9
Temazepam	25.4	32	26.2
Paracetamol	25.5	37	27.4
p-Aminobenzoic acid	25.7	6	27.4
Lorazepam	25.9	7	27.5
Oxazepam	27.3	25	28.3
Theophylline	27.4	16	31.3
p-Hydroxybenzoic acid	27.6	31	32.3
Piroxicam	28.6	21	32.7
Citric acid	29.3	2	32.7
Meloxicam	29.3	12	36.1
Sucrose	30	27	37.4
Mannitol	32	22	37.8
Lactose	40.5	9	40.4

The compounds that are thermodynamically miscible will have similar values of δ. There is an established classification system in the literature for predicting the miscibility of drug and polymers, based on the solubility parameter differences ($\Delta\delta$). According to Greenhalgh et. al. (Greenhalgh et al. 1999), compounds with $\Delta\delta < 7.0$ MPa$^{0.5}$ are likely to be miscible, while for $\Delta\delta > 10.0$ MPa$^{0.5}$, the compounds are completely immiscible. According to Foster et. al. (Forster et al. 2001), compounds that are miscible have $\Delta\delta < 2.0$ MPa$^{0.5}$. In Table 7 we observe that, there are several drugs and polymers with comparable solubility parameters or with $\Delta\delta < 2.0$ MPa$^{0.5}$. For example if we take a very well known drug, Paracetamol with a δ value of 25.5. The polymers, which have an almost equal value of, δ are with serial numbers 1, 34, 39, 20 with increasing value of $\Delta\delta$. Similarly, Paracetamol is almost immiscible with polymer of serial numbers 2, 12, 27, 22, 9 with increasing value of $\Delta\delta$. Therefore, the greater the miscibility between the polymer and drug, the more likely the polymer would be able to suppress the crystallinity of the drug. This is the basis for formation of amorphous solid dispersions (ASD's) for drug delivery. Through this method of comparison, one can identify the most compatible polymer and drug combinations having the best miscibility. This is an effective strategy to filter the polymer candidates generated based on their compatibility with the drug candidates.

The solubility parameters shown in Table 7 dictate the relative hydrophobicity of the novel polymers generated. The solubility parameter provides a numerical estimate of the intermolecular forces within a material and can be a good indication of solubility (Ilevbare et al. 2012). The higher the solubility parameter, more hydrophilic it is.

4.7 Sensitivity and Uncertainty Analysis

All the group contribution parameters used in the CAMD method have an error margin. This means that it is quite possible that some of the feasible molecules will be eliminated due to errors in the property predictions. In order to ensure the accuracy of the method, we performed sensitivity and uncertainty analysis.

We performed parameter sensitivity analysis to analyze the relative sensitivity of model output with respect to the changing parameter values and identifying the most important ones. The parameters in our case are the group contribution of the relevant groups specific to each of the

properties. We performed uncertainty analysis to determine the accuracy of the group contribution method based on the group contribution parameter values and their standard deviations.

We chose a sample molecule generated through the CAMD method, which in this case is molecule with serial number 25 and ranked 3rd in Table 5, and perform sensitivity and uncertainty analysis on this molecule and discuss the results obtained. The sensitivity analysis is done by sequentially varying the model parameters by fixing all the other parameters to their nominal values to determine the model output. Normalized sensitivity coefficient (NSC) values are evaluated from the values obtained using Eq. (19) (Chung 2009). NSC values indicate the importance of a parameter on the model output.

$$NSC = \frac{(\phi - \phi_0)/\phi_0}{(P - P_0)/P_0} \tag{19}$$

where, ϕ_0 is the nominal value of the model output at P_0 the nominal value of the parameter; similarly ϕ is the model output at P. The model output is evaluated using Eq. (10).

The sample molecule with serial number 25 is made up of 4 different groups, namely, CH_2COO, $CHCN$, $CONHCH_2$ and CH_2CO. The contribution parameter and standard deviation values for each of these groups can be obtained from Table 8.

Table 8: Group contribution parameters and standard deviations for molar glass transition temperature

Group	Molar glass transition function (Y_{gi}) (gm.K/mol)	Standard deviation (%)
CH_2COO	15447.25	18.91
$CHCN$	17695.43	34.17
$CONHCH_2$	23529.58	18.94
CH_2CO	13169.56	28.59

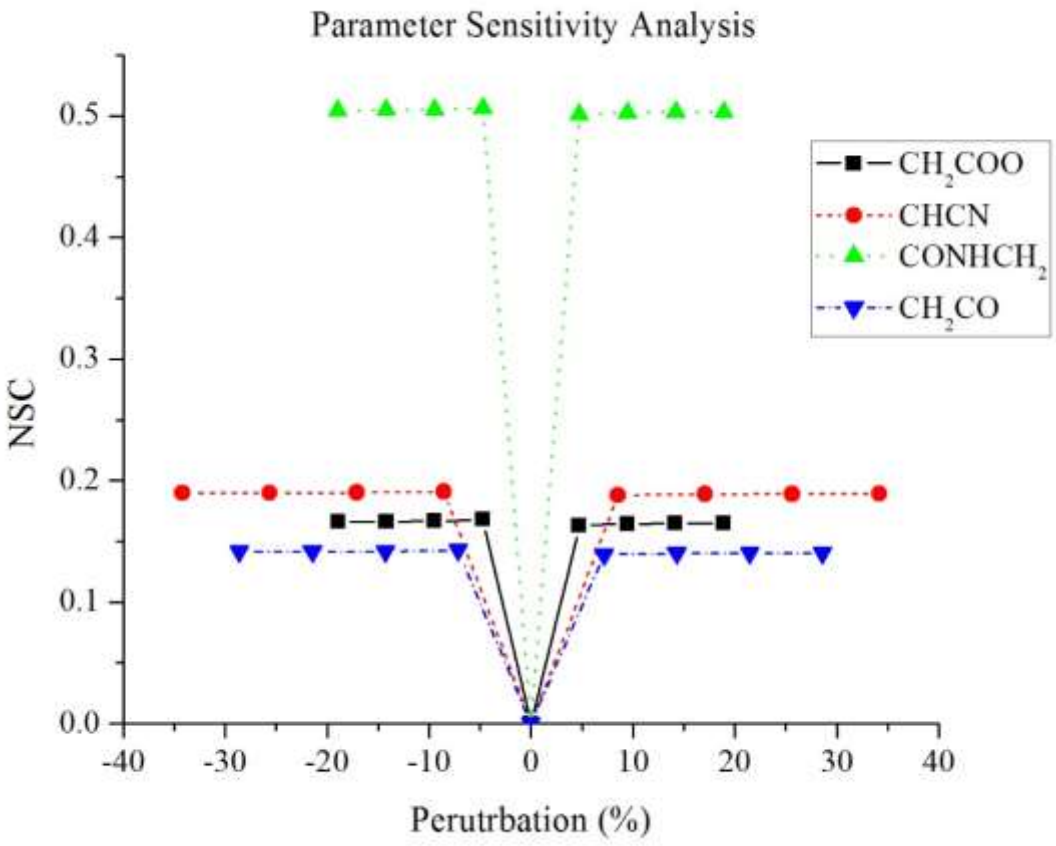

Figure 4: Sensitivity analysis of group contribution parameters

The contribution parameters for each group mentioned in Table 8 are varied according to their standard deviations, keeping the values of other groups a constant and observed the effect on the estimated T_g value. The corresponding NSC values are evaluated and plotted in Fig. 4. We observed that, the NSC values are maximum for the $CONHCH_2$ group, followed by $CHCN$, followed by CH_2COO, and finally CH_2CO group being the least sensitive. This indicated the sensitivity of groups from highest to lowest in the same order. We observe that the sensitivity increases with increase in the contribution parameter value. Since the glass transition temperature is estimated as given in Eq. (6), with increase or decrease in the contribution parameter value of a certain group, there is a corresponding increase or decrease in the NSC value.

We have done uncertainty analysis to see the variability of the group contributions parameters and their effect on the model output. This analysis determined if the parameter values

when taken to the extremes of their standard deviations, satisfy the model constraints. We varied the group parameter values according to the standard deviation values given in Table 8. A plot comparing the contribution parameter of molar glass transition temperature with the estimated glass transition temperature value is given in Fig. 5.

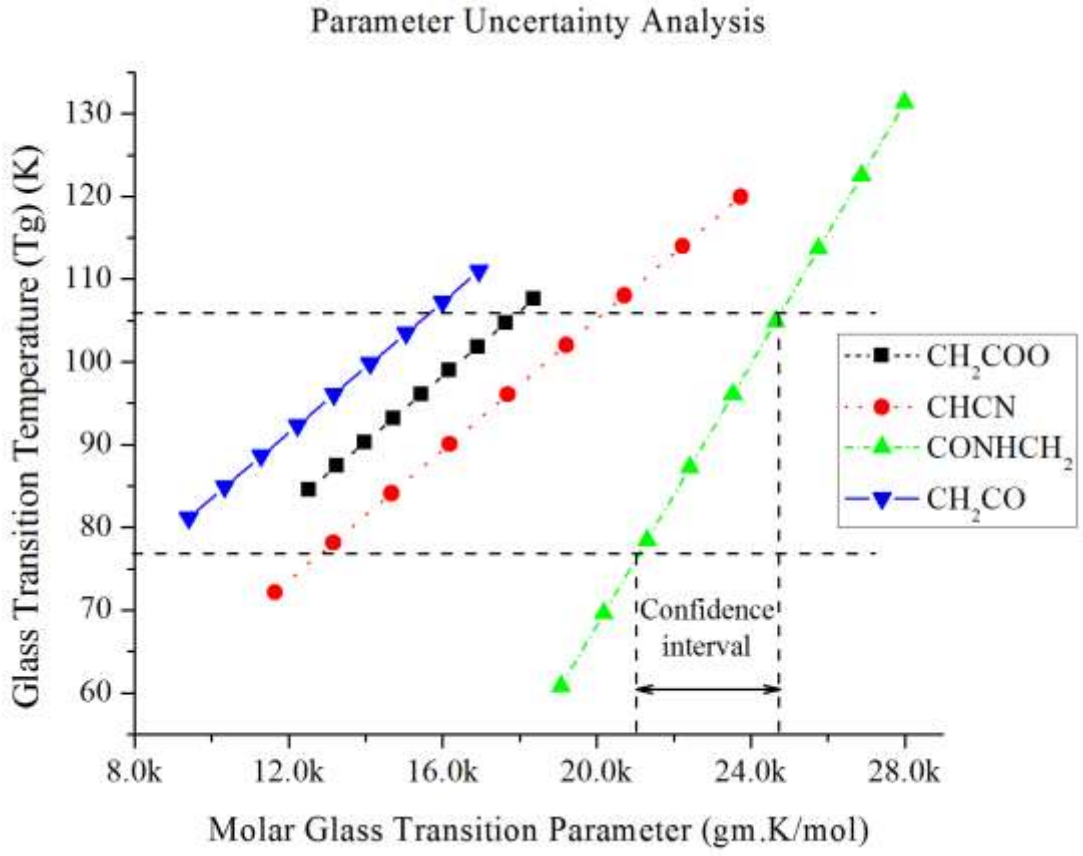

Figure 5: Uncertainty analysis of group contribution parameters

We observed that, there is a proportional change in the estimated property value, which in this case is the T_g value, with change in the contribution parameter value. The lines corresponding to the groups CH_2CO, CH_2COO, and $CHCN$ are parallel because they have an equal slope of 1 mol/gm as they appear once in the repeat unit. While the line corresponding to $CONHCH_2$ has a slope of 2 mol/gm because it appears twice in the repeat unit. Fortunately in our case, the estimated T_g value is within the acceptable bounds of 37 ºC to 177 º as described in Table 3, even when the contribution parameter values are varied to the extremes of their standard deviation values.

However, if the acceptable bounds of T_g are changed to 77 ºC K to 107 ºC as shown in Fig. 4, we observe that some of the estimated T_g values fall outside the bounds with change in the contribution parameter values. A minor part of the curves for the groups CH_2CO and CH_2COO fall outside the bounds, while a significant portion of the curves for the groups $CHCN$ and $CONHCH_2$ fall outside the bounds. This indicates that there is a high possibility of the molecule becoming a failure due to the standard deviation values of the contribution parameters. One solution to this issue is to improve the accuracy of the group contribution parameters by using greater sample size to estimate the parameter value. We can assign confidence intervals to the contribution parameter values by further analyzing the plot as shown in Fig. 4 for the $CONHCH_2$ group.

4.8 Conclusions

A CAMD framework is used to generate molecular structures of polymers with desired properties. We have successfully generated molecular structures of repeat units of polymers which have the potential to be used as efficient carrier materials for drug delivery. The properties used in the problem formulation, namely, glass transition temperature (T_g), expansion coefficient (α_f) and water absorption (W) were effective in reducing the number of possible candidates to a few. As the total number of groups in the repeat unit increased, the number of possible ways in which the repeat unit could be formed increased accordingly. This method does not provide us with a strategy on the how to form the repeat unit, once we have the groups. Hence, there is no distinguishing between the several possible repeat units, as the properties estimated for each of them are same. The formulation does not take into account the constraints based on bond angles. A group contribution method which could consider bond angles and be able to distinguish between different structures in a systematic manner is desired.

The generated polymer structures are ranked using desirability curves. The desirability curves are developed based on a desired property value. We were able to successfully rank the candidates based on the desirability developed using glass transition temperature (T_g) and water absorption (W). The desirability curve is an effective tool to rank the polymer candidates

according to their usability. The higher their desirability value, the more useful the polymer is for the intended application.

A solubility parameter analysis was done to further analyze and filter the polymer candidates. It served as an effective strategy to filter the polymer candidates based on their compatibility with the pharmaceutical drugs. Two compounds with the most similar solubility parameter value are the most miscible. This principle has been effectively used to develop the strategy.

The generated molecular structures using this methodology need further investigation for them to be used for drug delivery applications. An expert opinion from a polymer chemist about the validity of the generated structures is very essential. An opinion about the possibility of synthesizing the new polymers, the practicality and economics involved, will greatly help in progress of this work.

Sensitivity analysis was done for one of the candidate polymers generated and evaluated the NSC values. A change in the contribution parameter value corresponds to a change in the NSC value. The sensitivity of a group contribution parameter increases with increase in the contribution value. Uncertainty analysis revealed that contribution parameter values when changed to the extremes of their standard deviation can make the estimated property value fall out of the acceptable bounds. This can potentially lead to candidate failures. There is need for greater accuracy in the estimated group contribution parameter values to avoid greater uncertainties in the candidate selection process.

The MINLP optimization used to solve the CAMD problem give a local optimum solution. Thus there are multiple solutions based on the starting points. This is one of the major reasons for high computational times, because of the existence of multiple feasible solutions. An excellent way to avoid repeating solutions is to introduce constraints based on heuristics. For example, a constraint can be formed to update the bounds after each iteration to change the feasibility region and avoid repeatability. This would definitely help in eliminating the problem but would increase the complexity of the formulation.

The developed CAMD methodology helps in selecting the most favorable candidates having the desired properties. It greatly helps in the product development process by reducing the number of experimental trials, hence reducing the time and effort involved. It helps in identifying potential failures in the early development process, thereby avoiding late stage failures. We expect our work to greatly aid in the overall product development process.

4.9 Nomenclature

T_g	Glass transition temperature
α_f	Expansion coefficient
W	Water absorption
Y	Estimated property
p_i	Contribution of atom or group or bond
m	Number of occurrences of atom or group or bond in a chemical structure
$n_{\min}$	Minimum number of groups which could be present in the repeat unit
$n_{\max}$	Maximum number of groups which could be present in the repeat unit
n_i	Number of groups of type i
v_i	Valency of groups of type i
P_l	Lower bounds of the properties specified for a polymer repeat unit structure
P_u	Upper bounds of the properties specified for a polymer repeat unit structure
$P(n_i)$	Predicted property value
d_i	Desirability function
δ	Solubility parameter
V_i	Group contribution parameter for molar volume
ϕ_0	Nominal value of the model output
P_0	Nominal value of the parameter
ϕ	Model output at parameter value P

4.10 References

Andrianov, A. K. and L. G. Payne (1998). "Protein release from polyphosphazene matrices." Advanced Drug Delivery Reviews **31**(3): 185-196.

Attawia, M. A., M. D. Borden, K. M. Herbert, D. S. Katti, F. Asrari, K. E. Uhrich and C. T. Laurencin (2001). "Regional drug delivery with radiation for the treatment of Ewing's sarcoma: In vitro development of a taxol release system." Journal of Controlled Release **71**(2): 193-202.

Bae YH, K. S. (1998). Drug delivery. Frontiers in tissue engineering. M. A. Patrick CW, Mcintire LV Oxford**:** 261.

Barbucci, R. (2002). Integrated Biomaterials Science. New York, Kluwer Plenum

Bezemer, J. M., D. W. Grijpma, P. J. Dijkstra, C. A. van Blitterswijk and J. Feijen (2000). "Control of protein delivery from amphiphilic poly(ether ester) multiblock copolymers by varying their water content using emulsification techniques." Journal of Controlled Release **66**(2–3): 307-320.

Bicerano, J. (2002). Prediction of Polymer Properties. New York, Marcel Dekker. Inc.

Blanco, M. D., M. V. Bernardo, R. L. Sastre, R. Olmo, E. Muñiz and J. M. Teijón (2003). "Preparation of bupivacaine-loaded poly(ε-caprolactone) microspheres by spray drying: drug release studies and biocompatibility." European Journal of Pharmaceutics and Biopharmaceutics **55**(2): 229-236.

Brüggemann, I. T. a. O. (2013). "Polyphosphazenes: Multifunctional, Biodegradable Vehicles for Drug and Gene Delivery." Polymers 2013 **5**(161-187).

Camarda, K. V. and C. D. Maranas (1999). "Optimization in Polymer Design Using Connectivity Indices." Industrial & Engineering Chemistry Research **38**(5): 1884-1892.

Chiu Li, L., J. Deng and D. Stephens (2002). "Polyanhydride implant for antibiotic delivery—from the bench to the clinic." Advanced Drug Delivery Reviews **54**(7): 963-986.

Choi, H. J., Yang, R., Kunioka, M. (1995). "Synthesis and characterization of pH-sensitive and biodegradable hydrogels prepared by γ irradiation using microbial poly(γ-glutamic acid) and poly(ϵ-lysine)." Journal of Applied Polymer Science **58**(4): 807-814.

Chung, S.-W., Miles, Fayth L., Sikes, Robert A., Cooper, Carlton R., Farach-Carson, Mary C., Ogunnaike, Babatunde A. (2009). "Quantitative Modeling and Analysis of the Transforming Growth Factor ² Signaling Pathway." Biophysical journal **96**(5): 1733-1750.

Churi, N. and L. E. K. Achenie (1996). "Novel Mathematical Programming Model for Computer Aided Molecular Design." Industrial & Engineering Chemistry Research **35**(10): 3788-3794.

Cynthia D'Avila Carvalho Erbetta, R. J. A., Jarbas Magalhães Resende, Roberto Fernando de Souza Freitas, Ricardo Geraldo de Sousa (2012). "Synthesis and Characterization of Poly(D,L-Lactide-co-Glycolide) Copolymer." Journal of Biomaterials and Nanobiotechnology **3**: 208-225.

Derringer, G. and R. Suich (1980). "{Simultaneous optimization of several response variables}." Journal of quality technology **12**(4): 214-219.

Derringer, G. C. and R. L. Markham (1985). "A computer-based methodology for matching polymer structures with required properties." Journal of Applied Polymer Science **30**(12): 4609-4617.

Dossi, M., G. Storti and D. Moscatelli (2010). "Synthesis of Poly(Alkyl Cyanoacrylates) as Biodegradable Polymers for Drug Delivery Applications." Macromolecular Symposia **289**(1): 124-128.

Duvedi, A. P. and L. E. K. Achenie (1996). "Designing environmentally safe refrigerants using mathematical programming." Chemical Engineering Science **51**(15): 3727-3739.

Ertel, S. I. and J. Kohn (1994). "Evaluation of a series of tyrosine-derived polycarbonates as degradable biomaterials." Journal of Biomedical Materials Research **28**(8): 919-930.

Esposito, E. X., Hopfinger, A.J., Madura, J.D. (2004). Methods for Applying the Quantitative Structure-Activity Relationship Paradigm. **275:** 131-213.

Florence, A. T., D. Attwood and D. Attwood (2011). Physicochemical principles of pharmacy, Pharmaceutical Press.

Floudas, C. A. (1995). Nonlinear and mixed-integer optimization: fundamentals and applications, Oxford University Press.

Forster, A., J. Hempenstall, I. Tucker and T. Rades (2001). "Selection of excipients for melt extrusion with two poorly water-soluble drugs by solubility parameter calculation and thermal analysis." International Journal of Pharmaceutics **226**(1–2): 147-161.

Gani, R. and L. Constantinou (1996). "Molecular Structure Based Estimation of Properties for Process Design." Fluid Phase Equilibria **116**(1): 75-86.

Gasteiger, J. and T. Engel (2003). Chemoinformatics, Wiley-VCH.

Gaucher, G., P. Satturwar, M.-C. Jones, A. Furtos and J.-C. Leroux (2010). "Polymeric micelles for oral drug delivery." European Journal of Pharmaceutics and Biopharmaceutics **76**(2): 147-158.

Greenhalgh, D. J., A. C. Williams, P. Timmins and P. York (1999). "Solubility parameters as predictors of miscibility in solid dispersions." Journal of Pharmaceutical Sciences **88**(11): 1182-1190.

Gupta, J., Nunes, C., Vyas, S., Jonnalagadda, S. (2011). "Prediction of Solubility Parameters and Miscibility of Pharmaceutical Compounds by Molecular Dynamics Simulations." The Journal of Physical Chemistry B **115**(9): 2014-2023.

Hamdy Abdelkader, O. Y. A., and Hesham Salem (2008). "Formulation of Controlled-Release Baclofen Matrix Tablets II: Influence of Some Hydrophobic Excipients on the Release Rate and In Vitro Evaluation." AAPS PharmaSciTech **9**(2): 675-683.

Hancock, B. C. and M. Parks (2000). "What is the true solubility advantage for amorphous pharmaceuticals?" Pharmaceutical research **17**(4): 397-404.

Hansen, C. M. (1969). "The Universality of the Solubility Parameter." Product R&D **8**(1): 2-11.

Harmia, T., J. Kreuter, P. Speiser, T. Boye, R. Gurny and A. Kubi (1986). "Enhancement of the myotic response of rabbits with pilocarpine-loaded polybutylcyanoacrylate nanoparticles." International Journal of Pharmaceutics **33**(1–3): 187-193.

Harper, P. M., Gani, Rafiqul, Kolar, Petr, Ishikawa, Takeshi (1999). "Computer-aided molecular design with combined molecular modeling and group contribution." Fluid Phase Equilibria **158–160**(0): 337-347.

Harrington, E. C. (1965). "The desirability function." Industrial Quality Control(21): 494-498.

Heller, J., J. Barr, S. Y. Ng, H. R. Shen, K. Schwach-Abdellaoui, R. Gurny, N. Vivien-Castioni, P. J. Loup, P. Baehni and A. Mombelli (2002). "Development and applications of injectable poly(ortho esters) for pain control and periodontal treatment." Biomaterials **23**(22): 4397-4404.

Ilevbare, G. A., H. Liu, K. J. Edgar and L. S. Taylor (2012). "Understanding Polymer Properties Important for Crystal Growth Inhibition□ Impact of Chemically Diverse Polymers on Solution Crystal Growth of Ritonavir." Crystal Growth & Design **12**(6): 3133-3143.

Illum, L., A. N. Fisher, I. Jabbal-Gill and S. S. Davis (2001). "Bioadhesive starch microspheres and absorption enhancing agents act synergistically to enhance the nasal absorption of polypeptides." International Journal of Pharmaceutics **222**(1): 109-119.

Izawa, H., Kawakami, K., Sumita, M., Tateyama, Y., Hill, J.P., Ariga, K. (2013). "[small beta]-Cyclodextrin-crosslinked alginate gel for patient-controlled drug delivery systems: regulation of host-guest interactions with mechanical stimuli." Journal of Materials Chemistry B **1**(16): 2155-2161.

Jadhav, N. R., Gaikwad, V.L., Nair, K.J., Kadam, H.M. (2009). "Glass transition temperature: Basics and application in pharmaceutical sector." Asian J Pharm **3**: 82-89.

Jain, J. P., D. Chitkara and N. Kumar (2008). "Polyanhydrides as localized drug delivery carrier: an update." Expert Opinion on Drug Delivery **5**(8): 889-907.

Jain, J. P., W. Yenet Ayen, A. J. Domb and N. Kumar (2011). Biodegradable Polymers in Drug Delivery. Biodegradable Polymers in Clinical Use and Clinical Development, John Wiley & Sons, Inc.**:** 1-58.

Karunanithi, A. T., Achenie, Luke E. K., Gani, Rafiqul (2005). "A New Decomposition-Based Computer-Aided Molecular/Mixture Design Methodology for the Design of Optimal Solvents and Solvent Mixtures." Industrial & Engineering Chemistry Research **44**(13): 4785-4797.

Karunanithi, A. T., Achenie, Luke E. K., Gani, Rafiqul (2006). "A computer-aided molecular design framework for crystallization solvent design." Chemical Engineering Science **61**(4): 1247-1260.

Kassab, A. C., K. Xu, E. B. Denkbas, Y. Dou, S. Zhao and E. Piskin (1997). "Rifampicin carrying polyhydroxybutyrate microspheres as a potential chemoembolization agent." Journal of Biomaterials Science, Polymer Edition **8**(12): 947-961.

Kier, L. B. and H. L. Hall (1986). Molecular Connectivity in Structure Acivity Analysis. New York, John Wiley & Sons.

Konno, H. and L. S. Taylor (2006). "Influence of different polymers on the crystallization tendency of molecularly dispersed amorphous felodipine." Journal of pharmaceutical sciences **95**(12): 2692-2705.

Lakshmi, S., D. S. Katti and C. T. Laurencin (2003). "Biodegradable polyphosphazenes for drug delivery applications." Advanced Drug Delivery Reviews **55**(4): 467-482.

Lewis, D. H. (1990). Controlled release of bioactive agents from lactide/glycolide polymers. New York, Marcel Dekker.

Li, C., Yu, D.F., Newman, R.A., Cabral, F., Stephens, L.C., Hunter, N., Milas, L., Wallace, S. (1998). "Complete Regression of Well-established Tumors Using a Novel Water-soluble Poly(l-Glutamic Acid)-Paclitaxel Conjugate." Cancer Research **58**(11): 2404-2409.

Magdalena M. Stevanović, B. J., and Dragan P. Uskoković (2007). "Preparation and Characterization of Poly(D,L-Lactide-co-Glycolide) Nanoparticles Containing Ascorbic Acid." Journal of Biomaterials and Biotechnology **2007:84965**.

Maranas, C. D. (1996). "Optimal Computer-Aided Molecular Design: A Polymer Design Case Study." Industrial & Engineering Chemistry Research **35**(10): 3403-3414.

Marrero, J. and R. Gani (2001). "Group Contribution Based Estimation of Pure Component Properties." Fluid Phase Equilibria **183**: 183-184.

Mathiowitz, E. (1999). Encyclopedia of controlled drug delivery. New York, Wiley.

Moore, E. L. and T. J. Peters (2005). "Computational topology for geometric design and molecular design." Mathematics for Industry: Challenges and Frontiers. SIAM: 125-137.

Mumper, R. J., Hoffman, A.S., Puolakkainen, P.A., Bouchard, L.S., Gombotz, W.Z. (1994). "Calcium-Alginate Beads for the Oral Delivery of Transforming Growth Factor-B1 (TGF-B1): Stabilization of TGF-B1 by the Addition of Polyacrylic Acid Within Acid-Treated Beads." J. Controlled Rel. **30**: 241-251.

Nair, L. and C. Laurencin (2006). Polymers as Biomaterials for Tissue Engineering and Controlled Drug Delivery. Tissue Engineering I. K. Lee and D. Kaplan, Springer Berlin Heidelberg. **102:** 47-90.

Nicolas, J. and P. Couvreur (2009). "Synthesis of poly(alkyl cyanoacrylate)-based colloidal nanomedicines." Wiley Interdisciplinary Reviews: Nanomedicine and Nanobiotechnology **1**(1): 111-127.

Ostrovsky, G. M., L. E. Achenie and M. Sinha (2002). "On the solution of mixed-integer nonlinear programming models for computer aided molecular design." Comput Chem **26**(6): 645-660.

Phaechamud, T. (2008). "Variables Influencing Drug Release from Layered Matrix System Comprising Hydroxypropyl Methylcellulose." AAPS PharmaSciTech **9**(2): 668-674.

Randić, M. (2001). "The connectivity index 25 years after." Journal of Molecular Graphics and Modelling **20**(1): 19-35.

Robert, H., Marchessault1, François Ravenelle, Xiao Xia Zhu (2006). Polysaccharides for Drug Delivery and Pharmaceutical Applications. F. R. Robert H. Marchessault1, Xiao Xia Zhu, American Chemical Society.

Rosen, H. B., J. Chang, G. E. Wnek, R. J. Linhardt and R. Langer (1983). "Bioerodible polyanhydrides for controlled drug delivery." Biomaterials **4**(2): 131-133.

Shrivastav, A., Kim, H., Kim, Y. (2013). "Advances in the Applications of Polyhydroxyalkanoate Nanoparticles for Novel Drug Delivery System." BioMed Research International **2013**: 12.

Sola, D., A. Ferri, M. Banchero, L. Manna and S. Sicardi (2008). "QSPR prediction of N-boiling point and critical properties of organic compounds and comparison with a group-contribution method." Fluid Phase Equilibria **263**(1): 33-42.

Swarbrick, J., Boyan, H.C. (1991). Gels and jellies In:Encyclopedia of pharmaceutical technology Newyork, Marcel Dekker.

Timmerman, H., Mannhold, R., Krogsgaard-Larsen, P., Waterbeemd, H. (2008). Chemometric methods in molecular design, Wiley. com.

Tønnesen, H. H., Karlsen, J. (2002). "Alginate in Drug Delivery Systems." Drug Development and Industrial Pharmacy **28**(6): 621-630.

Ueda, H., Tabata, Y. (2003). "Polyhydroxyalkanonate derivatives in current clinical applications and trials." Advanced Drug Delivery Reviews **55**(4): 501-518.

Van Krevelen, D. W. (1990). Properties of Polymers. Amsterdam, Elsevier.

Venkatasubramanian, V., Chan, K., Caruthers, J.M. (1994). "Computer-aided molecular design using genetic algorithms." Computers & Chemical Engineering **18**(9): 833-844.

Venkatasubramanian, V., Chan, K., Caruthers, J.M. (1995). Genetic Algorithmic Approach for Computer-Aided Molecular Design. Computer-Aided Molecular Design, American Chemical Society. **589:** 396-414.

Vert, M., G. Schwach, R. Engel and J. Coudane (1998). "Something new in the field of PLA/GA bioresorbable polymers?" Journal of Controlled Release **53**(1–3): 85-92.

Wolber, G., Seidel, T., Bendix, F., Langer, T. (2008). "Molecule-pharmacophore superpositioning and pattern matching in computational drug design." Drug discovery today **13**(1): 23-29.

Yuan, H., K. Luo, Y. Lai, Y. Pu, B. He, G. Wang, Y. Wu and Z. Gu (2010). "A Novel Poly(l-glutamic acid) Dendrimer Based Drug Delivery System with Both pH-Sensitive and Targeting Functions." Molecular Pharmaceutics **7**(4): 953-962.

Zhao, Z., J. Wang, H.-Q. Mao and K. W. Leong (2003). "Polyphosphoesters in drug and gene delivery." Advanced Drug Delivery Reviews **55**(4): 483-499.

4.11 Appendix A

A list of polymers which are currently being used as carriers for pharmaceutical drugs and the corresponding groups extracted from the individual molecular structures of each polymer.

Table A1: List of polymers used in drug delivery as carrier materials

Polymer	Repeat unit structure	Corresponding groups
Polycaprolactone (PCL)	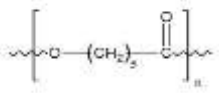	CH_2CO, CH_2O, CH_2
Poly (dimethyl siloxane) (PDMS)	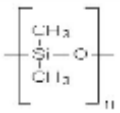	CH_3, SiO
Polyurethanes	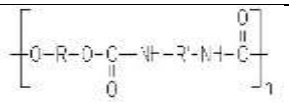	$CONH$, COO
Poly (vinyl chloride) (PVC)	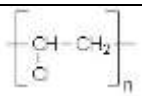	$CHCl$, CH_2
Poly (hexamethylene adipamide) (Nylon 6,6)	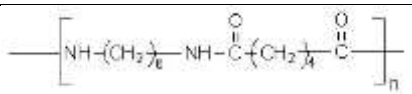	CH_2NH, $CONH$, CH_2CO
Poly (methyl methacrylate) (PMMA)	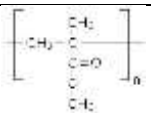	CH_3, CH_2, C, COO
Poly (lactide-co-glycolide) (PLGA)	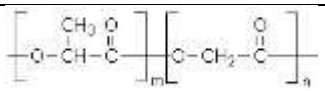	CH_3, CHO, CH_2CO
Polydioxanone (PDO)	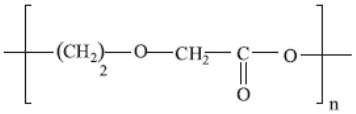	CH_2COO, CH_2O
Poly (sebacic acid)	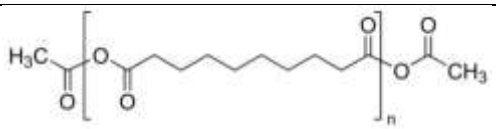	CH_2COO, COO, CH_2
Poly (ortho esters)	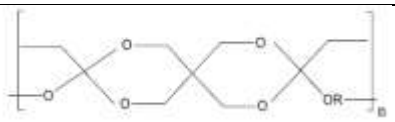	CH_2O, C, CH_2

Poly anhydrides	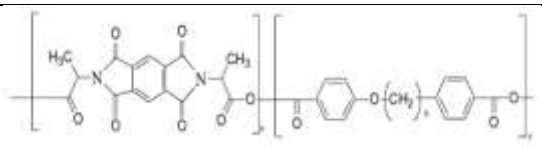	$CH_3, N, CH, CHCOO$
Poly (alkyl cyanoacrylate)	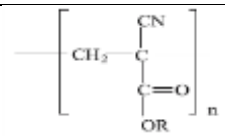	CH_2, CCN, COO
Poly (amino acids)	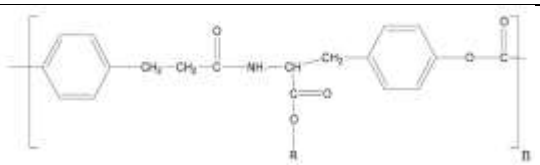	$CH_2CONH, COO, CHCOO$
Cellulose	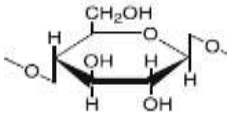	CH_2, CH, OH
Proteins	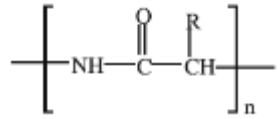	$CONH, CH$
Polyhydroxyalkanoates	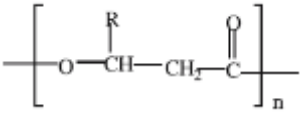	CHO, CH_2CO
Poly (propylene fumarate)	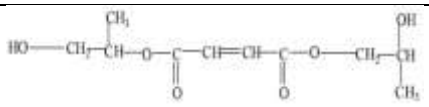	$OH, CH=CH, COO$

CHAPTER 5

Customization of Oral Drug Dosage Form – Innovation in Tablet Design

Abstract

Novel tablet designs (oral drug dosage forms) are proposed which could lead to desired drug release profiles. The targeted drug release profiles include constant or zero-order release, Gaussian release and pulsatile release. The proposed design are supported through mathematical modeling and simulations along with logical and sound explanations. A drug release model was used to simulate tablet designs; it successfully simulated a constant release and a pulsatile release. The duration of the drug release can be controlled by varying the dissolution rate of the polymer matrix in case of constant release. The delay between consecutive pulse releases can be controlled by varying the dissolution rate of the pH sensitive polymer barrier as well as its thickness.

Keywords: tablet customization, oral drug tablet, polymer matrix, drug release profile, polymer barrier, rigid polymer

5.1 Problem Description

In this chapter, we propose some innovative tablet designs (oral dosage form), which could lead to a desired drug release profile. A desired drug release profile is inspired by a desired plasma concentration profile of drug in the blood of the human body. A desired plasma concentration profile is a representation of the desired therapeutic for the patient (Fig. 1).

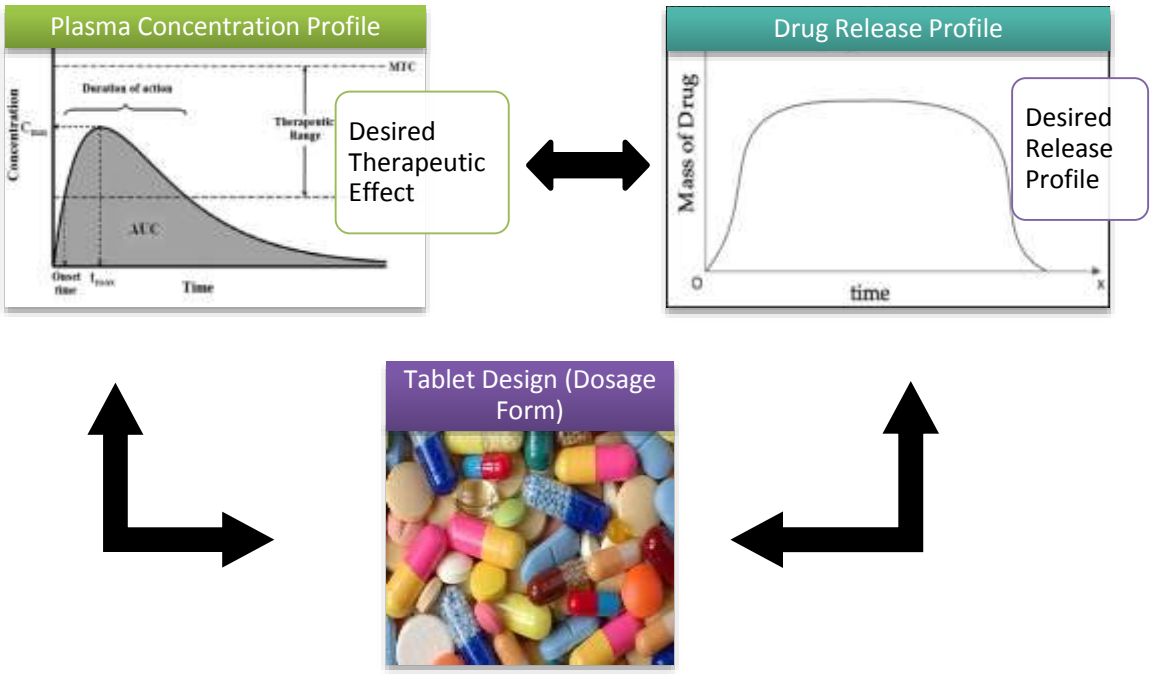

Figure 1: Interdependence of plasma profile, drug release profile and tablet design

We proposed tablet designs for specific desired release profiles such as a constant release (zero order) release, a Gaussian release and a pulsatile release. Different release profiles specified are desired for different kinds of diseases. This work is expected to have a significant impact on the approach to tablet design in the pharmaceutical industry. The customization of oral dosage form is inspired by the idea of providing desired therapeutic effect to each individual patient based on his/her physiological and genetic makeup. It is an important step towards the development of personalized medicine.

5.2 Background and Literature

The plasma concentration profile or the final concentration of blood in the plasma is dependent on the patient's metabolic rate. Once we know the amount of drug in the plasma and the bioavailability of the drug, one can estimate the amount of active pharmaceutical ingredient (API) that has to go into manufacturing the dosage form for each of the individual patients. In order to obtain the desired therapeutic effect specific to each patient, the tablets are cast into several shapes and sizes. A final customized tablet will ensure that the specific targeted patient will receive the most effective dosage of the API at a rate unique to that individual.

Most of the pharmaceutical drugs are manufactured in standard forms with limited range of dosage strengths. Thus a patient is forced to depend on a limited number of ways in which the dose could be administered for maximum effectiveness. This may sometimes lead to toxicity issues due to overdose of the drug, while it may lead to ineffectiveness of the drug in some patients due to insufficient drug dose. This generally varies from patient to patient based on their individual metabolic rates.

Drug delivery devices like reservoir or matrices are important means of delivering the drug at a given rate and duration. The delivery devices are chosen based on the type of drug and delivery kinetics. Matrices are considered more reliable in terms of delivery, less expensive, easier to formulate and less malfunctioning problem. There are several types of matrices such as inert, erodible and swellable. However, we restrict our discussion to swellable matrix given our area of interest.

5.2.1 Polymer Matrix Tablet

In a polymer matrix tablet, the drug is embedded inside a dry polymer. When the polymer comes in contact with the water, it swells and allows the drug to move freely through the swollen polymer. The transport of water through the swollen polymer and the rate of swelling of the polymer are two important factors governing the release of drug from the tablet. Some examples of polymers that are being used in synthesizing matrix tablets are: methylcellulose, hydroxypropyl methylcellulose, polyvinylpirrolyone, or sodium alginate (Wesselingh and Frijlink 2008).

The swelling of a matrix in an aqueous medium of a given drug and a chosen polymer determines the drug release rate from a system which is continuously transforming and then dissolves completely. Apart from the interactions between water, polymer and drug which are the primary factors for controlling the drug release rate, other variables which affect the drug release are drug to polymer ratio, drug solubility, polymer grade (molecular weight and viscosity), filter solubility, drug and polymer particle size and compaction pressure. Matrix shape and size and surface area to volume ratio also affect matrix hydration and drug release.

The underlying mechanisms controlling drug release from matrix of cellulose ethers are very complex. The process involves various physico-chemical process occurring simultaneously and controls the pattern of drug release (Huglin 1989, Colombo 1993). The processes are the

penetration of water into the system upon contact with aqueous media, the dissolution of incorporated drug particles, the swelling of the polymer, and diffusion of dissolved drug molecules through a partially or fully swollen polymer network as well as polymer dissolution. The physico-chemical processes can be strongly dependent on composition of the system (type and amount of drug and polymer). Thus, a mathematical model, which takes into account all relevant phenomenon, must be used.

In order to minimize the computational time and the number of parameters for model simulations, processes with minimum effect on the overall model should be ignored in the theory. Typically each model considers a specific geometry. The shape and dimension of a tablet can affect the drug release kinetics. In order to obtain constant drug release rates with swellable matrices hybrid matrices are used. Several manufacturing techniques are used for design of swellable matrix such as powder compression, granulation, extrusion and ultrasonic compression (Shah et al. 1996, Sheskey and Hendren 1999). There has been some development of multifunctional matrix drug delivery system. Here the geometry or assembly can be manipulated to obtain properties for different forms of controlled release.

In order to obtain constant drug release rates with swellable matrices hybrid matrices are used. For a zero order release, it is important to control the releasing area of the system. An approach introduced by Colombo et al. (Colombo et al. 2008), applied a coating covering different surface area of a hydrogel matrix. Therefore, the dimensionality of the swelling of a matrix could be changed without changing the diffusion characteristics of the drug. Matrices consisting of drug, polymer and filler were partially covered with permeable, semipermeable or erodible coatings.

The shape and geometry of the tablet have a significant effect on the drug release from a controlled release formulation. Several studies on drug release kinetics of polymer matrices proved that the shape and geometry of a tablet can be used to modulate the release rate (Cobby et al. 1974, Ford et al. 1987, Skoug et al. 1991). Reynolds et. al. (Reynolds et al. 2002), have demonstrated that the surface to volume ratio is an important factor in controlling the release rate in HPMC based tablet matrices. The study was done using soluble drugs such as promethazine HCl, diphenhydramine HCl, and propranolol HCl in order to achieve predominantly diffusion-controlled release. According to authors, the tablets with a given surface area to volume ratios gave similar release profiles irrespective of their shape, size and drug dosage. Tablets with lower surface

to volume ratio showed slower drug release. This was a very important discovery in the area of tablet matrix systems, because optimal drug release profiles can be obtained by changing the tablet shape and geometry without changing its formulation (Siepmann et al. 2000).

A donut-shaped matrix tablet design was proposed by Kim et. al. (Kim 1995), in order to achieve zero-order drug release kinetics. The release rate was programmed by adjusting the parameters such as size of the tablet, size of hole in the tablet, partial coating of the matrix and physic-chemical properties of the polymer used (Sangalli et al. 2003). A multilayered tablet system was synthesized by GeomatrixTM (Skye Pharma, London, U.K.). The drug release properties of this system were controlled by placing impermeable, swelling or erodible drug-free barrier layers on the bases of the cylindrical matrix. The core matrix is placed in an impermeable polymeric tube with one end opened. According to the device configuration, the mode of drug delivery can be obtained such as extended release, floating or pulsatile systems (Fig. 2) (Krögel and Bodmeier 1999). A novel Dome matrix technology was proposed based on Hydroxy Propyl Methyl Cellulose (HPMC) matrices of varying shapes which could give various release profiles described above (Losi et al. 2006, Colombo et al. 2008).

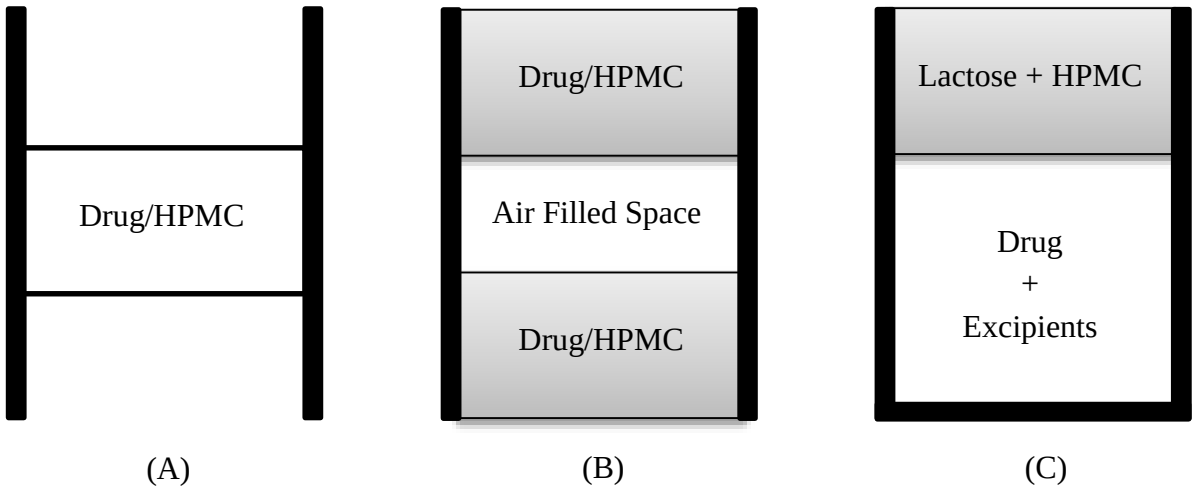

Figure 2: Schematic representation of prolonged release: (A) floating; (B) pulsatile release; (C) configurations in a multifunctional drug delivery system composed of HPMC matrices inserted in an impermeable polymer tube (Krögel and Bodmeier 1999).

Innovative tablet geometries could be studied that could allow accurate drug delivery due to changes in volume or surface/volume ratio modifications than to formulation changes. Dome

Matrix “release module assemblage” is a swellable matrix in the shape of a disc having one base convex and the other concave (Fig. 3). The release studies indicated different release behavior and kinetics for the concave, convex and flat base matrices. The convex base showed a faster drug release rate compared to a concave base, while the release rate for flat base was intermediate (Losi et al. 2006).

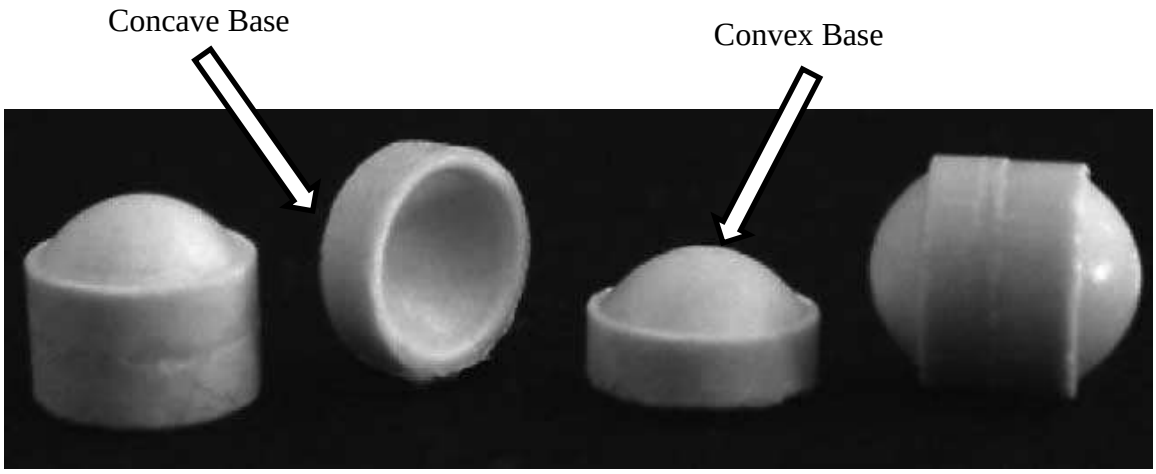

Figure 3: The Dome Matrix individual and assembled release modules (Losi et al. 2006)

5.3 Proposed Tablet Designs

We propose three different tablet configurations based on three different drug release profiles. A detailed explanation of each of the tablet configurations is described below.

5.3.1 Design 1 – Constant Release Profile

The first drug release profile is the constant release profile (zero-order release) as shown in Fig. 4.

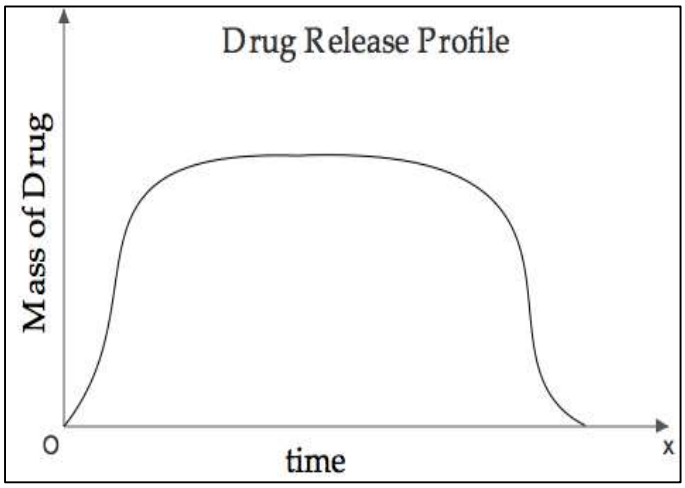

Figure 4: Constant or zero-order release profile

This tablet configuration leads to the zero-order release profile as shown in Fig. 5. Here, we show the front view and the top view of the solid drug tablet. The Tablet is cylindrical in shape with a thickness of length 2L and a radius of length R.

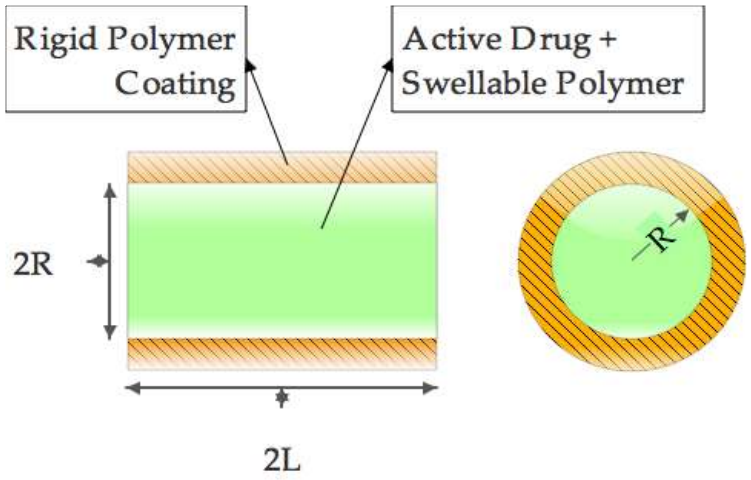

Figure 5: Tablet configuration for constant release profile – lateral view and cross-section

The tablet contains two different layers. The outer layer is a rigid polymer coating as shown in Fig. 5, while the inner layer is a regular oral tablet composition containing API, polymer and excipients. The rigid polymer in our case is defined as any polymer that does not allow drug permeation. Therefore only the curved part of the cylindrical tablet is coated with the rigid polymer, while the two flatter sides of the cylinder (front and rear) have the coating only on the perimeter. Hence, when this tablet enters the gastrointestinal (GI) tract and is exposed to the bodily fluids, the rigid polymer coating forces the tablet to release the drug only through the lateral sides

of the cylindrical tablet. The process of drug release is diffusion as in any other drug enclosed polymer matrix system. In this case, the area through which the drug diffusion is taking place is given by ($Area = \pi R^2$), on both sides of the cylinder. The rigid polymer on the curved surface ensures that this area of diffusion is always constant. Hence the drug diffuses at a constant rate from the tablet, which will lead to a constant release profile (Fig. 4) until the entire drug is diffused. We have simulated this design in the following sections using a drug release model.

5.3.2 Design 2 – Gaussian Release Profile

We propose a second design that will lead to a Gaussian release profile as shown in Fig. 6. A Gaussian release profile is obtained when the drug release rate continuously increases with time till it reaches a peak and then falls at the same rate.

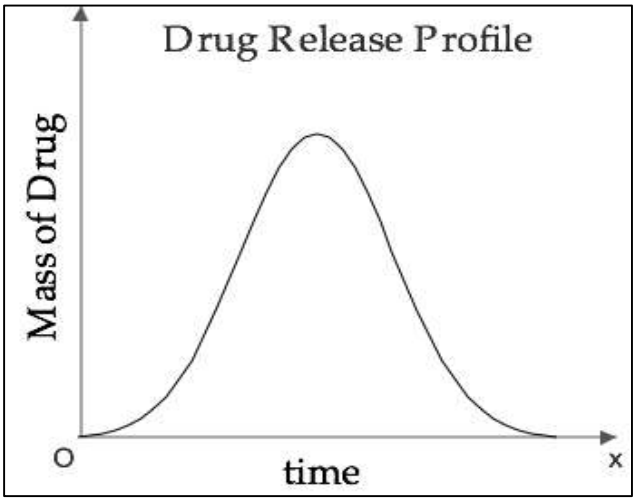

Figure 6: Gaussian Release Profile

For this profile the tablet design looks like a hexagon from the front (lateral view) and circular from the top (Fig. 7). This can be more aptly described as a cylindrical tablet with tapered edges. This tablet has a thickness of 2L and the circular lateral ends have a radius of R. This tablet has its curved surface coated with a rigid polymer as in design 1. However, we coat one of the lateral sides with the rigid polymer.

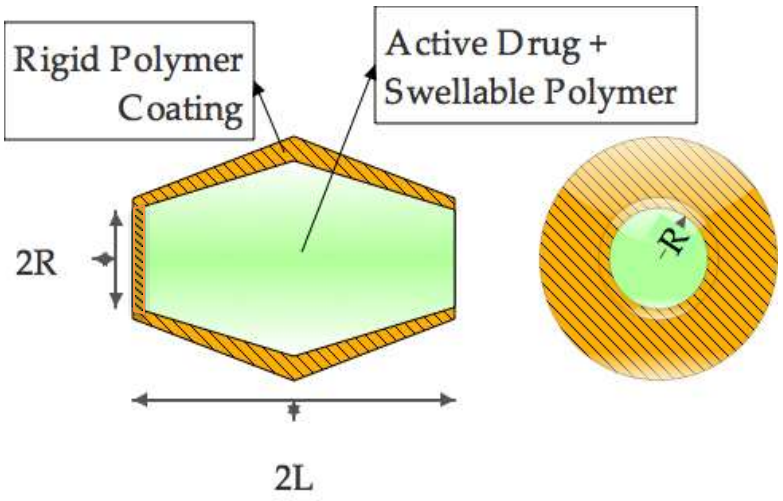

Figure 7: Tablet configuration for Gaussian release profile – lateral view and cross-section

When this tablet encounters the bodily fluids, the drug is forced to diffuse only through the one open lateral side (not coated with the rigid polymer). As the drug diffuses, and the solid drug/swollen polymer interface moves towards the center, there is an increase in the radius of the area of diffusion. This increase in diffusion area leads to an increase in the drug release rate until it reaches the center of the tablet, where the radius of diffusion is at its maximum. Once the interface crosses the center of the tablet, the diffusion area decreases leading to a steady decrease in the rate of drug release until the entire drug is released. This process in overall leads to a Gaussian release profile.

5.3.3 Design 3 – Pulsatile Release Profile

The third release profile we propose is the pulsatile release profile wherein the drug is released as small packets with a small time delay between each packet of drug release (Fig. 8).

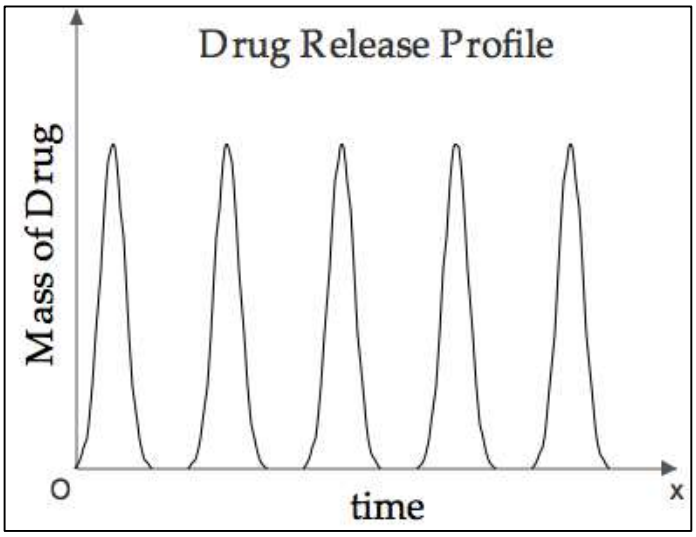

Figure 8: Pulsatile Release Profile

For this profile the tablet design is very similar to the design for a constant release profile (Fig. 5). This is a cylindrical tablet with a thickness of 2L and radius R. This tablet has its curved surface coated with a rigid polymer as in design 1. One major addition to this design is the pH sensitive polymer barriers along the length of the cylindrical tablet (Fig. 9).

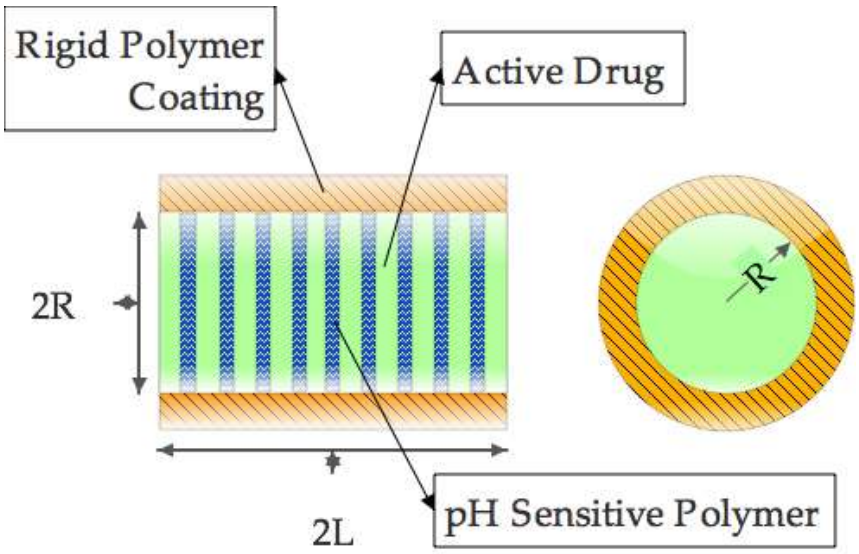

Figure 9: Tablet configuration for pulsatile release profile – lateral view and cross-section

When this tablet reaches the area in the GI tract with the proper pH, the pH-sensitive polymer dissolves exposing the drug to the bodily fluids. The drug is then released in a similar fashion as described above due to polymer swelling, drug diffusion and water diffusion. The pH

sensitive barriers arranged at equidistant places along the length of the tablet introduce a time delay after each packet of drug is released. The delay time can be adjusted by varying the thickness of the pH sensitive polymer. Through this design a pulsatile release profile is achieved.

5.4 Results and discussions

We used the drug release model discussed in the previous chapters to simulate some profiles that could be obtained through the tablet configurations proposed in this work. We were able to successfully simulate a constant release profile (Fig. 10) and a pulsatile release profile (Fig. 11).

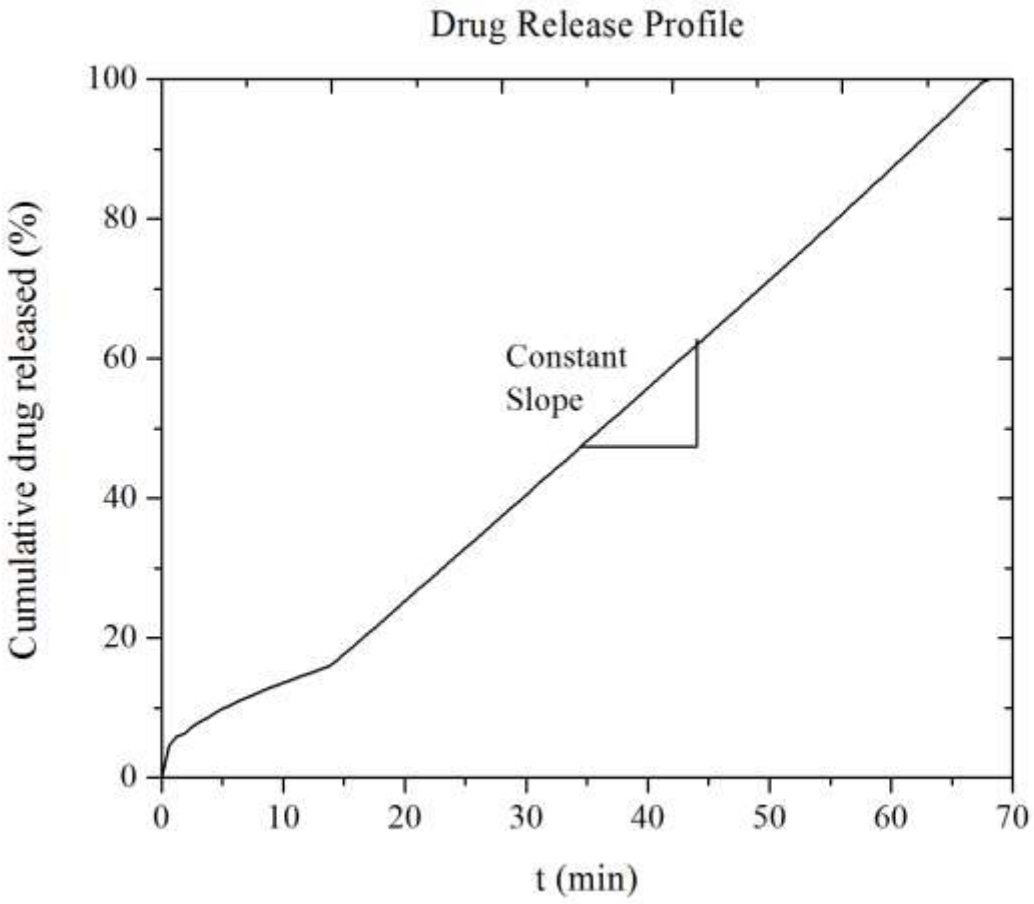

Figure 10: Simulated constant release profile for design 1. Constant slope indicates a zero-order release

We observe that the model predicts the initial burst release of the drug followed by a constant release profile as expected. The total time for drug release can be changed by varying the

dissolution rate of the polymer. We simulated a pulsatile release profile as shown in Fig. 11 for tablet design 3.

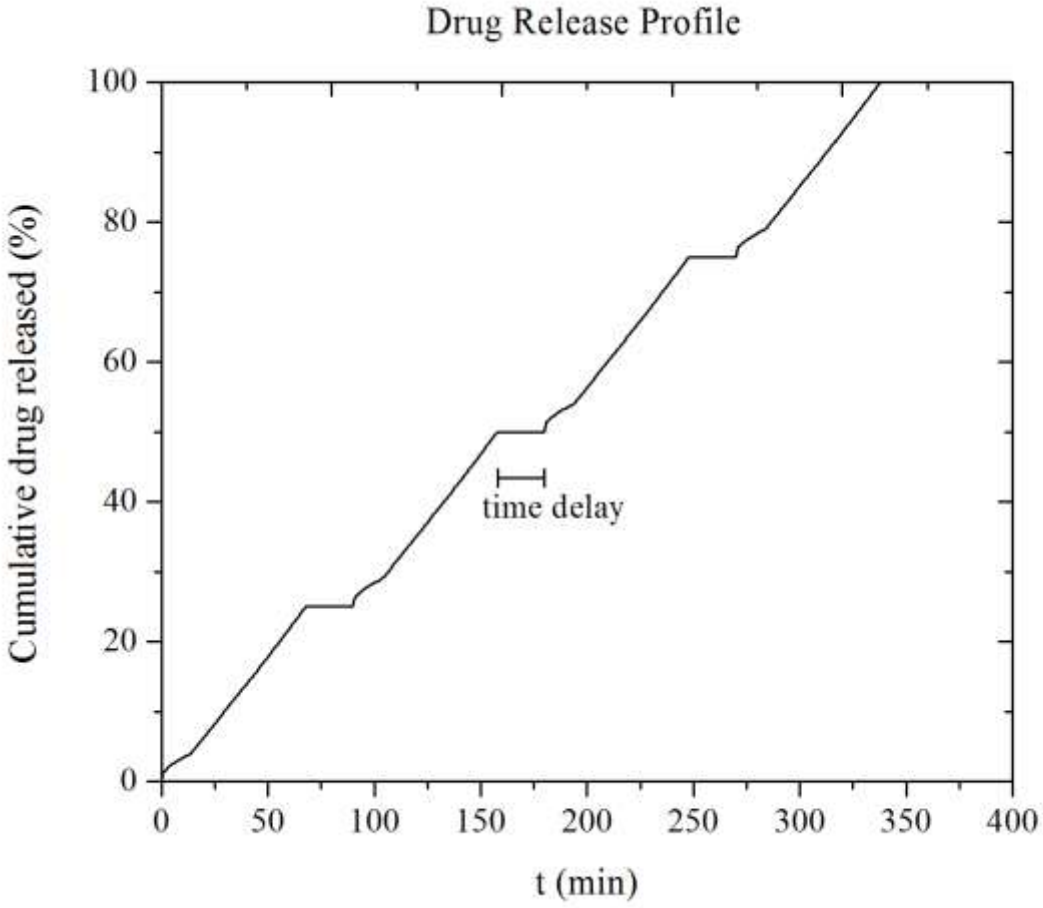

Figure 11: Simulated pulsatile release profile for design 3. Time delay indicates the delay between two consecutive pulse releases

When the first pulse of drug is released, there is a gap before the next pulse as shown in Fig. 11. There is no drug release during this gap, indicating that degradation of the pH sensitive polymer barrier is taking place. It is possible to increase or decrease this time gap by correspondingly changing the thickness of the polymer barrier or by using different polymers with different dissolution rate constants.

5.5 Conclusions

We proposed tablet configurations (dosage form designs) which could potentially lead to desired drug release profiles such as a constant or zero-order release profile, Gaussian release profile and a pulsatile release profiles. The proposed configurations are theoretically sound with simple designs that could be manufactured with little difficulty. The practicality of the designs can only be ascertained through thorough experiments and availability of the desired polymers for different applications discussed in this work. These include rigid polymers, swelling polymers and pH sensitive polymers.

We simulated the release profiles that could be obtained using the drug release model. We were able to successfully simulate the profiles for constant release and pulsatile release. The dissolution time of a constant release tablet can be altered by changing the dissolution rate of the polymer (using different polymers with varying dissolution rate). The time gap between each pulse release in a pulsatile release profile can be controlled by controlling the thickness of the pH sensitive barrier and the dissolution rate of the pH sensitive polymer. The total dose of drug can be varied by varying the drug loading of the tablet. We need a good model to simulate the tablet design 2, leading to a Gaussian release profile.

A desired drug release profile is inspired by a desired plasma concentration profile or a desired therapeutic effect. This work inspires the idea of personalized medicine. We will be able to design tablet configurations based on the requirements of a specific individual patient, his physiological and genetic makeup, and the desired therapeutic effect. This will greatly improve the patient compliance, improve the efficiency of the drug tablet, and reduce the dosage frequency.

5.6 References

Cobby, J., M. Mayersohn and G. C. Walker (1974). "Influence of shape factors on kinetics of drug release from matrix tablets I: Theoretical." Journal of pharmaceutical sciences **63**(5): 725-732.

Colombo, P. (1993). "Swelling-controlled release in hydrogel matrices for oral route." Advanced Drug Delivery Reviews **11**(1–2): 37-57.

Colombo, P., P. Santi, R. Bettini, O. Strusi, F. Sonvico and G. Colombo (2008). New modules, new assemblage kits and new assemblies for the controlled release of substances, WO Patent 2,008,067,829.

Ford, J. L., M. H. Rubinstein, F. McCaul, J. E. Hogan and P. J. Edgar (1987). "Importance of drug type, tablet shape and added diluents on drug release kinetics from hydroxypropylmethylcellulose matrix tablets." International journal of pharmaceutics **40**(3): 223-234.

Huglin, M. R. (1989). "Hydrogels in medicine and pharmacy Edited by N. A. Peppas, CRC Press Inc., Boca Raton, Florida, 1986 (Vol. l), 1987 (Vols 2 and 3). Vol. 1 Fundamentals, pp. vii + 180, £72.00, ISBN 0-8493-5546-X; Vol. 2 Polymers, pp. vii + 171, £72.00, ISBN 0-8493-5547-8; Vol. 3 Properties and Applications, pp. vii + 195, £8000, ISBN 0-8493-5548-6." British Polymer Journal **21**(2): 184-184.

Kim, C.-j. (1995). "Compressed donut-shaped tablets with zero-order release kinetics." Pharmaceutical research **12**(7): 1045-1048.

Krögel, I. and R. Bodmeier (1999). "Development of a multifunctional matrix drug delivery system surrounded by an impermeable cylinder." Journal of controlled release **61**(1): 43-50.

Losi, E., R. Bettini, P. Santi, F. Sonvico, G. Colombo, K. Lofthus, P. Colombo and N. A. Peppas (2006). "Assemblage of novel release modules for the development of adaptable drug delivery systems." Journal of controlled release **111**(1): 212-218.

Losi, E., R. Bettini, P. Santi, F. Sonvico, G. Colombo, K. Lofthus, P. Colombo and N. A. Peppas (2006). "Assemblage of novel release modules for the development of adaptable drug delivery systems." Journal of Controlled Release **111**(1–2): 212-218.

Reynolds, T. D., S. A. Mitchell and K. M. Balwinski (2002). "Investigation of the effect of tablet surface area/volume on drug release from hydroxypropylmethylcellulose controlled-release matrix tablets." Drug development and industrial pharmacy **28**(4): 457-466.

Sangalli, M. E., A. Maroni, L. Zema, M. Cerea, U. Conte and A. Gazzaniga (2003). "A study on the release mechanism of drugs from hydrophilic partially coated perforated matrices." Il Farmaco **58**(9): 971-976.

Shah, N. H., A. S. Railkar, W. Phuapradit, F.-W. Zeng, A. Chen, M. H. Infeld and A. Malick (1996). "Effect of processing techniques in controlling the release rate and mechanical strength of hydroxypropyl methylcellulose based hydrogel matrices." European journal of pharmaceutics and biopharmaceutics **42**(3): 183-187.

Sheskey, P. J. and J. Hendren (1999). "The Effects of Roll Compaction Equipment Variables, Granulation Technique, and HPMC Polymer Level on Controlled-Release Matrix Model Drug Formulation." Pharmaceutical technology **23**: 90-107.

Siepmann, J., H. Kranz, N. Peppas and R. Bodmeier (2000). "Calculation of the required size and shape of hydroxypropyl methylcellulose matrices to achieve desired drug release profiles." International journal of pharmaceutics **201**(2): 151-164.

Skoug, J. W., M. T. Borin, J. C. Fleishaker and A. M. Cooper (1991). "In vitro and in vivo evaluation of whole and half tablets of sustained-release adinazolam mesylate." Pharmaceutical research **8**(12): 1482-1488.

Wesselingh, J. A. and H. W. Frijlink (2008). Mass Transfer from Solid Oral Dosage Forms. Pharmaceutical Dosage Forms - Tablets, CRC Press**:** 1-50.

CHAPTER 6

Research Summary

In chapter 2, we successfully developed a drug release model to predict the release behavior of an oral drug from the solid drug tablet inside the GI tract of the body. A solution strategy was proposed to solve the moving boundary problem encountered in solving the drug release model. Using this model, we studied the effects of model parameters such as the polymer degradation rate constant (k_d), on the tablet dissolution rate. We specifically studied the effect on the thickness of the solid tablet (G) as well as the total tablet including the swollen gel layer (S). The value of G continuously decreased with time, while the value of S initially increased and then decreased as expected. The profiles indicated a burst release during the initial stages of the release process.

The solution that we have employed in this model to solve the moving boundary problem is an approximate solution. There is need for a more efficient solution to the moving boundary problem that would lead to more accurate predictions. A major assumption in the model is that the drug release takes place only along the tablet thickness (axial direction) leading to a 2-D model. We will extend this work by considering the release in all directions (a 3-D model), which is more realistic but more computationally demanding. The model solution strategy employed in this work is a discrete approach, where the time and space are divided into small fractions and the model is solved in each of these fractions. A better solution would be needed.

The developed model will provide insights into the various mass transport, diffusion and degradation processes involved in the mechanism of drug release from a swelling polymer matrix. This model will greatly aid in simulating some of the in vitro dissolution tests and reduce the number of experiments, and hence reduce the time and effort involved.

In chapter 3, we successfully developed a pharmacokinetic model incorporating the drug release, transit, absorption and elimination processes inside the GI tract of the human body. The advantage of the suggested approach is that it can be used to test hypothesis about the mechanism involved in drug delivery into the blood circulatory system. The model is very flexible and can be applied to different patients with varying body weights. We incorporated the

model within an optimization framework to estimate the optimal geometry of the tablet, which will give the maximum efficacy.

This pharmacokinetic model is based on the ACAT model, which represents the GI tract as a series of well-mixed continuous stirred tanks (CSTR's); however, the GI tract is a continuous tube more closely represented by for example by a piece-wise tubular vessel with constant cross section and axial dispersion. We are pursuing this angle as well with the understanding that higher model complexity and model accuracy would result. The tubular flow model would account for spatial variation of drug concentration inside the compartments. We plan to extend the model to allow it to predict a plasma profile of a general shape. This will make it possible to design the optimal dosage form and optimal dosage regimen to obtain a desired plasma profile in a desired shape. The model can be extended for predicting drug behavior in model animals such as rats and dogs by adapting the model to represent the physiology. This will be greatly beneficial to the pharmaceutical industry in performing animal studies and help in reducing the number of test subjects.

In chapter 4, we used a CAMD framework to generate molecular structures of polymers with desired properties. We have successfully generated molecular structures of repeat units of polymers that have the potential to be used as efficient carrier materials for drug delivery. We discussed an efficient methodology to rank the generated polymers based on their desirability. The higher their desirability value, the more useful is the polymer for the intended application. We discussed a method to filter out the polymer candidates based on their compatibility with the available pharmaceutical drugs. We used solubility parameter analysis to determine the compatibility between a polymer and a drug.

In the CAMD methodology, we used a group contribution method to predict polymer properties such as glass transition temperature (T_g), expansion coefficient (α_f) and water absorption (W). A mixed integer nonlinear optimization technique was used to successfully generate some novel polymer structures. There is a limited availability of group contribution parameters to only some polymer properties. We plan to extend this work by developing group contribution parameters for other desired polymer properties such as diffusion coefficients of water and drug in the polymer and porosity of the polymer. We designed simple homopolymers

in this work. It would be a value addition to extend the work to design co-polymers satisfying desired property constraints. This work deals with generating polymer repeat units by linear arrangement of the identified groups. It would be interesting to incorporate side chain formation in the design of the polymer.

The generated molecular structures using this methodology need further analysis and investigation for them to be practically used for drug delivery applications. An expert opinion from a polymer chemist about the validity of the generated structures is very essential. An opinion about the possibility of synthesizing the new polymers, the practicality and economics involved, will greatly help in progress of this work. The developed CAMD methodology greatly helps in the product development process by reducing the number of experimental trials, hence reducing the time and effort involved. It helps in identifying potential failures in the early development process, thereby avoiding late stage failures, which tend to be very expensive.

In chapter 5, we proposed tablet configurations (dosage form designs) which could potentially lead to desired drug release profiles such as a constant or zero-order release profile, Gaussian release profile and a pulsatile release profiles. The proposed configurations are theoretically sound with simple designs which could be manufactured with little difficulty. The practicality of the designs can only be ascertained through thorough experiments and availability of the desired polymers for different applications discussed in this work. These include rigid polymers, swelling polymers and pH sensitive polymers.

A desired drug release profile is inspired by a desired plasma concentration profile or a desired therapeutic effect. This work inspires the idea of personalized medicine. We will be able to design tablet configurations based on the requirements of a specific individual patient, his physiological and genetic makeup, and the desired therapeutic effect. This will greatly improve the patient compliance, improve the efficiency of the drug tablet and reduce the dosage frequency.

The development of a good modeling platform to predict the behavior of drug inside the body facilitates the drug development and design process. It helps in selecting the most favorable candidates for the drug development based on the desired properties and greatly reduces the number of experiments needed for drug development. This further reduces the time and effort

required significantly. It aids in reducing the dependence on trial-and-error methods used for drug development and design. The developed model follows a two-way approach i.e., given the drug tablet; it can predict the plasma concentration profile and evaluate the pharmacokinetic parameters like peak plasma concentration, area under the curve and bioavailability. Given the target plasma profile or the corresponding pharmacokinetic parameters, the model can evaluate the optimal design parameters of the drug tablet. This research will greatly aid in the development of personalized medicine, which is the future of drug industry. Personalized medicine is the development of specific drug for specific patient based on individual's physiology and genetic makeup. These personalized drugs will be more effective for each individual, since right amount of drug will be given to the patient at the right time with maximum efficiency.

Many advanced models have been developed and are being developed to predict the release of drug from a polymer matrix system. Many of these models have increased in complexity and have become more accurate due to improvement in the simulation programs that are being used to solve the underlying mathematical problems. It would be very useful to understand and model the effect of different kinds of excipients on the drug release behavior. The modeling framework developed is more focused on the macroscopic environment of the GI tract in the human body. The model is useful to predict the amount of drug released, absorbed and eliminated. However, we did not focus on the microscopic environment such as, the different processes through with the drug absorption takes place, or the different processes through which drug elimination takes place. Much more advanced models are available which focus more on these microscopic processes in detail. Our model can be modified to include these microscopic process based on the requirement of the client. It would also be very useful to modify the current model using physiologically based pharmacokinetic (PBPK) modeling to be used for pharmacokinetic studies in animals such as rats and dogs. The current model has the ability to be used along with or combine with other models to further enhance the predictability and usability. This could have a significant impact by saving a lot of time and money during animal studies. The molecular design framework using group contributions is a simple method to design the polymer structures. The uncertainties involved in the group contribution parameters make the CAMD process less accurate. Much more advanced property prediction models are available which could be adapted to make the molecular design more accurate and efficient. The major limitations with the

proposed tablet designs are the economics involved in manufacturing these tablets, customized to each patient. In the current pharmaceutical industry, standard shapes, sizes and dosages of the oral tablet are used which is much more economical compared to designing individual tablets specific to each patient. Based on all the recent advances, we can expect a significant improvement in the development of accurate and efficient computational models for improving the overall drug discovery and development process.